KCRS25

Kidney Cancer Research Summit

Abstracts

July 17–18, 2025

Boston • MA

Contents

Oral Abstract Presentations

1 **Pembrolizumab plus lenvatinib for previously untreated advanced non–clear cell renal cell carcinoma: 3-year follow-up of the phase 2 KEYNOTE-B61 study** Laurence Albiges 2

2 **Combination casdatifan plus cabozantinib in previously treated patients with clear cell renal cell carcinoma: results from an expansion cohort of ARC-20 (NCT05536141)** Toni Choueri 2

3 **Derepression of Human Endogenous Retroviruses in ccRCC: Implications for Immunotherapy** Qinqin Jiang 3

4 **CD163+ Tumor-Associated Macrophages and Clinical Outcomes to First-Line Nivolumab Therapy in Patients with Metastatic Clear Cel Renal Cell Carcinoma: Insights from the HCRN GU16-260 Trial** Berkay Simsek 4

5 **Integrative clinical, genomic, transcriptomic, and immunopathologic characterization of circulating KIM-1 in metastatic RCC** Marc Machaalani 5

6 **Lower Checkpoint Gene Expression is Associated with Primary Resistance to Nivolumab-Ipilimumab Combination in Advanced Renal Cell Carcinoma** Rana McKay 7

Rapid Abstract Presentations

7 **Phase 2 trial of metastasis directed radiotherapy without systemic therapy (MRWS) for oligometastatic clear cell renal cell carcinoma (ccRCC) and investigation of circulating tumor DNA (ctDNA)** Chad Tang 9

8 **The actionable microbial gut checkpoint MAdCAM-1 in patients with advanced renal cell carcinoma** Carolina Alves Costa Silva 10

9 **Characterizing Carbonic Anhydrase 9 and HIF-2α RNA Expression in Clear Cell Renal Cell Carcinoma (ccRCC)** Yu-Wei Chen 11

10 **Investigating the Mechanisms of Neoadjuvant Olaparib and Cediranib in Renal Cancer: Results of Arms 1 to 3 of the WIndow of opportunity in REnal cancer (WIRE) Clinical Trial** James Jones on behalf of the WIRE Trial Group 12

11 **Exploring Health-Related Quality of Life Across the Disease Spectrum in Renal Cell Carcinoma: A Conceptual Domain Analysis** Koral Shah 13

12 **Evaluating Global Disparities in Clinical Trial Availability for Renal Cell Carcinoma** Ruchi Agarwal 14

13 **Quality-adjusted time without symptoms or toxicity (Q-TWiST) analysis of belzutifan versus everolimus in previously treated advanced renal cell carcinoma (RCC): LITESPARK-005 (LS-005)** Thomas Powles, MD 15

14 **Influence of sex on immunosurveillance and metastatic tropism in novel mouse models of clear cell renal cell carcinoma** Doris Zheng 17

15 **Real-World Evidence Shows No Survival Advantage with Contemporary First-Line Strategies in Papillary Renal Cell Carcinoma: A Call for Randomized Trials** Miguel Zugman 18

Trials in Progress Oral Presentations

16 **LASER – a Phase 2 trial of 177Lu-PSMA-617 as Systemic Therapy for Renal Cell Carcinoma (NCT06964958)** Praful Ravi 19

17 **A Phase 1, multiple-dose study to evaluate the safety and tolerability of first-in-class XmAb819 (ENPP3 x CD3) in subjects with relapsed or refractory clear cell renal cell carcinoma (ccRCC) (NCT05433)** Chet Bohac 20

18 **EXACT: A Randomized phase II trial of XL092 (Zanzalintinib) in combination with immunotherapy in patients who progress on Adjuvant therapy in Clear Cell RCC [NCT06863311]** Karie Runcie 21

19 **A Phase 0 Pilot Study of Memory-like Natural Killer (NK) Cell Immune Therapy in Patients with Renal Cell Carcinoma or Urothelial Carcinoma (NCT06318871** Wenxin (Vincent) Xu 22

20 **Phase II trial of ivonescimab in patients with advanced clear cell renal cell carcinoma previously treated with immune checkpoint blockade: IVORY Trial (NCT06940518)** Nazli Dizman 23

21 **Short TeRm Intensified Pembrolizumab (KEytruda) and Tivozanib for Hogh-Risk Renal Cell Carcinoma – STRIKE! (A033201) - NCT06661720** Bradley A. McGregor 25

Posters

22 **Final results of the phase 3 COSMIC-313 study comparing first-line cabozantinib plus nivolumab and ipilimumab with nivolumab plus ipilimumab in patients with advanced renal-cell carcinoma** Laurence Albiges 27

23 **Molecular Residual Disease (MRD) Guided Adjuvant ThErapy in Renal Cell Carcinoma (RCC) -MRD GATE RCC** Arnab Basu 27

24 **TGF-Beta alters CD8+ T cell phenotype and drives resistance to immune checkpoint inhibitors (ICI) in renal cell carcinoma (RCC)** Rishabh Rout 28

25 **Determining the impact of HIF2α inhibition on T cell function in clear cell renal cell carcinoma** Katrine Madsen 29

26 **Subgroup analysis of the efficacy and safety of cabozantinib ± atezolizumab in patients from CONTACT-03 who received first-line treatment with immuno-oncology–based combinations** Bradley A. McGregor 31

27 **Characterization of aberrant alternative splicing landscape in patients with metastatic renal cell carcinoma** Benjamin Mercier 31

28 **Microbial metabolic pathways to abrogate immunotherapy toxicity and promote anti-tumor response in metastatic renal cell cancer** Shahla Bari 32

29 **An artificial intelligence model to predict somatic mutations from histopathology in metastatic renal cell carcinoma** Regina Barragan-Carrillo 32

30 **Meta-analysis of single-cell RNA sequencing of tumor-infiltrating T-cells in clear cell renal cell carcinoma reveals distinct phenotypes and prediction markers of expanded T-cell clonotypes** Yuexin Xu 33

31 **Lymphocyte Heat Shock Signature Predicts Response to Immune Checkpoint Blockade in Renal Cell Carcinoma** Ethan Burns 34

32 **Interplay of Tumor-Intrinsic and Microenvironmental Gene Expression Predicts Immune Checkpoint Blockade Response in Metastatic Renal Cell Carcinoma** Nicholas Salgia 35

33 **Fusion Derived Oncogenic Programs Shape the Immune Landscape in translocation Renal Cell Carcinoma** Prathyusha Konda 37

34 **Hypoxia and immune suppression shapes therapeutic outcomes and metastases in clear cell renal cell carcinoma** Lynda Vuong 38

35 **FGD1 Splice Variant as a Novel Biomarker for Inferior Clinical Outcomes and Development of Brain and Bone Metastasis in Clear Cell Renal Cell Carcinoma** Alex Soupir 39

36 **International Neoadjuvant Kidney Cancer Consortium guidelines on assessing pathological response after neoadjuvant therapy in kidney cancer** James Jones 41

37 **Integrative multi-omic characterization of the immune landscape in renal cell carcinoma** Jennifer Pfei 42

38 **Presence of tertiary lymphoid structures and exhausted tissue-resident T cells determines clinical response to PD-1 blockade in renal cell carcinoma** Lena Wirth 43

39 **Intratumoral Viral Transcriptomic Signatures Stratify Immune Phenotypes and Clinical Outcomes in Renal Cell Carcinoma (RCC)** Mustafa Saleh 44

40 **Investigating the determinants of immunotherapy response in the primary tumor of clear cell renal cell carcinoma (RCC)** Cerise Tang 45

41 **Single-cell dissection of immunosuppressive myeloid subclusters driving resistance to immune checkpoint therapy in renal cell carcinoma (RCC)** Soki Kashima 45

42 **The Impact of Belzutifan on Tumor Reduction Procedures and Healthcare Resource Utilization in Von Hippel–Lindau (VHL) Disease** Rimas V. Lukas 46

43 **AURKA Connects NSD1 and SETD2 in an Epigenetic Axis Governing Mitotic Fidelity in ccRCC** Ruhee Dere 48

44 **Overview of Tivozanib (Tivo) safety in phase 3 clinical trials in patients with metastatic renal cell carcinoma (mRCC)** Pedro C. Barata 48

45 **Tumor matrix directed IL12/A3 fusion cytokine secreted by CD70-CAR NK cells markedly enhances anti-ccRCC responses with limited systemic exposure** Fuguo Liu 49

46 **Integrated Efficacy and Safety Exposure Response (ER) Analysis of Tivozanib (TIVO) for the Treatment of Renal Cell Cancer (RCC)** Bradley A. McGregor 51

47 **TCF1+ CD4+T Cells Mediate Response to Anti-CTLA-4 Therapy in a Sarcomatoid RCC Mouse Model** Hui Jiang 52

48 **Immunotherapy Response Correlates in Metastatic Clear Cell Renal Cell Carcinoma from Circulating Cell-Free Epigenomes** Razane El Hajj Chehade 52

49 **Preclinical efficacy of combined CDK4/6 and mTORC1 inhibition in translocation renal cell carcinoma** Shikha Gupta 53

50 **Clinical characteristics, determinants and subsequent therapy of primary refractory metastatic renal cell carcinoma (mRCC): An International Metastatic Database Consortium (IMDC) study** Marc Eid 54

51 **Antioxidant dependencies in fumarate hydratase–deficient kidney cancer** Blake Wilde 55

52 **Spatial Transcriptomic Mapping Reveals Immune-inflamed Niches in Sarcomatoid Chromophobe Renal Cell Carcinoma** Yan Tang 56

53 **Microenvironmental characteristics of disease relapse after nephrectomy in clear cell renal cell carcinoma** Yu Fujiwara 56

54 **Allogeneic HSPC-engineered CD70-directed CAR-NKT cells for renal cell carcinoma targeting tumor, microenvironment, and alloreactive T cells** Yan-ruide Li 58

55 **The Prognostic Role of Circulating Tumor DNA (ctDNA) Clearance as a Biomarker in Localized and Metastatic Renal Cell Carcinoma (RCC): A Single-Center Experience** Adanma Ayanambakkam 59

56 **NPRL2 loss enhances DNA damage while isolating cGAS-STING pathway and conferring immunotherapy resistance** Xiande Liu 59

57 **VHL and TP53 mutation status are not associated with response or progression-free survival in metastatic renal cell carcinoma treated with VEGF-targeted therapies** Daniela Castro 61

58 **Dissecting the Interplay between Bap1 and Pbrm1 in Renal Cell Carcinoma** Bingqing Xie 61

59 **Real-World Efficacy and Safety of Belzutifan in Sporadic Metastatic Renal Cell Carcinoma: A Multicenter Study from The City of Hope Enterprise** Charles Nguyen 62

60 **Systemically Administered Oncolytic Vaccinia Virus Enhances the In Vivo Antitumor Effects of RTKI and Anti-PD-1 Based Therapies in an Immunocompetent Renal Cancer Model** Ngoc Huong Giang Tran 63

61 **Predicting Immunotherapy Response in ccRCC using Deep Learning on Histopathological Slides** Satwik Rajaram 64

62 **The SLC1A1/EAAT3 Dicarboxylic Amino Acid Transporter is an Epigenetically Dysregulated Nutrient Carrier that Sustains Oncogenic Metabolic Programs** Treg Grubb 65

63 **Plasma Proteomic Profiling Reveals Distinct Mitochondrial Signatures in Chromophobe Renal Cell Carcinoma** Clara Steiner 65

64 **Defining Cancer Initiating Cells and their Vulnerabilities in Renal Cell Carcinoma** Zohreh Mehrjoo 66

65 **Treatment Patterns and Attrition Rates for Metastatic Non-Clear Cell Renal Cell Carcinoma in the US** Zeynep Irem Ozay 67

66 **Patient Perceptions of Biomarker Testing in Kidney Cancer (KC) from the International Kidney Cancer Coalition (IKCC) Global Patient Survey (GPS)** Eric Jonasch 68

67 **Generating Syngeneic NF2 models of Unclassified Renal Cell Carcinoma** Nicole Rittenhouse 70

68 **Targeting the BBOX1-TBK1-mTORC1 Axis in Clear Cell Renal Cell Carcinoma** Chengheng Liao 70

Trials in Progress Posters

69 **Testing Cabozantinib with or without Atezolizumab in Patients with Advanced Papillary Kidney Cancer (NCT05411081)** Benjamin Maughan 72

70 **A Phase 1 Clinical Trial of the Farnesyltransferase Inhibitor KO-2806 in Combination with Cabozantinib in Renal Cell Carcinoma** Adanma Ayanambakkam 73

71 **Educational Video Intervention to Enhance Latinx Participation in Genitourinary Oncology Clinical Trials: A Randomized Study** Regina Barragan-Carrillo 74

Oral Abstract Presentations

1

Pembrolizumab plus lenvatinib for previously untreated advanced non–clear cell renal cell carcinoma: 3-year follow-up of the phase 2 KEYNOTE-B61 study

Laurence Albiges[1], Howard Gurney[1], Jae Lyun Lee[2], Vagif Atduev[2], Cristina Suarez[3], Miguel A. Climent[3], David Pook[3], Piotr Tomczak[3], Philippe Barthelemy[4], Craig Gedye[5], Louis Lacombe[5], Thomas Ferguson[5], Viktor Stus[5], Pawel Wiechno[5], Mustafa Erman[5], Yuksel Urun[6], Jerry Cornell[6], Joe Burgents[6], Manish Sharma[6], Martin Voss[7]

[1]Institut Gustave Roussy, [2]Asan Medical Center, University of Ulsan College of Medicine, [3]Vall d´Hebron Institute of Oncology (VHIO), Hospital Universitari Vall d´Hebron, [4]Institut de Cancerologie Strasbourg Europe, [5]ICON Cancer Centre Adelaide, [6]Ankara University, [7]Memorial Sloan Kettering Cancer Center

Background

First-line pembrolizumab plus lenvatinib showed durable responses in participants with advanced non–clear cell renal cell carcinoma (nccRCC) in the single-arm, phase 2 KEYNOTE-B61 study (NCT04704219). Responses were observed across subtypes including papillary, chromophobe, and unclassified histologies. We present results from KEYNOTE-B61 with approximately 18 months of additional follow-up from the previous analysis.

Methods

Adults with previously untreated, advanced nccRCC and measurable disease per RECIST v1.1 received pembrolizumab 400 mg intravenously every 6 weeks for up to 18 cycles (approximately 2 years) plus lenvatinib 20 mg by mouth once daily until intolerable toxicity, progressive disease, or participant withdrawal. The primary end point was objective response rate (ORR) per RECIST v1.1 by blinded independent central review (BICR). Secondary end points included duration of response (DOR) and progression-free survival (PFS) per RECIST v1.1 by BICR, overall survival (OS), and safety and tolerability. Histologic subtypes were determined by investigator assessment and retrospectively reviewed by central pathology.

Results

Overall, 158 participants received pembrolizumab plus lenvatinib. Median study follow-up (time from first dose to the data cutoff date of January 27, 2025) was 41.6 months (range, 35.4-46.4). Of 158 participants, 93 (58.9%) had papillary, 29 (18.4%) had chromophobe, and 20 (12.7%) had unclassified histologies, and 16 (10.1%) had translocation (n = 6), medullary (n = 1), or other (n = 9) histologic subtypes. As of the data cutoff date, 121 of 158 participants (76.6%) had discontinued treatment, most commonly due to disease progression (n = 81, 51.3%). A total of 61 of 158 participants (38.6%) received subsequent anticancer therapy, most commonly cabozantinib (n = 38, 24.1%). In all participants, ORR was 50.6% (n = 80; 95% CI, 42.6-58.7), with 16 complete responses and 64 partial responses. ORR was generally consistent across histologic subtypes, including chromophobe (33.3%) and papillary

Table

	Total N = 158	Papillary n = 93	Chromophobe n = 29
Median PFS (95% CI), months	17.9 (15.0-21.1)	18.3 (15.0-21.0)	11.3 (6.7-29.0)
24-mo PFS rate, %	39.2	34.7	44.4
36-mo PFS rate, %	26.4	19.0	26.6
Median OS (95% CI), months	41.5 (32.8-NR)	37.5 (27.1-NR)	NR (21.7-NR)
24-mo OS rate, %	66.5	64.5	69.0
36-mo OS rate, %	53.7	50.4	62.1

(52.9%). Median DOR was 23.5 months (range, 1.5+ to 40.2+); 34.6% of responders remained in response for ≥36 months per Kaplan-Meier estimates. In all participants, median PFS was 17.9 months (95% CI, 15.0-21.1); the 24- and 36-month PFS rates were 39.2% and 26.4%, respectively. Median OS was 41.5 months (95% CI, 32.8 to not reached [NR]); the 24- and 36-month OS rates were 66.5% and 53.7%, respectively. Based on histologic subtype, median PFS was 18.2 months (95% CI, 15.0-21.0) for participants with papillary nccRCC and 11.3 months (95% CI, 6.7-29.0) for participants with chromophobe nccRCC (table). Median OS was 37.5 months (95% CI, 27.1-NR) and NR (95% CI, 21.7-NR) for papillary and chromophobe histology, respectively. Grade 3 or 4 treatment-related adverse events occurred in 95 participants (60.1%) and most commonly included (≥5%) hypertension (25.9%), proteinuria (7.6%), diarrhea (6.3%), and weight decreased (6.3%). No deaths due to treatment-related adverse events occurred.

Conclusions

After a minimum of 3 years of follow-up, pembrolizumab plus lenvatinib continued to demonstrate durable responses and promising survival outcomes in the first-line setting for advanced nccRCC. With additional follow-up, 3 additional complete responses from the previous data cutoff were observed. No new safety signals have been reported with extended follow-up. Results from KEYNOTE-B61 support the use of pembrolizumab plus lenvatinib as a first-line treatment option for patients with nccRCC regardless of histology.

Keywords

Immunotherapy; renal cell carcinoma; non-clear cell renal cell carcinoma; pembrolizumab; lenvatinib

2

Combination casdatifan plus cabozantinib in previously treated patients with clear cell renal cell carcinoma: results from an expansion cohort of ARC-20 (NCT05536141)

Toni Choueri[1], Moshe Ornstein[2], Pedro C. Barata[3], Marc Matrana[4], Jaime Merchan[5], Craig Gedye[6], Clara Hwang[7], Rohit Kumar[8], Jae Lyun Lee[9], Yinghui Guan[10], Mohammad Ghasemi[10], Syed Quadri[10], Chris Negro[10], Jianfen Chen[10], Paul Foster[10], Deepti Warad[10], Bradley A. McGregor[1], Sun Young Rha[11], Alexandra Drakaki[12]

[1]Dana-Farber Cancer Institute, [2]Cleveland Clinic, [3]University Hospitals Seidman Cancer Center, [4]Oschsner Health, [5]University of Miami Leonard M. Miller School of Medicine, University of Miami, [6]ICON Cancer Centre Adelaide, [7]Henry Ford Cancer–Detroit, [8]James Graham Brown Cancer Center, University of Louisville, [9]Asian Medical Center, University of Ulsan College of Medicine, [10]Arcus Biosciences, Inc., [11]Yonsei Cancer Center, Yonsei University College of Medicine, [12]David Geffen School of Medicine, University of California, Los Angeles

Background

Hypoxia-inducible factor 2-alpha (HIF-2α) is highly dysregulated in clear cell renal cell carcinoma (ccRCC), resulting in increased expression of proteins involved with angiogenesis, proliferation, and cancer cell survival. Casdatifan is an orally bioavailable small-molecule HIF-2α inhibitor that has demonstrated monotherapy activity in patients receiving 2L+ treatment for ccRCC. We investigated the safety and efficacy of casdatifan plus the anti-vascular endothelial growth factor receptor tyrosine kinase inhibitor (VEGFR-TKI) cabozantinib in previously treated patients with ccRCC in an expansion cohort (casdatifan plus cabozantinib) of the phase 1, open-label ARC-20 (NCT05536141) trial.

Methods

Patients enrolled in the casdatifan plus cabozantinib expansion cohort were previously treated with immunotherapy (IO) alone or combined with anti-VEGF therapies. Casdatifan 100 mg and cabozantinib 60 mg were given orally once daily. Endpoints included the incidence of treatment-emergent adverse events (AEs) and objective response rate (ORR) by RECIST v1.1. The efficacy evaluable population was defined as patients who received any study treatment and achieved a minimum of 12 weeks follow-up. This study is ongoing; data as of March 14, 2025, are reported.

Results

Overall, 42 patients with a median (range) follow-up of 3.7 (1.1–9.1) months were enrolled. At the data cutoff date, prior treatment settings included adjuvant only (n = 8/42) and locally advanced/metastatic (1L n = 29/42; 2L n = 5/42). Twenty-five (60%) patients had received prior IO alone, and 17 (41%) patients had received prior IO plus VEGFR-TKI treatment. All grade AEs occurred in 98% of patients, with the most common being anemia (69%) and fatigue (57%). Most common (> 5%) grade ≥ 3 AEs were anemia (n = 10 [24%]), hyponatremia (n = 4 [10%]), and hypoxia (n = 3 [7%]). No casdatifan-related grade 4 or 5 AEs were observed. AEs leading to casdatifan only, cabozantinib only, or any study drug dose reductions occurred in 10 (24%), 16 (38%), and 22 (52%) patients, respectively. Two (5%) patients discontinued due to an AE related to casdatifan (hypoxia and drug hypersensitivity; n = 1 each). For patients in the efficacy evaluable population (n = 24), 1 (4%) patient achieved a complete response, and 10 (42%) patients achieved a partial response for a confirmed ORR of 45.8% (Table). Activity was seen across all IMDC risk groups.

Table. Clinical Activity With Casdatifan Plus Cabozantinib Combination Therapy in Previously Treated Patients With Clear Cell Renal Cell Carcinoma

	Patients With 12 Weeks of Follow-Up[a] (n = 24)
Follow-up, months, median (range)	5.3 (2.8–9.1)
Confirmed ORR[b], % (n)	45.8% (11)
(95% CI)	(25.6%, 67.2%)
Best overall response, n (%)	
CR	1 (4%)
PR[b]	10 (42%)
SD	12 (50%)
PD	1 (4%)

Data cutoff date: 14 March 2025.

[a]All eligible patients who received any study treatment and achieved a minimum of 12 weeks follow-up or discontinued due to progression or AE.

[b]Inclusive of 1 patient who had confirmed PR after 14 March 2025.

Conclusions

In previously treated patients with ccRCC, casdatifan 100 mg plus cabozantinib 60 mg had a manageable AE profile with promising clinical activity. These data support continued evaluation of this combination in the phase 3 PEAK-1 clinical trial.

Keywords

Casdatifan, hypoxia-inducible factor 2-alpha

3

Derepression of Human Endogenous Retroviruses in ccRCC: Implications for Immunotherapy

Qinqin Jiang

Dana-Farber Cancer Institute

Background

Clear cell renal cell carcinoma (ccRCC) often responds to immune checkpoint inhibitors (ICIs) despite having a relatively low burden of non-synonymous mutations, distinguishing it from other cancers like melanoma or mismatch repair-deficient colorectal cancer that are typically responsive to ICIs. ccRCC has historically been considered an immunogenic tumor due to characteristics such as spontaneous remissions, response to high-dose interleukin-2 (IL-2), and abundant T-cell infiltration. However, paradoxically, high T-cell infiltration in ccRCC correlates with poor prognosis and inconsistent ICI responses.

Over 70% of ccRCCs harbor inactivated pVHL tumor suppressor, which leads to the stabilization of HIF2α, a transcription factor critical for tumor growth. Recent studies suggest that HIF2α regulates the expression of endogenous retroviruses (ERVs)—ancient viral elements embedded in the human genome—whose expression is typically suppressed by DNA methylation. Notably, ccRCC has been found to express high levels of ERVs, and this correlates with better responses to ICIs. One specific ERV, ERVE-4, has been shown to produce an HLA-bound peptide recognized by donor-derived T cells in a patient who achieved complete remission after allogeneic stem cell transplantation (allo-SCT). Since ERVE-4 is transcriptionally activated by HIF2α and expressed in ccRCC but not normal tissues, it, along with other HIF2-regulated ERVs, could serve as potential tumor-specific antigens. This raises the possibility of targeting ERV-derived peptides as a novel immunotherapy strategy for ccRCC.

Methods

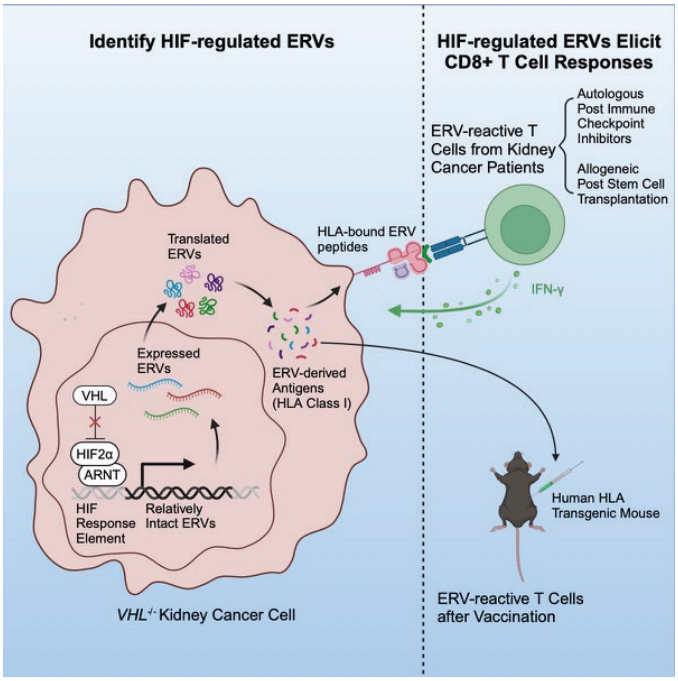
To assess whether ERVs in ccRCC are transcribed, translated, and presented by HLA complexes, a multi-omics approach was employed. RNA-seq, ChIP-seq, PRO-seq, single-cell RNA-seq and single-cell ATAC-seq were used to profile ERV transcription and regulatory mechanisms. Polysome-seq was conducted to identify ERV transcripts actively undergoing translation, while HLA immunoprecipitation followed by mass spectrometry (HLA-IP/MS) was employed to detect HLA-bound ERV-derived peptides. The immunogenicity of these peptides was evaluated using IFNγ ELISpot assays in both humanized mouse models and primary immune cells derived from ccRCC patients.

Results

RNA-seq and RT-qPCR analyses identified several HIF2α-responsive ERVs in ccRCC cell lines, such as ERVE-4, ERV3.2, and ERV4700, which were upregulated by active HIF2α and downregulated upon its inhibition. Additionally, treatment with the DNA methyltransferase inhibitor GSK3685032 induced the expression of ERV4700, suggesting that epigenetic mechanisms also regulate ERV activation.

Polysome-seq confirmed that these ERVs, including ERVE-4 and ERV3.2, were actively translated, and HLA-IP/MS identified 22 ERV-derived peptides presented by HLA complexes, including several that were tumor-specific. Single-cell RNA-seq and scATAC-seq further demonstrated that these ERVs were primarily expressed in tumor cells, indicating their specificity to ccRCC.

To assess the immunogenicity of these ERV-derived peptides, humanized HLA-A*11:01 mice were immunized with a mix of these peptides, and several of the predicted strong binders elicited T-cell responses, confirming their potential immunogenicity. Next, we incubated these peptides with immune cells from patients who had responded to immunotherapies. Peripheral blood mononuclear cells (PBMCs) from kidney cancer patients revealed reactivity to multiple ERV-derived peptides both before and after allo-SCT. The T-cell response increased in complete responders (CRs) post-transplant, further supporting the idea that ERV-derived peptides can trigger immune responses. Additionally, the T-Scan platform identified ERV-derived peptides recognized by T cells from patients with tumors harboring VHL mutations, reinforcing the hypothesis that HIF2-responsive, ERV-derived peptides presented on ccRCC cells are immunogenic.



Conclusions

This study uncovers a novel mechanism by which HIF2α enhances the immunogenicity of ccRCC through the transcriptional activation of ERVs. It provides compelling evidence that ERV-derived peptides can be translated, presented by HLA complexes, and recognized by T cells, positioning them as promising tumor-specific antigens. These findings support the potential of targeting ERVs for the development of next-generation immunotherapies in ccRCC.

Keywords

HIF, ERV, neoantigen, cancer vaccine

4

CD163+ Tumor-Associated Macrophages and Clinical Outcomes to First-Line Nivolumab Therapy in Patients with Metastatic Clear Cel Renal Cell Carcinoma: Insights from the HCRN GU16-260 Trial

Berkay Simsek[1], Morgan A. Paul[2], Wanling Xie[2], Nourhan El Ahmar[1], Sayed Matar[3], Yasmin Nabil Laimon[1], Gabriel Roberti De Oliveira[1], Razan Mohanna[1], Andrew Delcea[1], Toni Choueri[2], David Braun[4], Maxine Sun[2], Naomi B. Haas[5], Hans J. Hammers[6], Mehmet Bilen[7], Mark N. Stein[8], Jeffrey A. Sosman[9], Gordon J. Freeman[2], Catherine Wu[2], David McDermott[10], Michael B. Atkins[11], Sabina Signoretti[1]

[1]Brigham and Women's Hospital, [2]Dana-Farber Cancer Institute, [3]Yale School of Medicine, [4]Yale New Haven Hospital, [5]Hospital of the University of Pennsylvania, [6]UT Southwestern, [7]Winship Cancer Institute at Emory University, [8]Columbia University Medical Center, [9]Northwestern University Feinberg School of Medicine, [10]Beth Israel Deaconess Medical Center, [11]Georgetown Lombardi Comprehensive Cancer Center

Background

Tumor-associated macrophage (TAM) infiltration has been shown to modulate response to immune checkpoint inhibitors in various cancers, but its role in metastatic clear cell renal cell carcinoma (mccRCC) remains unclear. Here, we investigated the role of CD163+ TAMs as a potential determinant of clinical outcomes to first-line anti-PD-1 therapy (nivolumab) in patients with mccRCC enrolled in the HCRN GU16-260 trial. Moreover, as recent data suggest that the interaction between TAMs and tumor infiltrating lymphocytes (TILs) promotes T cell exhaustion, we explored the spatial relationship between CD163+ TAMs and CD8+ TILs in different states of exhaustion (i.e. terminally exhausted (TE) and non-terminally exhausted (NTE) CD8+ TILs).

Methods

Pre-treatment tumor samples from 67 patients were analyzed by multiplex immunofluorescence to identify CD163+ TAMs, $CD8^+PD\text{-}1^+TIM\text{-}3+$ and/or LAG-3+ (TE CD8+), and $CD8^+PD\text{-}1^+TIM\text{-}3^-LAG\text{-}3^-$ (NTE CD8+) TILs. Associations between the natural log of density of $CD163^+$ TAMs with progression-free survival (PFS) and objective response rate (ORR) were assessed using univariable Cox and logistic regression models, respectively. An optimized cutoff was determined using minimum p value for ORR. For each tumor, the density of TE CD8+ TILs and the density of NTE CD8+ TILs were calculated within a 30 μm radius area centered on CD163+ TAMs (proximal area) and outside of this area (non-proximal area), using the 'sf' package within R software. The densities of TE and NTE CD8+ TILs were compared in proximal versus non-proximal areas across all tumor samples using the Wilcoxon signed-rank test. For each CD8+ TIL population (TE and NTE), the enrichment in proximity of CD163+ TAMs was assessed by calculating the difference in densities in proximal and non-proximal areas normalized by the density in the overall tumor area. The level of enrichment in TE CD8+ TILs versus NTE CD8+ TILs in proximity of CD163+ TAMs was compared using the Wilcoxon signed-rank test.

Results

The density of $CD163^+$ TAMs, analyzed as a continuous variable was positively associated with ORR (OR: 2.21, 95% CI: 1.33 to 3.69, p=0.002) and PFS (HR: 0.77, 95% CI: 0.61 to 0.97, p=0.028). At an optimized cutoff, patients with high density of $CD163^+$ TAMs (n=34, 50.7%) had higher ORR (65% vs. 15%, p<0.001) and longer median PFS (16.6 months, 95% CI: 5.5-32.9 vs. 5.5 months, 95% CI: 4.1-10.6, p=0.009) compared to patients with low density of CD163+ TAMs (n=33, 49.3%). The density of CD163+ TAMs was moderately correlated with the density of TE CD8+ TILs (Spearman correlation, r= 0.55) and weakly correlated with the density of NTE CD8+ TILs (r= 0.32). Proximity analysis showed that the density of TE CD8+ TILs was significantly higher in the area proximal to the CD163+ TAMs compared to the non-proximal area (median density: 123.3/mm2 vs. 37.2/mm2; p < 0.001). Similarly, the density of NTE CD8+ TILs was significantly higher in the area proximal to the CD163+ TAMs compared to the non-proximal area (median density: 127.2/mm2 vs. 66.8/mm2; p < 0.001). The level of enrichment in proximity of CD163+ TAMs was higher for TE CD8+ TILs compared to NTE CD8+ TILs (0.77 vs. 0.58; p = 0.0011).

Conclusions

High levels of $CD163^+$ TAMs are associated with improved outcomes to anti-PD-1 therapy in mccRCC. In addition, exhausted CD8+ TILs preferentially localize in proximity of $CD163^+$ TAMs in ccRCC tissues, supporting that TAM-T cell interactions are critical for driving T cell dysfunction. Taken together, our data are consistent with the hypothesis that the efficacy of PD-1 blockade may be in part mediated by reprogramming TAMs from a pro-tumorigenic to an anti-tumorigenic state.

Keywords

Tumor-associated macrophage, cytotoxic T-cell, exhaustion, spatial

5

Integrative clinical, genomic, transcriptomic, and immunopathologic characterization of circulating KIM-1 in metastatic RCC

Marc Machaalani[1], Renée Maria Saliby[2], Caiwei Zhong[1], Eddy Saad[1], Clara Steiner[1], Emre Yekeduz[1], Liliana Ascione[1], Mustafa Saleh[1], Jad El Masri[1], Pablo Barrios[1], Xiaowen Liu[3], Ti Cai[3], Maxine Sun[1], Gwo-Shu Mary Lee[1], Wanling Xie[1], Sabina Signoretti4, David McDermott5, Toni Choueiri[1], Wenxin (Vincent) Xu[1]

[1]Dana-Farber Cancer Institute, [2]Yale New Haven Hospital, [3]Beth Israel Deaconess Medical Center, Harvard Medical School, [4]Brigham and Women's Hospital, [5]Beth Israel Deaconess Medical Center

Background

Kidney injury molecule-1 (KIM-1) is a transmembrane protein that is overexpressed in renal cell carcinoma (RCC). The JAVELIN Renal 101 trial established avelumab+axitinib as a standard treatment regimen for advanced renal cell carcinoma (RCC). We evaluated the prognostic value of KIM-1 and explored the association between KIM-1 levels and underlying tumor biology in RCC, leveraging translational analyses including genomic, transcriptomic, and immunohistochemistry data.

Methods

KIM-1 was measured in plasma at baseline (C1D1) and at 12 weeks (C3D1) using an electrochemiluminescence-based assay. Cox regression analyses were performed for progression-free survival (PFS) and overall survival (OS) and adjusted for baseline clinical characteristics. The predictive performance of our models for 18-month OS was evaluated using time-dependent receiver operating characteristic (ROC) curves. Associations between KIM-1 levels and clinical and translational data were evaluated using the Wilcoxon rank-sum test for categorical groups. Differential gene expression (DGE) and gene set enrichment analysis (GSEA) were performed using DESeq2, with KIM-1 treated as a continuous variable.

Table

Multivariable Cox regression models evaluating the association of baseline KIM-1 levels plus the change in KIM-1 levels from baseline to 12 weeks with progression-free survival and overall survival*

	Progression-free survival		Overall survival	
	Adjusted HR (95% CI)**	Adjusted *P*-value**	Adjusted HR (95% CI)**	Adjusted *P*-value**
Baseline log10 KIM-1 (continuous)	1.29 (1.12, 1.50)	<0.001	1.88 (1.52, 2.32)	<0.001
Change from C1 to C3 (>30% vs. <30%)	2.37 (1.75, 3.20)	<0.001	3.21 (2.15, 4.78)	<0.001

*We used a landmark analysis from cycle 3. For overall survival, no patients were excluded. For progression-free survival, 66 patients were excluded: 7 due to short follow-up, and 59 due to progress after cycle 1.
**Adjusted for International mRCC Database Consortium (IMDC) risk groups

Abbreviations: HR, hazard ratio; CI, confidence interval; C1, cycle 1; C3, cycle 3.

Results

Plasma for analysis was available from 612 patients (69% of the ITT population), including 323 treated with avelumab+axitinib and 289 with sunitinib. Elevated baseline KIM-1 levels were correlated with higher tumor burden as assessed by the sum of tumor diameters (Spearman's ρ=0.55; P<0.0001). Lower KIM-1 levels were found at baseline in patients with IMDC favorable versus intermediate (185.09 vs. 330.95 pg/ml; P<0.001) and poor (185.09 vs. 1,285.51 pg/ml; P<0.001) risk, and in intermediate versus poor (330.95 vs. 1,285.51 pg/ml; P<0.001) risk groups.

Loss-of-function (LOF) BAP1 mutations were associated with higher tumor KIM-1 RNA expression (P<0.0001) and plasma protein expression (742.29 vs. 280.47 pg/ml; P=0.038) which remained significant after adjustment for tumor burden, as well as greater decreases in KIM-1 on avelumab+axitinib (-578.4 vs. -75.8 pg/ml; P=0.01) but not on sunitinib. Transcriptomic analysis showed that the expression of HAVCR1, the gene encoding KIM-1, showed the strongest association with KIM-1 protein levels (Spearman's ρ=0.31; P<0.0001), and that higher KIM-1 levels were associated with interferon gamma response whereas lower KIM-1 levels were associated with a hypoxia transcriptional program. Higher KIM-1 levels were also associated with enrichment for proliferative versus angiogenic gene expression signatures (P=0.013).

At 12 weeks, a greater decrease in KIM-1 was observed on avelumab+axitinib versus sunitinib (-65.55% vs. -31.02%; P<0.001). Patients with PD-L1 positive tumors had a greater decrease in KIM-1 (-56.80% vs. -33.49%; P=0.001) across arms. Tumors of patients who had a decrease in KIM-1 had a higher baseline total CD8+ infiltration (1.54% vs. 1.05%; P=0.004), including within the tumor center (1.48% vs. 0.92%; P=0.004). In all patients, lower KIM-1 at baseline or at 12 weeks was associated with longer PFS and OS (Table). Landmark analyses showed that increases in KIM-1 from baseline to 12-week follow-up were associated with shorter PFS and OS (Table). Lower KIM-1 levels were found among patients with partial response (PR) versus progressive disease (327.84 vs. 759.82 pg/ml; P=0.04), complete response versus PR (94.22 vs. 327.84 pg/ml; P<0.001), and exceptional versus intermediate response (117.13 vs. 325.81 pg/ml; P=0.003). The 18-month AUC was 0.67 for baseline KIM-1 and 0.71 for 12-week KIM-1 for predicting OS. Adding baseline KIM-1 to IMDC improved the 18-month AUC from 0.69 to 0.75. The highest predictive performance was observed when IMDC was combined with 12-week KIM-1, corresponding to AUC of 0.78.

Conclusions

We present the first integrative clinical, transcriptomic, genomic, and immunopathologic evaluation of circulating KIM-1. High KIM-1 is correlated with poor prognosis in RCC and aggressive biology as characterized by mutational and transcriptomic analyses. Prospective studies are needed for the clinical implementation of KIM-1 as a biomarker in RCC.

Keywords

KIM-1; Circulating Biomarker; Clinical Trial; mRCC; Proteomics

6

Lower Checkpoint Gene Expression is Associated with Primary Resistance to Nivolumab-Ipilimumab Combination in Advanced Renal Cell Carcinoma

Rana McKay[1], Adam Dugan[1], Unnati Jariwala[1], Karyn Ronski[1], Jacob Mercer[1], Eddy Saad[2], Jad El Masri[2], Marc Machaalani[2], Mustafa Saleh[2], Cody Rose[2], Maxine Sun[2], Sabina Signoretti[3], David Braun[4], Sumanta Pal[5], Toni Choueiri[2]

[1]University of California, San Diego, [2]Dana-Farber Cancer Institute, [3]Brigham and Women's Hospital, [4]Yale New Haven Hospital, [5]City of Hope Comprehensive Cancer Center

Background

Immunotherapy combinations have emerged as the standard of care for patients with advanced renal cell carcinoma (RCC). While the combination of first-line (1L) nivolumab and ipilimumab has demonstrated long-term durability with 90-month progression-free survival (PFS) of 23%, primary progressive disease (PD) occurs in up to 20% of patients. There is an urgent clinical need to identify negative selection markers for patients unlikely to respond to nivolumab-ipilimumab therapy.

Methods

We used Tempus Lens to select records for 106 patients with RCC who received 1L ipilimumab-nivolumab treatment from the Tempus multi-modal database. Eligible patients had tumor samples collected within one year of treatment initiation and were processed using xT (DNA-seq) and xR (RNA-seq) assays. Treatment response was investigator-assessed within 90 days of therapy start and categorized as progressive disease (PD) versus non-PD, which includes stable disease, partial response, or complete response. RNA-seq data were normalized, log2-transformed, and batch-corrected and used to measure checkpoint and angiogenic gene expression (Transcripts per million, TPM). Immunologic phenotype was assessed by TMB (mt/Mb), MSI status, PD-L1 (IHC, 22c3); immune infiltration was estimated by quanTIseq (RNA).

	Response to Nivolumab + Ipilimumab within 90 days of Treatment Initiation		
	SD, PR, CR (n=51)	**PD (n=55)**	**P value**
TMB (mt/Mb)	4.21 (2.63, 6.32)	3.16 (2.11, 4.21)	0.068
MSI High, N (%)	1 (2.0%)	1 (1.8%)	>0.999
Checkpoint Gene Expression			
TIGIT	**2.05 (1.23, 2.72)**	**1.30 (0.82, 2.12)**	**0.004**
CTLA4	**2.53 (1.72, 3.68)**	**1.87 (1.07, 3.08)**	**0.014**
PD-1	**2.32 (1.67, 3.73)**	**1.89 (1.13, 2.77)**	**0.017**
LAG-3	3.07 (2.32, 4.03)	2.55 (1.85, 3.67)	0.052
CD274 (PD-L1)	2.41 (2.01, 3.09)	2.26 (1.81, 2.84)	0.106
PD-L2	3.67 (3.22, 4.23)	3.45 (2.73, 4.18)	0.117
TIM3	5.15 (4.57, 5.88)	5.26 (4.14, 5.77)	0.426
Angiogenic Gene Expression			
VEGFA	8.07 (7.24, 8.38)	7.97 (6.85, 8.39)	0.766
KDR	6.43 (5.34, 7.21)	6.21 (5.70, 7.32)	0.924
ESM1	5.21 (4.26, 5.91)	4.72 (3.64, 5.72)	0.232
ANGPTL4	8.85 (7.90, 9.48)	8.64 (7.27, 9.22)	0.397
CD34	6.32 (5.36, 7.12)	6.26 (5.60, 6.91)	0.747
Immune cell proportions			
B cells	3.74 (2.90, 4.70)	3.78 (2.71, 4.79)	0.762
M1 Macrophages	6.4 (4.6, 10.9)	4.7 (2.8, 9.1)	0.083
M2 Macrophages	5.28 (4.07, 6.81)	5.82 (3.77, 6.94)	0.733
NK cells	2.91 (2.16, 3.72)	2.54 (1.96, 2.95)	0.095
Neutrophils	14.0 (11.0, 17.0)	13.2 (9.8, 15.8)	0.162
CD8 T cells	1.02 (0.22, 3.61)	0.55 (0.00, 2.71)	0.099
Tregs	3.27 (2.21, 5.11)	2.52 (1.62, 3.53)	0.007
Total Immune cells	39.0 (35.0-49.0)	37.0 (30.0-44.0)	0.033
CR=complete response, PR=partial response, SD=stable disease, PD=progressive disease, Gene expression=log2 (TPM)			

Results

Of the 106 patients, 55 experienced PD as the best response. The cohort was predominantly male (73%) and white (86%), with a median age at diagnosis of 59 years. Clinical characteristics were similar between treatment response categories, including rates of clear cell RCC (82% vs. 76%, p=0.480) and primary nephrectomy (47% vs. 53%, p=0.560). Patients with primary PD were more likely to have liver metastases (20% vs. 5.9%, p=0.032). There was no significant difference in PD-L1 (IHC) expression between groups (p=0.542). However, patients with primary PD exhibited significantly lower gene expression of CTLA4, TIGIT, and PD-1 as well as lower proportions of immune cells (Table 1). We observed a trend toward lower LAG3 expression and TMB in the PD group. Strong positive correlations were demonstrated between LAG3 expression and other checkpoint genes (all $p<0.002$). No significant differences were found in angiogenic gene expression or somatic tumor alterations between response groups.

Conclusions

In patients with advanced RCC treated with 1L nivolumab-ipilimumab, we identified distinct transcriptomic patterns of primary resistance characterized by lower expression of immune checkpoint genes. These findings suggest that tumors with reduced checkpoint pathway activity may be less responsive to dual checkpoint inhibition, possibly reflecting an immune-cold microenvironment with limited T-cell infiltration and activation. Future prospective validation of these findings, including IHC, could inform precision medicine strategies for patients with advanced RCC.

Keywords

Immunotherapy, progressive disease, tumor microenvironment, checkpoints.

Rapid Abstract Presentations

7

Phase 2 trial of metastasis directed radiotherapy without systemic therapy (MRWS) for oligometastatic clear cell renal cell carcinoma (ccRCC) and investigation of circulating tumor DNA (ctDNA)

Chad Tang, Alex Sherry, Aaron Seo, Kieko Hara, Haesun Choi, Suyu Liu, Xiaowen Sun, Anya Montoya, Ethan Ludmir, Amishi Y. Shah, Eric Jonasch, Amado J. Zurita-Saavedra, Craig Kovitz, Christopher Battey, Sarah Ratzel, Giannicola Genovese, Kanishka Sircar, Jose Karam, Nizar Tannir, Pavlos Msaouel

MD Anderson Cancer Center

Background

Current treatment for frontline ccRCC focuses on systemic therapy doublets. Although effective, such combinations exhibit substantial toxicities and healthcare costs. An underutilized option is MRWS, which may facilitate a prolonged systemic therapy-free interval in select patients. Unfortunately, no reliable prognostic markers exist to select patients for MRWS. Although ctDNA assays may guide patient selection, implementation in ccRCC has proven challenging due to limited ctDNA shedding. Therefore, advanced sequencing and bioinformatic pipelines are needed to enhance ctDNA reliability in ccRCC.

Methods

This phase 2 single-arm trial (NCT03575611) enrolled patients with oligometastatic ccRCC and up to 5 metastases. All patients had either never received systemic therapy or ceased >1 month earlier. Patients were treated with MRWS, consisting of predominately stereotactic radiation therapy to all sites of disease. Subsequent rounds of MRWS were administered if limited progression was observed. The co-primary endpoints were progression free survival (PFS) and systemic therapy free survival (STFS). For the latter, a median STFS of > 24 months (mo) was prespecified as the threshold for success. Individualized ctDNA panels (Myriad Genetics) were created from tumor whole genome sequencing and applied to serial plasma samples. Molecular residual disease (MRD) status was determined based on whether ctDNA was detected (MRD+) or not (MRD-).

Results

Between July 2018 to May 2023, 121 oligometastatic ccRCC patients were enrolled. Median follow up was 36 mo (range 13-61 mo). Most patients (72%) had 1 site of metastatic disease and had never received systemic therapy (70%). The median PFS was 18 mo (95% CI: 16-25 mo) and STFS was 34 mo (95% CI: 28-54 mo). The lower bounds of 95% CI of the median STFS exceeded the prespecified 24 mo threshold for success. Two-year PFS and STFS were 40% and 75%, respectively. Median OS was not reached, and 2- and 3-year OS were 94% and 86%, respectively. Nine (8%) patients experienced patients 3+ toxicities at least possibly attributed to MRWS. There were no grade 5 toxicities.

MRD+ was detected in 56% of patients at baseline and associated with significantly shorter STFS (HR 2.9, 95% CI 1.4-6.1, P=0.003). Patients who were MRD+ and MRD- at baseline exhibited a 27 vs. 54 mo median STFS, respectively. Three months after MRWS, 31% of MRD + patients converted to MRD-. Positive MRD status at 3 month follow up was strongly associated with shorter STFS (HR 4.3, 95% CI 2.0-9.0, P<0.001).

Conclusions

MRWS exhibited excellent tolerability and facilitated prolonged time off systemic therapy without compromising OS. Our ctDNA approach appears to be a promising baseline prognostic biomarker for STFS and a dynamic marker of MRWS response.

Keywords

Radiation Therapy, Metastasis Directed Therapy, Oligometastatic Kidney Cancer, circulating tumor DNA

8

The actionable microbial gut checkpoint MAdCAM-1 in patients with advanced renal cell carcinoma

Carolina Alves Costa Silva[1], Marc Machaalani[2], Renée Maria Saliby[3], Caiwei Zhong[2], Wanling Xie[2], Edoardo Pasolli[4], Cécile Dalban[5], Marine Fidelle[6], Gwo-Shu Mary Lee[2], Roxanne Birebent[6], Eddy Saad[2], Clara Steiner[2], Ronan Flippot[6], Janice Barros-Monteiro[7], Bernard Escudier[6], Lisa Derosa[6], Laurence Zitvogel[6], Toni Choueiri[2], Laurence Albiges[6]

[1]Oncoclínicas, [2]Dana-Farber Cancer Institute, [3]Yale New Haven Hospital, [4]Task Force on Microbiome Studies, University of Naples Federico II, [5]Clinical Research and Innovation Department, Centre Léon Bérard, [6]Institut Gustave Roussy, [7]Translational Research, UNICANCER, Paris – France

Background

Despite therapeutic advances, treatment resistance remains a major clinical challenge in advanced RCC (aRCC). The MAdCAM-1/$\alpha 4\beta 7$ axis plays a pivotal role in mediating immune-microbial crosstalk, contributing to gut dysbiosis-associated treatment resistance. In this study, we evaluated the clinical relevance of both baseline levels and longitudinal dynamics of soluble MAdCAM-1 (sMAdCAM-1) as a biomarker of dysbiosis-related immune dysregulation in aRCC patients.

Methods

We measured sMAdCAM-1 in plasma samples from 612 patients treated in the phase 3 JAVELIN Renal 101 (1st line avelumab + axitinib vs. sunitinib, NCT02684006), 278 patients treated in the phase 2 NIVOREN (>2nd line nivolumab post-TKI, NCT03013335) and the prospective study ONCOBIOTICS (with paired with fecal metagenomics, NCT04567446) using a Luminex assay. Quantitative data are described by the number of patients with available data, the number of missing values, the mean, standard deviation, median, minimum and maximum values, and the 1st and 3rd quartile values (Q1-Q3). Optimal cutoff was determined using the maximum log-rank statistic. Cox regression models analyzed associations with progression-free survival (PFS) and overall survival (OS). We profiled each metagenome's taxonomic composition with MetaPhlAn-4. For alpha diversity, we computed the per-sample Richness and Shannon indexes using the vegan R package. Differences between groups were assessed using the Wilcoxon-Mann-Whitney test. For beta-diversity, we computed the between-samples Bray-Curtis dissimilarities using the implementation available in the Vegan R package. Differential abundance analysis on taxonomic profiles between groups were performed using the LefSE software.

Results

The OS-based optimal cutoff was 180 ng/ml (25% percentile) in the JAVELIN Renal 101 population. Patients with higher sMAdCAM-1 at baseline demonstrated significantly improved survival outcomes: progression-free survival of 13.9 vs. 8.4 months ($p<0.01$) and 18-month overall survival (OS) of 84.2% vs 68.1% ($p<0.01$). These associations remained independent of IMDC risk group. Combining sMAdCAM-1 with IMDC scores improved 18-month OS prediction (AUC: 0.72 vs. 0.68, p=0.01). We further evaluated sMAdCAM-1 dynamics between cycles 1 and 3 in the JAVELIN Renal 101 trial. Persistently low sMAdCAM-1 levels were associated with poor survival across both treatment arms (Table 1). Patients harboring low sMAdCAM-1 level had a gut microbiota composition dominated by proinflammatory species such as Proteobacteria (Hafnia alvei, Suterella wadsworthensis), Paraprevotella clara, and Bacteroidales (Odoribacteraeae (Butyricimonas virosa), Rikenellaceae (Alistipes shahii, A. onderdonkii), Tanarellaceae (Parabacteroides merdae) family members. Additionally, low baseline sMAdCAM-1 correlated with elevated proinflammatory cytokines interleukin-6 (IL-6), IL-8, and VEGF levels in the JAVELIN Renal 101 and NIVOREN cohorts.

Table 1. Cox proportional hazards models for longitudinal sMAdCAM-1 categories.

	PFS		OS	
	HR (95% CI)	p-value	HR (95% CI)	p-value
High-High	0.53 (0.37, 0.76)	0.001	0.34 (0.23, 0.52)	<.001
Low-High	0.59 (0.36, 0.98)	0.041	0.64 (0.37, 1.12)	0.116
High-Low	0.52 (0.29, 0.92)	0.024	0.49 (0.26, 0.92)	0.026
Low-Low	ref	ref	ref	ref

Conclusions

Baseline and persistently low sMAdCAM-1 levels demonstrated significant associations with inferior survival outcomes and a distinct pro-inflammatory microbial-immune phenotype in aRCC patients. Our findings position sMAdCAM-1 as both: (1) a dynamic biomarker for tracking dysbiosis-driven immune dysregulation, and (2) a potential therapeutic target for microbiota-directed interventions in treatment-resistant disease.

Keywords

Renal cell carcinoma; Microbiota; gut dysbiosis; MAdCAM-1; biomarker.

9

Characterizing Carbonic Anhydrase 9 and HIF-2α RNA Expression in Clear Cell Renal Cell Carcinoma (ccRCC)

Yu-Wei Chen[1], Shayan Nazari[1], Andrew Elliott[1], Ninad Kulkami[1], Norm Smith[1], Rashad Nawfal[2], Pedro C. Barata[3], Aditya Bagrodia[3], Brent Rose[3], David McDermott[4], Sabina Signoretti[5], Marc Machaalani[2], Shankar Shiva[2], Michael Hofman[2], Neeraj Agarwal[6], Sumanta Pal[7], Toni Choueri[2], Rana McKay[1]

[1]*University of California, San Diego,* [2]*Dana-Farber Cancer Institute,* [3]*University Hospitals Seidman Cancer Center,* [4]*Beth Israel Deaconess Medical Center,* [5]*Brigham and Women's Hospital,* [6]*Huntsman Cancer Institute at the University of Utah,* [7]*City of Hope Comprehensive Cancer Center*

Background

ccRCC is frequently driven by VHL loss, leading to HIF-2α stabilization and upregulation of downstream targets such as carbonic anhydrase 9 (CA9). While CA9 is a well-established diagnostic marker of HIF pathway activation, its prognostic and predictive roles remain unclear. Emerging evidence suggests that high CA9 and HIF-2α expression may be associated with improved outcomes in ccRCC. With the recent approval of the HIF-2α inhibitor belzutifan, understanding whether these markers predict treatment response is critical for guiding biomarker-driven therapy.

Methods

Next-generation sequencing of DNA (592-gene panel or whole exome) and RNA (whole transcriptome) were performed on ccRCC specimens through Caris Life Sciences to comprehensively characterize genomic and transcriptomic alterations. Expression levels of CA9 and HIF-2α were quantified based on RNA transcripts per million (TPM) and categorized as High or Low using the >75th vs <25th percentile cutoff. Overall survival (OS) was defined as the time from initial diagnosis to death or last known follow-up. Time on treatment (TOT) was defined as the duration from the start of systemic therapy to treatment discontinuation.

Results

A total of 764 ccRCC specimens were analyzed. Of these, 433 (56.7%) were derived from primary kidney tumors, while the remaining samples were from metastatic sites, including lung (n=71, 9.3%), bone (n=70, 9.2%), endocrine (n=43, 5.6%), liver (n=23, 3%), lymph node (n=23, 3%), CNS (n=19, 2.5%), GI (n=4, 0.5%) and other sites (n=78, 10.2%). VHL alterations occurred in 82% (626/764) ccRCC tumors. The median age was 63. CA9 and HIF-2α expression levels were relatively higher in primary kidney tumors compared to metastatic sites. Expression levels of CA9 and HIF-2α were comparable across racial and ethnic subgroups. High CA9 expression (Q4 vs Q1) was associated with improved OS (mOS: 95 vs 42 months; HR 0.55, p = 0.005). Similarly, high HIF-2α expression (Q4 vs Q1) correlated with longer survival (mOS: 54.8 vs 38.3 months; HR 0.56, p < 0.001). Among belzutifan-treated patients (n=80), CA9 expression was not associated with OS (mOS: NE vs 17.3, p:0.851) or TOT of belzutifan (mTOT: 3.49 vs 2.34, p: 0.175). HIF-2α expression was not associated with OS (mOS: 16.2 vs 13.4, p:0.89) or TOT of belzutifan among VHL mutant patients (2.96 vs 2.96; p: 0.91). There were limited VHL wild-type ccRCC patients (n=9) treated with belzutifan in our cohort.

Conclusions

This comprehensive analysis of 764 ccRCC specimens demonstrates that VHL alterations are present in the majority of ccRCC tumors. CA9 and HIF-2α expression were consistent across racial and ethnic groups but showed higher expression in primary tumors compared to metastatic sites. High expression of both CA9 and HIF-2α were associated with significantly improved overall survival in the general ccRCC population. However, neither CA9 nor HIF-2α expression levels predicted response to belzutifan therapy. These findings enhance our understanding of HIF pathway biology in ccRCC and provide important context for the potential clinical application of CA9 PET imaging and HIF-2α inhibitor therapy in diverse patient populations.

Keywords

ccRCC, CA-9, HIF-2

10

Investigating the Mechanisms of Neoadjuvant Olaparib and Cediranib in Renal Cancer: Results of Arms 1 to 3 of the WIndow of opportunity in REnal cancer (WIRE) Clinical Trial

James Jones[1], Rebecca Wray[1], Ines Horvat Menih[2], Martin Thomas[3], Sulekha Said[3], Helen Mossop[4], Maria Aquino[3], James Arimtage[3], Harriet Baker[2], Carley Batley[5], James Blackmur[6], Sarah Burge[1], Anita Chhabra[3], Farhana Easita[5], Tim Eisen[5], Kate Fife[3], Angela Godoy[5], Richard Goodwin[7], Will Ince[3], Rose John[3], Alexander Laird[6], Natalia Lukashchuk[7], Athena Matakidou[3], Thomas Mitchell[8], Andrew Priest[2], Andrew Protheroe[9], Sreenidhi Ranjit[3], Anthony Riddick[3], Jamal Sipple[3], Amy Strong[3], Helen Su[5], Mark Sullivan[9], Silvia Tarantino[3], Gemma Tsang-Pells[5], Stephan Ursprung[10], Lauren Wallis[5], Anne Warren[3], James Wason[4], Sarah Welsh[11], Younghwa Kim[7], John Stone[7], Mireia Crispin-Ortuzar[1], Ferdia Gallagher[2], on behalf of the WIRE Trial Group

[1]University of Cambridge, Department of Oncology, [2]University of Cambridge, Department of Radiology, [3]Cambridge University Hospitals NHS Foundation Trust, [4]University of Newcastle, [5]University of Cambridge, [6]Western General Hospital, Edinburgh, [7]AstraZeneca, 8University of Cambridge, Department of Surgery, [9]Oxford University Hospitals NHS Foundation Trust, [10]Beatson West of Scotland Cancer Centre, [11]Royal Devon University Healthcare NHS Foundation Trust

Background

New treatments are required for patients with resistance to current renal cell cancer (RCC) therapies. In contrast to the success of immunotherapy and VEGF directed therapies, few treatments have successfully targeted the RCC cell directly. Pre-clinical data suggests that PARP inhibitors have activity against RCC, and PARP inhibitors have been investigated in advanced RCC either alone or combined with VEGF directed therapy. Neoadjuvant window of opportunity studies allow us to understand drug mechanism by comparing the tumour before and after treatment. WIRE (WIndow of opportunity in REnal Cancer) is a phase II, multi-centre, multi-arm, non-randomised, neoadjuvant clinical trial platform (NCT03741426) investigating novel RCC treatments. Here we report updated outcome data for arms 1-3 and ongoing translational analysis.

Methods

WIRE enrols patients with clear cell RCC, planned to have surgery, stage cT1b+, cN0/1, cM0/1, with no contraindication to IMP. A Bayesian adaptive design with pre-defined stop/go criteria efficiently assigns patients to each arm. Arms 1-3 comprised: 1. cediranib (a VEGF inhibitor), 2. cediranib + olaparib (a PARP inhibitor), 3. olaparib. Patients received 14-28 days of IMP before surgery. The primary endpoint is a ≥30% reduction in dynamic contrast enhanced (DCE) MRI assessed vascular permeability (median Ktrans) post-treatment compared to baseline. Secondary endpoints include a ≥30% increase in IHC-assessed tumour CD8+ T cell density post-treatment compared to baseline, and percentage change in MRI assessed tumour volume. Extensive tissue and blood samples are taken during the trial for mechanistic analysis.

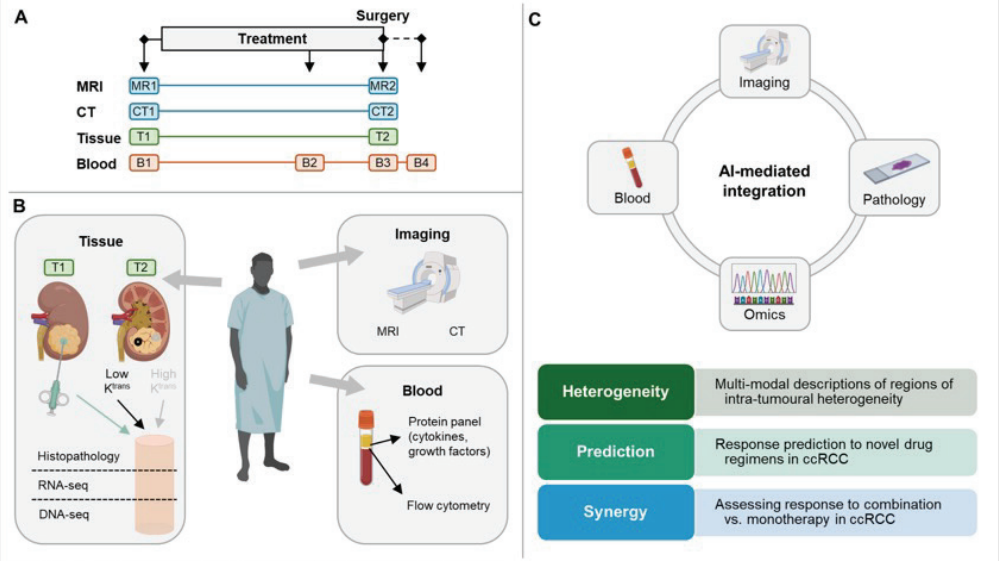


Figure 1. Multimodal data integration in the WIRE Trial

A. Trial schematic showing imaging, tissue and blood collection events. B. Key translational analysis performed on the trial. Biopsies and multi-region tissue samples from nephrectomy will be assessed by histopathology and transcriptomics. Serial blood samples are analysed for cytokine and immune cell profiles. Results will be compared to tumour response as measured by DCE-MRI and CT scanning. C. AI approaches will be used to integrate multiple data modalities to understand tumour response to therapy.

Results

29 patients were recruited (arm 1=6, arm 2=16, arm 3=7), 28/29 were male, median age 61 years (range 48-75 years). 8 patients had M1 disease. Treatment was well tolerated, and importantly all patients had surgery within the planned window. 3 patients were not evaluable for the primary endpoint due to inadequate dose of IMP (<70% compliance rate in total doses of IMP within 7 days prior to presurgical imaging).

The numbers of evaluable patients which met the primary endpoint for Ktrans reduction were arm 1 (cediranib): 4/6 (67%), arm 2 (cediranib + olaparib): 4/14 (29%), arm 3 (olaparib): 0/6 (0%). For the secondary endpoint of increase in tumour CD8+ T cell density, the numbers were arm 1: 3/6 (50%), arm 2: 9/14 (64%), arm 3: 1/6 (17%). There were reductions in MRI-assessed tumour volume in arms 1 and 2 compared to arm 3 (median change & [range], arm 1: -9.01% [-43.78% to -4.78%]; arm 2: -11.47% [-37.47% to 10.53%]; arm 3: 8.29% [-5.43% to 13.28%]).

In exploratory analysis, there was significant induction of VEGF-A and Placental Growth Factor (PlGF) in plasma prior to surgery compared to baseline in the combination arm 2 (VEGF-A p=0.0330, PlGF p=0.00071). There were no correlations between degree of angiogenic cytokine induction and MRI assessed change in Ktrans or tumour volume.

Conclusions

Responses as measured by Ktrans were observed particularly in the cediranib only arm, less so in the combination arm and not at all in the olaparib arm. Within a short duration of therapy, consistent tumour volume reductions occurred in both cediranib containing arms. Greater induction of PlGF and VEGF-A in the combination arm indicates possible synergy between cediranib and olaparib.

Ongoing translational work is investigating the relationship between other DCE-MRI metrics assessed during the trial. Transcriptomics and digital pathology will be performed comparing baseline biopsies with multiple regions sampled at nephrectomy. These methods will define tumour environments associated with response or non-response. Machine learning approaches will be used to integrate the multiple data modalities (Figure 1). Arm 4, using volrustomig – a PD-1/CTLA-4 bispecific antibody is actively recruiting.

Keywords

Neoadjuvant, window of opportunity, angiogenesis, PARP, AI

11

Exploring Health-Related Quality of Life Across the Disease Spectrum in Renal Cell Carcinoma: A Conceptual Domain Analysis

Koral Shah[1], Paulo Gustavo Bergerot[2], Daniela Castro[1], Benjamin Mercier[1], Elizabeth Nally[3], Adil Ali[4], Thomas E. Hutson[5], Axel Bex[6], Sarah P. Psutka[7], Brian Rini[8], Elizabeth Plimack[9], Viraj A. Master[10], Viktor Grünwald[11], Laurence Albiges[12], Toni Choueri[13], Sumanta Pal[1], David Cella[14], Thomas Powles[15], Cristiane Decat Bergerot[2]

[1]City of Hope Comprehensive Cancer Center, [2]Oncoclínicas & Co, Medica Scientia Innovation Research (MEDSIR), [3]Barts Cancer Institute, [4]Department of Urology, Emory University School of Medicine, [5]Texas Oncology, [6]Netherlands Cancer Institute, [7]Department of Urology, University of Washington, [8]Division of Hematology and Oncology, Department of Medicine, Vanderbilt University Medical Center, [9]Fox Chase Cancer Center, [10]Emory University School of Medicine, [11]Essen University Hospital, [12]Institut Gustave Roussy, [13]Dana-Farber Cancer Institute, [14]Department of Medical Social Sciences, Northwestern University Feinberg School of Medicine, [15]Barts Cancer Institute, Queen Mary University of London, Barts Health NHS Trust

Background

Understanding how health-related quality of life (HRQOL) concerns vary by disease stage is essential for developing patient-reported outcome measures (PROMs) that reflect the lived experiences of individuals with renal cell carcinoma (RCC). This study aimed to explore differences in the perceived relevance of HRQOL domains between patients with localized and metastatic RCC using a provisionally grouped item set derived from validated instruments.

Methods

This is a secondary analysis of a prospective international study conducted from August 2022 and October 2024, with participants from the United States, Europe, and Brazil (Bergerot et al., JCO 2025). In Phase 1, a 54-item was developed using the Functional Assessment of Cancer Therapy–Kidney Symptom Index (FKSI-19), the European Organization for Research and Treatment of Cancer Core Quality of Life Questionnaire (EORTC QLQ-C30), and the EuroQol (EQ-5D). Items were provisionally grouped into four conceptual domains: physical disease-related symptoms (DRS-P), emotional symptoms (DRS-E), treatment side effects (TSE), and function/well-being (FWB). Patients with localized or metastatic RCC rated item relevance. We calculated the mean number of relevant items per domain and conducted ANOVAs to compare groups, reporting partial eta squared (η^2) for effect size.

Results

A total of 200 patients (localized n=83; metastatic n=117) were included. Patients with metastatic RCC reported greater relevance of physical symptoms (DRS-P: M=39.2, SD=6.0) compared to those with localized disease (M=35.3, SD=6.7; $F(1,198)=17.53$, $p<.001$, $\eta^2=0.081$). Similarly, metastatic patients reported higher treatment side effect burden (TSE: M=12.2, SD=2.3 vs. 10.6, SD=2.5; $F(1,198)=19.47$, $p<.001$, $\eta^2=0.089$). No significant difference was observed in emotional symptoms (DRS-E; $p=0.260$). Conversely, patients with localized RCC more often endorsed concerns related to function and well-being (FWB: M=17.6, SD=3.5) than those with metastatic disease (M=15.5, SD=2.9; $F(1,198)=20.52$, $p<.001$, $\eta^2=0.094$).

Conclusions

Given the differences in trajectory and treatment modalities across localized and metastatic RCC, our findings underscore the evolving nature of HRQOL concerns across the RCC continuum. While physical symptoms and treatment side effects were highly relevant across both groups, their prominence among metastatic patients suggests the burden of advanced disease and systemic therapies. In contrast, patients with localized disease prioritized functional limitations and emotional concerns, potentially linked to surveillance-related anxiety. These insights support the need for stage-specific PROMs and highlight the importance of integrating both physical and emotional dimensions of care in RCC. Validation of such a tool for both localized and metastatic RCC is underway in forthcoming studies.

Keywords

Health-related quality of life, patient-reported outcome measures, metastatic renal cell carcinoma, localized renal cell carcinoma

12

Evaluating Global Disparities in Clinical Trial Availability for Renal Cell Carcinoma

Ruchi Agarwal[1], Jaya Goud[2], Miguel Zugman[2], Daniela Castro[2], Xiaochen Li[2], Koral Shah[2], Lily Lau[3], Aaron Lee[4], Salvador Jaime-Casas[2], Hedyeh Ebrahimi[2], Gabriela Regalado-Porras[5], Sharon Choi[6], Nora Sobrevilla-Moreno[7], Erika Ruiz-Garcia[7], Shivanee Kooner[8], Skylar Reid[9], Nasr Chaudhary[10], Rana McKay[6], Sumanta Pal[2], Regina Barragan-Carrillo[7]

[1]University of Pennsylvania, [2]City of Hope Comprehensive Cancer Center, [3]University of California, Irvine, [4]University of California, Berkeley, [5]ABC Medical Center, [6]University of California, San Diego, [7]National Cancer Institute of Mexico, [8]University of Southern California, [9]Rensselaer Polytechnic Institute, [10]University of California, Merced

Background

Clinical trials are the cornerstone for generating high-quality evidence to improve patient outcomes. In metastatic renal cell carcinoma (RCC), research over the past two decades has resulted in a fourfold increase in median overall survival (Lancet, 2024). However, most clinical trials are conducted in high-income countries (HICs), limiting the inclusion of diverse patient populations (JCO CCI, 2020). We aimed to assess the global distribution of RCC clinical trials and identify disparities by country income level.

Methods

We queried the National Clinical Trials database for all trials enrolling patients with RCC between June 1, 2019, and June 1, 2024. We excluded non-interventional studies, pediatric trials, and trials for non-RCC malignancies. Participating countries were categorized using the World Bank Ranking (WBR): high-income (HICs), upper-middle-income (UMICs), lower-middle-income (LMICs), and low-income countries (LICs). For each eligible trial, we documented RCC subtype, sponsor, trial phase, disease stage, and multinational status. Descriptive statistics were used to summarize trial characteristics. We assessed the association between country income level and trial availability using the Kruskal-Wallis test and Poisson regression to evaluate associations with RCC incidence, mortality, WBR, health expenditure, and gross national income (GNI).

Results

A total of 357 eligible trials were identified. Most (N = 273; 76%) were conducted exclusively in HICs, while only 84 trials (24%) included participation from UMICs, LMICs, or LICs. There were no significant differences in RCC subtype or disease stage across income groups. Pharmaceutical-sponsored trials were more common in non-HICs compared to HICs (64.3% vs. 39.6%, $p < 0.001$), whereas government and academic-sponsored trials were more frequent in HICs (60.4% vs. 35.7%, $p < 0.001$). Although early-phase trials predominated in all regions, late-phase trials were more common in non-HICs (25% vs. 8.1%, $p < 0.001$). Multinational trials were significantly more prevalent in non-HICs (45.2% vs. 15.8%, $p < 0.001$). The odds of having an RCC trial available significantly decreased with lower income classification (OR: UMICs 0.20; LMICs 0.05; LICs 0.013 vs. HICs). Poisson regression showed that GNI, health expenditure, and mortality were significantly associated with the number of clinical trials per country.

Conclusions

RCC clinical trials are largely concentrated in high-income countries, with limited inclusion of UMICs, LMICs, and LICs. Countries outside the HIC group are more reliant on pharmaceutical industry funding and international collaborations to access clinical research. Addressing these disparities by expanding clinical trial access in non-HICs is essential to promote global equity in RCC care and ensure the generalizability of trial findings across diverse populations.

Keywords

Renal Cell Carcinoma, Clinical Trials, Global Disparities, Income Level

13

Quality-adjusted time without symptoms or toxicity (Q-TWiST) analysis of belzutifan versus everolimus in previously treated advanced renal cell carcinoma (RCC): LITESPARK-005 (LS-005)

Thomas Powles, MD[1], Guillermo De Velasco, MD[2], Toni Choueri, MD[3], Gregory Chen, PhD[4], Ying Xiao, MHSA[5], Reshme Shinde, MPH, PhD[6], Patrick Moneuse, MSc[4], Emanuele Del Fava, PhD[4], Rodolfo Perini, MD[6], Donna Vickery, MD[6], Laurence Albiges, MD, PhD[7], Brian Rini, MD[8]

[1]Barts Cancer Institute, Queen Mary University of London, Barts Health NHS Trust, [2]Medical Oncology Department, 12 de Octubre University Hospital, [3]Dana-Farber Cancer Institute, [4]MSD, Zurich, Switzerland, [5]MSD (UK) Limited, London, UK, [6]Merck & Co, Inc., [7]Institut Gustave Roussy, [8]Division of Hematology and Oncology, Department of Medicine, Vanderbilt University Medical Center

Background

Belzutifan significantly prolonged progression-free survival vs. everolimus in the phase 3 LS-005 trial (NCT04195750) among patients with advanced RCC who had previously received immune checkpoint and antiangiogenic therapies. Q-TWiST is an established framework that integrates efficacy, safety, and patient health utility data into one interpretable index. This analysis applied the Q-TWiST method to quantify the net health benefits of belzutifan versus everolimus, based on the final analysis of LS-005 (15Apr2024 cutoff)

Methods

Patients' survival time after randomization was divided into 3 mutually exclusive health states: time with grade 3-4 toxicity before investigator-assessed disease progression (TOX); time without symptoms of progression or grade 3-4 toxicity (TWiST); and time from progression until death (REL, i.e., relapse). In each treatment arm, Q-TWiST was calculated as the sum-product of restricted mean time spent in the three states and state-specific utility weights. Standard set of utility weights used in literature (1 for TWiST, 0.5 for TOX and REL) were considered, with threshold utility analysis performed to assess the impact of the different health state utility. Treatment effects were summarized as differences in restricted mean time spent in each state, difference in Q-TWiST, and relative gain in Q-TWiST (difference divided by everolimus mean overall survival). Bootstrap resampling was performed to obtain 95% confidence intervals (CIs)

	Belzutifan, mean months (N=374)	Everolimus, mean months (N=372)	Difference (95% CI), months
TOX	1.45	1.22	0.23 (-0.29, 0.76)
TWiST	10.73	6.07	4.66 (3.28, 6.02)
REL	12.02	16.25	-4.23 (-6.45, -1.84)
Q-TWiST (LS-005 utility set)	18.52	17.72	0.80 (-0.96, 2.87)
Q-TWiST (standard utility set)	17.47	14.81	2.66 (1.06, 4.49)

Results

With a maximum follow-up of 49 months, patients treated with belzutifan had significantly longer TWiST, significantly shorter time in REL, and numerically longer time in TOX than those treated with everolimus (Table). Mean Q-TWiST difference significantly favored belzutifan by 2.66 months (95% CI: 1.06, 4.49; relative gain: 11.32%) when applying standard utility weights. In a sensitivity analysis using the utility weights of TOX and REL varying between 0 to 1, the mean Q-TWiST difference varies from 0.54 to 4.43 months, and the associated relative gain varied from 2.28% to 18.82%. Scenario analysis using an alternative TOX definition of all-cause SAE showed minimal impact on results.

Conclusions

Belzutifan showed a statistically significant and clinically important improvement in quality-adjusted survival time compared to everolimus among patients with advanced RCC who had previously received immune checkpoint and antiangiogenic therapies.

Keywords

RCC, QTWiST, Belzutifan

14

Influence of sex on immunosurveillance and metastatic tropism in novel mouse models of clear cell renal cell carcinoma

Doris Zheng, Hui Jiang, Nicole Rittenhouse, Amrita Nargund Mangalvedhekar, Zizhuo Yang, Liangliang Ji, David Solit, Lynda Vuong, A. Ari Hakimi

Memorial Sloan Kettering Cancer Center

Background

Sex bias in renal cell carcinoma (RCC) is marked by males having twice the incidence and mortality rates of females, along with larger, higher-grade tumors and greater metastatic burden. Several hormonal, genetic, and behavioral reasons have been identified, however, the role that the immune system plays in this remains unclear. This is in part due to the historical lack of relevant and reliable animal models that recapitulate human disease. We therefore sought to utilize two newly developed syngeneic ccRCC mouse models to first establish and characterize the features of mouse ccRCC sex bias, and subsequently to determine whether a strong immunological basis exists.

Methods

Because of the known heterogeneity in ccRCC, we evaluated these sex-specific differences in both an immune checkpoint blockade (ICB)-resistant (Vhl-/- p53-/- Rb1-/- Myc-overexpression) & an ICB-responsive (Vhl-/- Cdkn2a/2b-/- Bap1-/-) model developed by our lab. Tumor cells were orthotopically implanted by sub-renal capsular injection into the kidneys of male and female WT or immune-deficient (ID, NSG- NOD.Cg-Prkdcscid Il2rgtm1Wjl/SzJ) mice, and tumor growth was longitudinally monitored using ultrasound imaging. In addition, metastatic derivatives of these cells lines were injected intravenously. At necropsy, liver and lung metastases were quantified and immune populations in the tumor and peripheral blood were analyzed by flow cytometry.

Results

WT females developed smaller primary tumors with lower penetrance compared to WT males, while ID mice showed no sex differences, indicating that the gender bias is dependent on the immune system. Flow cytometry revealed females had more circulating T-cells. Interestingly in tumors, CD8+ T-cells in the ICB-resistant model correlated with larger tumors (males), while in the ICB-responsive model, they correlated with smaller tumors (females), suggesting CD8+ T-cells can have pro-tumor/anti-tumor effects depending on the microenvironment.

Metastases were observed exclusively in ID mice in both models. However, while the ICB-responsive model had a higher incidence of lung metastases in females and no sex-related differences in liver metastases, male mice injected with ICB-resistant cells had higher incidence of both lung and liver metastases. This suggests a critical role of immune surveillance in restricting both liver and lung ccRCC metastases; gender specific organ tropism was model-dependent.

Given that WT mice did not develop metastases, metastatic derivatives of the two lines were used to evaluate metastatic seeding in an immunocompetent setting. In both models, WT females had significantly fewer liver metastases compared to males. In the ICB-responsive model, this correlated with elevated levels of ILC1s in the liver tumors. In the lung, both models exhibited distinct phenotypes: males developed more lung masses in the ICB-resistant model, whereas females showed a higher burden in the ICB-responsive model. Males with fewer lung metastases had significantly greater populations of monocytes, DCs, and T-cells, compared to females having a greater abundance of macrophages, suggesting different sex- dependent mechanisms for immunosurveillance in the lung.

Conclusions

Overall, our findings highlight deterministic sex-related immunologic differences in immune surveillance and metastatic tropism in ccRCC and support the need for further mechanistic studies.

Keywords

Immunosurveillance, metastatic tropism

15

Real-World Evidence Shows No Survival Advantage with Contemporary First-Line Strategies in Papillary Renal Cell Carcinoma: A Call for Randomized Trials

Miguel Zugman[1], Jennifer R. Rider[2], Nazli Dizman[3], Salvador Jaime-Casas[1], Vitor Abreu Goes[1], Koral Shah[1], Daniela V. Castro[1], Benjamin Mercier[1], Peter Zang[1], Hedyeh Ebrahimi[1], Regina Barragan-Carrillo[1], Diwyanshu Sahu[4], Prithviraj Vikramsinh Mandora[4], JoAnn Hsu[1], Wesley Yip[1], Charles B. Nguyen[1], Alex Chehrazi-Raffle[1], Robert Miller[2], Thomas Powles[5], Toni Choueiri[6], Sumanta K. Pal[1]

[1]City of Hope Comprehensive Cancer Center, [2]ConcertAI LLC, [3]MD Anderson Cancer Center, [4]ConcertAI LLC, Bengaluru, Karnataka, India, [5]Barts Health NHS Trust Saint Bartholomew's Hospital, [6]Dana-Farber Cancer Institute

Background

Papillary renal cell carcinoma (pRCC) is the most common non-clear cell RCC subtype, yet prospective evidence guiding first-line systemic therapy remains limited. The phase 2 PAPMET trial in molecularly unselected pRCC and the phase 3 SAVOIR trial in MET-driven pRCC demonstrated clinical benefit, but neither showed overall survival improvement and were limited by small sample size (Pal et al., Lancet 2021; Choueiri et al., JAMA Oncol 2020). In this context, as IO-based combinations have gained traction in clinical practice following promising activity in single-arm studies, we leveraged real-world data (RWD) to characterize evolving treatment patterns and associated outcomes in pRCC.

Methods

Patients with pRCC were retrospectively identified from the ConcertAI Patient360™ RCC Dataset, a US-based de-identified, human curated comprehensive real-world dataset, generated from multiple electronic medical record systems and linked with medical and pharmacy claims as well as third party date of death information. Histology was defined by ICD-O-3 codes (8260/3, 8050/2, 8050/3, 8052/2, 8052/3, 8130/2, 8130/3) and NCI System codes (C27886, C27887), excluding clear cell papillary RCC (8323/1). Among patients with metastatic disease who received first-line systemic therapy, regimens were categorized as tyrosine kinase inhibitors (TKIs), IO (monotherapy or IO/IO), MET inhibitors (METi), mTOR inhibitors (mTORi), or IO-based combinations (IO/TKI or IO/METi). Temporal trends, demographics, and outcomes were assessed. Real-world PFS (rwPFS) and overall survival (rwOS) were estimated using Kaplan–Meier methods and compared across treatment groups. Cox models evaluated associations between treatment and survival with adjustment for clinical and demographic factors.

Results

Of 391 patients with pRCC, 385 (98.5%) had metastatic disease, of whom 216 (55.2%) initiated first-line systemic therapy between January 1, 2016, and May 1, 2024, and were included in the analyses. Median age was 65.6 years (IQR, 56.4–76.3), and 75.6% were male. Most were treated in community settings (89.4%). Patients were primarily White (61.0%) or Black/African American (26.0%); 5.5% were Hispanic or Latino. Most were from the South (40.3%), Midwest (16.1%), or Northeast (15.6%). TKIs were the most frequently used first-line regimen (49.5%), followed by IO (21.8%), METi (15.3%), IO/TKI or IO/METi (10.6%), and mTORi (2.8%). TKIs predominated from 2016 to 2019, after which IO and IO-based combinations became the most common first-line therapies. Median rwPFS was 5.4 months (95% CI, 4.07–7.06) for TKIs, 5.0 (2.52–6.30) for IO, 4.9 (2.95–8.93) for METi, 2.4 (1.80–12.74) for IO/TKI or IO/METi, and 2.0 (0.32–3.21) for mTORi. Median OS was 14.6 months (10.50–19.90) for TKIs, 18.7 (15.00–26.10) for IO, 14.8 (9.80–24.80) for METi, 9.3 (5.19–37.45) for IO/TKI or IO/METi, and 6.9 (0.32–11.10) for mTORi. Results were similar after adjustment for age, gender, race, geographic region, practice setting, stage at diagnosis, and ECOG.

Conclusions

In this national RWD cohort of metastatic pRCC, a shift toward IO and IO/TKI or IO/METi combinations was observed in recent years. However, survival outcomes remained similar across treatment groups. These findings underscore the need for phase 3 randomized trials. Ongoing studies such as STELLAR-304 (NCT05678673) and SAMETA (NCT03091192) reflect the current clinical equipoise and are essential to defining optimal first-line therapy in metastatic pRCC.

Keywords

Papillary renal cell carcinoma; Real-world evidence; Immune checkpoint inhibitors; Tyrosine kinase inhibitors; MET inhibitors

Trials in Progress Oral Presentations

16

LASER – a Phase 2 trial of 177Lu-PSMA-617 as Systemic Therapy for Renal Cell Carcinoma (NCT06964958)

Praful Ravi, Wanling Xie, Stephanie Berg, Michael Serzan, Bicky Thapa, Srinivas Viswanathan, Wenxin (Vincent) Xu, Bradley A. McGregor, Toni Choueri, Heather Jacene

Dana-Farber Cancer Institute

Background

There is an unmet need for therapeutic targets beyond immune checkpoint (IO), VEGF and HIF in-hibition in advanced clear cell renal cell carcinoma (ccRCC). PSMA (prostate-specific membrane an-tigen) is highly expressed on the cell surface of prostate cancer as well as the neovasculature of other tumors, including RCC. A high degree of PSMA expression has been noted with RNA-sequencing and immunohistochemistry (IHC) in ccRCC and a high rate of detection of ccRCC has been seen with use of PSMA-PET/CT, confirming the validity of PSMA as a therapeutic target. 177Lu-PSMA-617 (LuPSMA) is a beta-emitting PSMA-targeting radiopharmaceutical with proven efficacy in advanced prostate cancer. There is therefore a clear biologic and clinical rationale for evaluating LuPSMA in PSMA-positive advanced ccRCC.

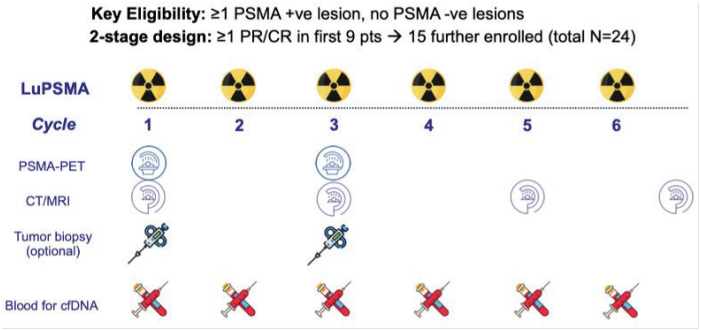
Methods

NCT06964958 is an investigator-initiated, single-arm, single-center phase 2 trial at Dana-Farber Cancer Institute. The primary objective is to evaluate the objective response rate (ORR) per RECIST 1.1 of LuPSMA in patients with PSMA-positive, advanced ccRCC. Key secondary objectives include safety, progression-free (PFS) and overall survival (OS). Exploratory objectives include imaging, blood and tissue-based biomarkers of response and resistance to therapy, with optional baseline and on-therapy biopsies to be performed in up to 10 patients. Correlative investigations will focus on evaluating SUV thresholds on PSMA-PET/CT associated with response, IHC for DNA damage repair markers in tissue, and spatial transcriptomic and single-nucleus RNA-seq (sNuc-seq) to characterize the inflammatory and immune milieu and understand the interplay between the immune system and response to LuPSMA. Key eligibility criteria include prior receipt of ≥1 IO and ≥1 VEGF-TKI, the presence of PSMA-positive disease (≥1 lesion with avidity >liver) and the absence of PSMA-negative measurable lesions. Eligible patients will receive 2 cycles of LuPSMA and undergo an interim PSMA-PET, with the option of receiving up to 4 further cycles if there is continued presence of PSMA-avid disease. Radiographic assessment by CT/MRI will occur every 12 weeks. The study will employ a Simon's optimal two-stage design, with the aim of detecting an ORR of 25% (similar to ORR of belzutifan in the post-IO/TKI setting). 9 patients will be enrolled in stage 1, and the study will proceed to stage 2 and enrol a further 15 patients (for a total of 24 patients overall) if ≥1 response is seen in stage 1. If ≥3 responses are seen among 24 evaluable patients, the treatment will be declared effective. The probability of concluding that the treatment is effective is 0.9 if the true rate is ≥25%, and ≤0.1 if the true rate is ≤5%. There is a 63% chance of stopping early with a true ORR of 5%. The trial is due to activate in June 2025.

Significance & Vision

LASER is one of the first trials of radiopharmaceutical therapy (RPT) in advanced ccRCC and evaluates a novel therapeutic target in this disease. Should promising activity be observed, this study would pave the way for a larger, randomized phase 2/3 study in the post-IO and post-TKI setting. Insights from this study will also inform future RPT trials evaluating other targets including CAIX. Furthermore, the planned imaging, blood and tissue correlatives will provide unique scientific in-sights into the mechanisms of response and resistance to LuPSMA in RCC, and potentially lead to identification of other therapeutic targets and inform future clinical and translational research evaluating RPT in RCC.

Trial Schema



Keywords

PSMA; radiopharmaceutical; Lu177; clear cell RCC

17

A Phase 1, multiple-dose study to evaluate the safety and tolerability of first-in-class XmAb819 (ENPP3 x CD3) in subjects with relapsed or refractory clear cell renal cell carcinoma (ccRCC) (NCT05433)

Chet Bohac[1], Sumanta Pal[2], Randy Sweis[3], Ritesh Kotecha[4], Karie Runcie[5], Mehmet Bilen[6], David Braun[7], Scott Tykodi[8], Christopher Holmes[9], Vithika Suri[1], Jitendra Kanodia[1], Engie Salama[1], Jacky Woo[1], Lingling Li[1], Yuanquan Yang[10], Robert Franklin[11], Joseph Maly[12], Claud Grigg[13], Shuchi Gulati[14], David J. VanderWeele[15], Benjamin Garmezy[16]

[1]Xencor, [2]City of Hope Comprehensive Cancer Center, [3]University of Chicago, [4]Memorial Sloan Kettering Cancer Center, [5]Columbia University, [6]Winship Cancer Institute at Emory University, [7]Yale New Haven Hospital, [8]Fred Hutchinson Cancer Center, [9]Duke University Medical Center, [10]The Ohio State University Wexner Medical Center, [11]University of Cincinnati Medical Center, [12]Norton Cancer Center, [13]Atrium Health, [14]University of California Davis Comprehensive Cancer Center, [15]Northwestern Memorial Hospital, [16]Sarah Cannon Research Institute

Background

Despite advances in the treatment of metastatic ccRCC, few patients are cured. Therapies exploiting novel targets are needed. Antigen screening identified ENPP3 (ectonucleotide pyrophosphatase/phosphodiesterase family member 3) as having consistent high expression in ccRCC and low expression in normal tissue. ENPP3 is a transmembrane ectoenzyme involved in hydrolysis of extra-cellular nucleotides. XmAb819 is a 2+1 bispecific antibody with high-avidity bivalent ENPP3 binding and mid-affinity monovalent CD3 binding. XmAb819 is engineered for preferential engagement and T-cell-mediated cytolysis of high ENPP3-expressing cancer cells.

Methods

This is a multicenter, open-label, dose-escalation/expansion study enrolling up to 190 participants with advanced ccRCC. The primary objective is safety and tolerability; the secondary objective is preliminary anti-tumor activity. Part A, dose escalation, establishes a priming dose, step-up dose(s), a cohort-limit dose, and the dosing schedule for both intravenous (IV) and subcutaneous (SC) administration. Part B, dose expansion, evaluates the safety and efficacy of the recommended dose established in Part A. All subjects will have disease progression on standard-of-care therapies. XmAb819 will be administered weekly; cohort-limit doses will be administered in 21-day cycles until disease progression or unacceptable toxicity. Adverse events are graded using CTCAE v5.0; CRS using ASTCT Consensus Grading (Lee, 2019). Efficacy is assessed per investigator using RECIST v1.1.

Enrollment and dose escalation continues in both the IV and SC cohorts.

Significance & Vision

XmAb819 is an investigational, novel bispecific T-cell engager engineered to bind and kill high ENPP3-expressing cells. The XmAb819-01 study is a trial designed to enroll patients with ccRCC, a solid tumor that overexpresses ENPP3. Initial evidence of anti-tumor activity in ccRCC has been observed, and tolerability supports continued dose escalation.

Trial Schema

The dosing period consists of priming, step-up, and target doses.

Keywords

Clear cell renal cell carcinoma, bispecific, t-cell engager

18

EXACT: A Randomized phase II trial of XL092 (Zanzalintinib) in combination with immunotherapy in patients who progress on Adjuvant therapy in Clear Cell RCC [NCT06863311]

Karie Runcie[1], Rana McKay[2], Eric A. Singer[3], Elshad Hasanov[3], Jennifer M. King[4], Melissa A. Reimers[5], Ian Okazaki[6], Alexander Wei[7], Mark N. Stein[7]

[1]Columbia University, [2]University of California, San Diego, [3]The Ohio State University Comprehensive Cancer Center, [4]Indiana University, [5]Washington University in St. Louis, [6]University of Minnesota, [7]Columbia University Medical Center

Background

The randomized phase III KEYNOTE-564 trial demonstrated that adjuvant pembrolizumab improves disease-free survival and overall survival compared to placebo in patients with clear cell renal cell carcinoma (ccRCC) at intermediate-high and high risk for recurrence after surgery with curative in-tent. At 2 years of follow-up about 20% of patients on KEYNOTE-564 had disease recurrence. Treatment options post adjuvant progression are not well established. Zanzalintinib (Zanza) is a next-generation anti-VEGFR multi-targeted tyrosine kinase inhibitor which has demonstrated safety and activity in ccRCC including treatment-refractory disease. Pre-clinical data shows that anti-PD-1 immune checkpoint inhibition is synergistic with Zanza. Nivolumab (nivo) is an anti-PD-1 immune checkpoint inhibitor that is well tolerated and approved in advanced ccRCC. We hypothesize that Zanza and Zanza + Nivo in combination are well tolerated and improve the overall response rate at 6 months in patients who have progressed on or after adjuvant pembrolizumab compared to the historical control of cabozantinib post- ICI.

Methods

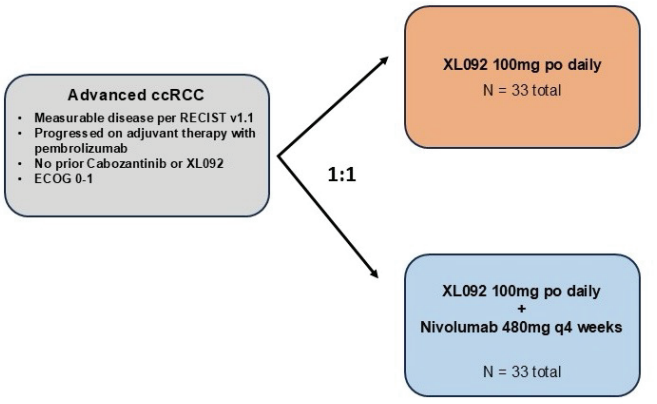
This is a multicenter open-label randomized phase II trial evaluating Zanza and Zanza plus Nivo both compared to the historical control, cabozantinib, in subjects who progress on or after adjuvant pembrolizumab. Eligible patients include those patients with measurable disease per RECIST 1.1 who progress on or after adjuvant pembrolizumab. 70 patients will be randomized 1:1 to receive either Zanza 100mg by mouth daily or Zanza 100mg by mouth daily in combination with Nivolumab 480mg intravenously every 4 weeks until disease progression. The primary endpoint is overall response rate at 6 months as per investigator assessed RECIST 1.1. Secondary endpoints include progression-free survival at 6 months, overall survival, duration of response and adverse events as per CTCAE v5. 10 patients will undergo paired baseline and on treatment biopsies to evaluate tissue based molecular predictors of response and resistance and serial ctDNA will be evaluated. For each arm, a single stage design will be used to test the null hypothesis that the population partial and complete response proportion (P) ≤ 0.330 versus the alternative that P ≥ 0.530 via Z test. To assure a minimum of 85% power for a one-sided 0.10 level of significance test, we need to recruit 33 pa-tients per arm. This trial is enrolling patients through the Hoosier Cancer Research Network. The study is activated at Columbia University. Sites pending activation include The Ohio State University, University of California, San Diego, University of Indiana, University of Minnesota, and Washington University in St. Louis.

Significance & Vision

Zanzalintinib is a multitargeted tyrosine kinase inhibitor which has demonstrated efficacy and tolerability in metastatic ccRCC. Treatment options for patients who progress on adjuvant pembrolizumab are ambiguous. The EXACT Trial seeks to determine if Zanzalitinib and Zanzalitinib plus Nivolumab are effective treatments in patients who progress on adjuvant pembrolizumab.

Trial Schema

This study is in collaboration with Exelixis Inc.



Primary endpoint: ORR

Secondary endpoints: PFS, OS, AE

Exploratory endpoints: % change in ctDNA, % change in intratumoral CD8+ T cells, CD4 T cells, Tregs and myeloid cells, radiomics and tumor kinetic analysis

Keywords

Clear cell RCC, renal cell carcinoma, tyrosine kinase inhibitors (TKIs)

19

A Phase 0 Pilot Study of Memory-like Natural Killer (NK) Cell Immune Therapy in Patients with Renal Cell Carcinoma or Urothelial Carcinoma (NCT06318871)

Wenxin (Vincent) Xu[1], Wanling Xie[1], Fuguo Liu[1], Grace Birch[1], Casey Welch[1], Maily Nguyen[1], Mila Stanojevic[1], Srinivas Viswanathan[1], Bradley A. McGregor[1], Jerome Ritz[1], David Braun[2], Sarah Nikiforow[1], Rizwan Romee[1], Toni Choueiri[1]

[1]*Dana-Farber Cancer Institute*, [2]*Yale New Haven Hospital*

Background

PD-1 based combination therapies improve survival in advanced renal cell carcinoma (RCC) and urothelial carcinoma (UC), but most patients still experience subsequent disease progression and death. Natural killer (NK) cells are immune effector lymphocytes specialized in the elimination of malignant cells and play an important role in the immune response against RCC and UC. However, prior efforts to develop NK cell-based therapies have been limited by the short half-life of NK cells (10-14 days). Cytokine induced memory-like (CIML) NK cells have prolonged survival, enhanced proliferation, and improved cytotoxicity and prior trials have demonstrated clinical activity in myeloid malignancies and head/neck cancer.

Methods

We are performing the first study of CIML NK cell therapy among patients with RCC and UC. Patients are eligible who have advanced RCC (including clear cell, chromophobe and translocation RCC) or UC and progression after ≥1 prior treatment regimens, including prior therapy with PD-1/PD-L1 inhibitors. Participants undergo apheresis for autologous NK cell collection followed by fludarabine and cyclophosphamide lymphodepleting chemotherapy. On day 0, patients receive CIML NK cells (which have undergone a 6-day maintenance culture) followed by subcutaneous IL-2 for up to 5 doses to promote CIML NK cell growth and expansion.

We plan to enroll 5-10 patients for this pilot study. The primary outcome is feasibility defined as the ability to collect cells, generate product, and administer CIML NK plus 6-day maintenance culture cells to patients. The feasibility endpoint will be met if 60% or more patients are successful per the feasibility criteria. Exploratory objectives will evaluate the safety and efficacy of this regimen.

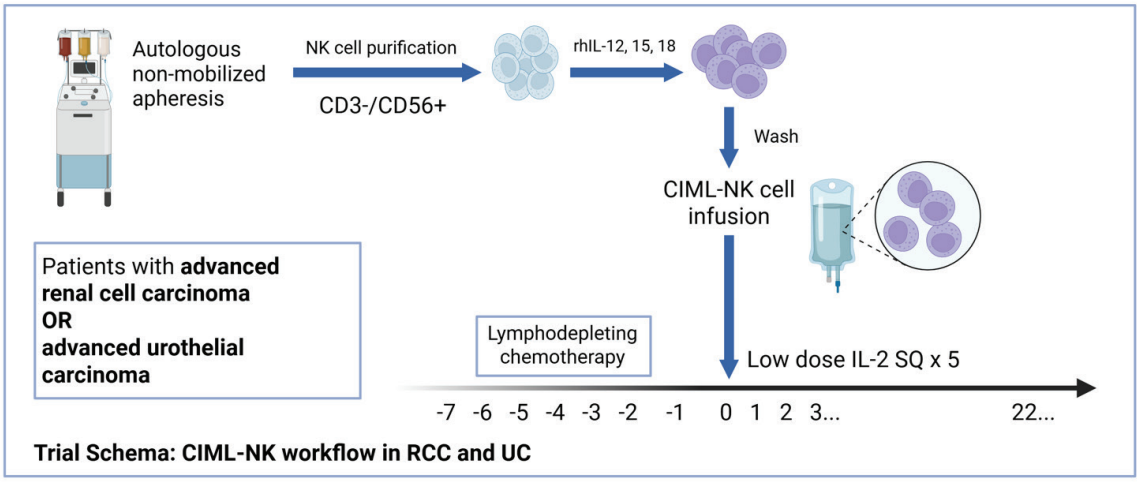
Significance & Vision

In this study, we are evaluating the feasibility of treating patients with autologous CIML NK cells. This is the first use of CIML NK cell-based therapy for RCC and UC. Correlative studies will evaluate the phenotype and function of CIML NK cells and determinants of treatment response. This data will inform the development of novel NK cell based therapies in RCC and UC, including NK chimeric antigen receptor strategies.

Keywords

Clinical trial, renal cell carcinoma, cell therapy, natural killer cells

Trial Schema



Trial Schema: CIML-NK workflow in RCC and UC

20

Phase II trial of ivonescimab in patients with advanced clear cell renal cell carcinoma previously treated with immune checkpoint blockade: IVORY Trial (NCT06940518)

Nazli Dizman, Rebecca S. Slack-Tidwell, Rahul A. Sheth, Omar Alhalabi, Matthew T. Campbell, Paul G. Corn, Sangeeta Goswami, Andrew Johns, Eric Jonasch, John K. Lin, Amishi Y. Shah, Jianbo Wang, Amado J. Zurita-Saavedra, Jianjun Gao, Nizar Tannir, Andrew W. Hahn, Pavlos Msaouel

MD Anderson Cancer Center

Background

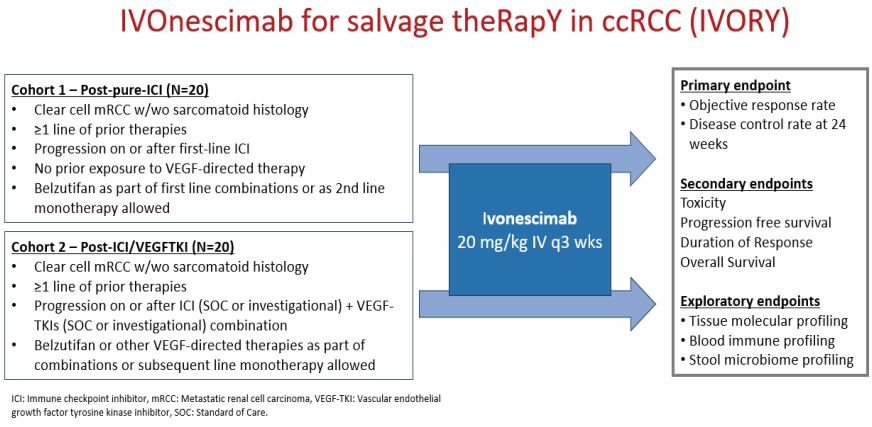
Immune checkpoint inhibitor (ICI)-based combinations, whether in the form of dual ICIs, or an ICI combined with a vascular endothelial growth factor tyrosine kinase inhibitor (VEGF-TKI), constitute the first-line treatment for metastatic clear cell renal cell carcinoma (mccRCC). However, in the subsequent-line setting, the addition of ICIs to VEGF-TKIs did not demonstrate superior activity compared to VEGF-TKI monotherapy in two phase III clinical trials (CONTACT-03 Pal et al. Lancet 2023, TiNivo-2 Choueiri et al. Lancet 2024). This highlights the urgent need for novel approaches to overcome ICI resistance in further-line settings. Ivonescimab is a novel first-in-class tetravalent bispecific antibody blocking PD1/PD-L1 and VEGF/VEGFR signaling, thereby simultaneously inhibit-ing both immune escape and angiogenesis in the tumor microenvironment, two canonical mechanisms of mccRCC pathogenesis. In treatment-naïve non-small cell lung cancer, ivonescimab has recently shown superior clinical activity over pembrolizumab (HARMONi-2 Xiong et al. Lancet 2025).

Ivonescimab may offer several advantages over the use of separate combination agents in mRCC: (1) enabling spatial proximity of concurrent PD-1 and VEGF inhibition within the tumor microenvironment, (2) providing integrated, synchronized inhibition of two key pathways potentially to address tumor heterogeneity, (3) avoiding pharmacokinetic variability and provide more predictable dosing and drug levels, improving efficacy and reducing the risk of suboptimal therapeutic exposure. Further, preclinical studies suggest that the cooperative inhibition of VEGF and PD-1, two key pathways implicated in mccRCC pathogenesis, may result in synergistic anti-tumor activity. Accordingly, we hypothesize that dual PD-1 and VEGF blockade via ivonescimab will restore treatment sensitivity in mccRCC following progression on prior VEGF and/or ICI therapies.

Methods

This is a phase II, single-arm, open-label, investigator-initiated study evaluating ivonescimab mono-therapy in patients with previously treated mccRCC. All participants must have received prior ICI therapy. Cohort 1 will enroll patients with no prior exposure to VEGF-directed agents, while Cohort 2 will enroll patients who had disease progression on a prior VEGF-directed therapy. Participants will receive the recommended phase II dose of Ivonescimab (20 mg/kg IV every 3 weeks) and continue treatment until disease progression or unacceptable toxicities. Figure 1 presents the study schema. Each cohort will enroll 20 patients and follow a Bayesian Optimal Phase 2 (BOP2) design, with simultaneous monitoring of two efficacy endpoints: objective response rate (ORR), defined as complete or partial response at any time, and disease control rate (DCR), defined as complete response, partial response or stable disease at 24 weeks, per RECIST 1.1. In cohort I, the null hypothesis is ORR= 10% or DCR= 30%, while the alternative hypothesis is ORR= 30% or DCR= 50%. The regimen will be deemed acceptable if more than 4 patients experience an objective response, or more than 9 patients experience disease control, providing 87% power with a 10% type I error

Trial Schema



ICI: Immune checkpoint inhibitor, mRCC: Metastatic renal cell carcinoma, VEGF-TKI: Vascular endothelial growth factor tyrosine kinase inhibitor, SOC: Standard of Care.

rate. In cohort II, the null hypothesis is ORR= 5% or DCR= 20% and the alternative hypothesis is ORR= 20% or DCR= 40%. The regimen will be considered acceptable if more than 2 patients experience an objective response, or more than 6 patients experience disease control, with 84% power and 10% type I error rate. Tissue, blood, and stool correlatives will be collected at baseline, during therapy and at the end of treatment to identify changes in specific immune-cell and gut microbiome subsets and elucidate the dynamic evolution of tumor and immune-cell compartments as well as their spatial relationships following ivonescimab.

Significance & Vision

This is the first clinical trial testing ivonescimab in RCC. Potential clinical activity signals and translational insights obtained will (1) shape the understanding of approaches to revert ICI-resistance and (2) open venues for further clinical testing of this agent in mccRCC. NCT: NCT06940518

Keywords

Kidney Cancer, Ivonescimab, Bispecific, PD-1, VEGF

21

Short TeRm Intensified Pembrolizumab (KEytruda) and Tivozanib for Hogh-Risk Renal Cell Carcinoma – STRIKE! (A033201) - NCT06661720

Bradley A. McGregor

Dana-Farber Cancer Institute

Background

Pembrolizumab (pembro) for one year following resection of localized high risk clear cell renal cell carcinoma (ccRCC) with a phase 3 trial resulted in improvement in relapse free survival and overall survival (Choueiri, NEJM 2024) However, 20% of patients still experience a relapse within 2 years with no biomarker yet identified to predict who will respond to or needs adjuvant therapy. Addition of a tyrosine kinase inhibitor (TKI) to immunotherapy (IO) is a standard of care in metastatic ccRCC but to date no studies have studied the addition of a TKI to IO in the adjuvant setting. Subsequently, STRIKE! Was developed to explore the benefit of 6 months of tivozanib (tivo) to pembro vs pembro alone in the adjuvant setting for resected high risk ccRCC.

Methods

Patients with a ECOG PS ≤2 and histologically confirmed diagnosis of RCC with clear cell component with or without sarcomatoid features who have undergone complete resection of the primary tumor with pathology revealing pT2 grade 4 disease or any grade ≥ T3 or TxN1 are eligible. In addition, patients who developed metastasis within a year of resection and underwent resection, definitive radiation or ablation of solid, isolated, soft tissue metastases (excluding brain and bone lesions) are eligible. Patients will be randomized 1:1 to pembro for 48 weeks with or without the addition of tivo 1.35 mg by mouth daily D1-21 q28D for 6 months. With no limit on dos holds or interruptions of tivo, dose reductions of tivo to 0.89 mg D1-21 q28D or tivo 0.89 mg every other day are allowed. No dose reductions of pembro are permitted. Following baseline imaging to confirm no disease, imaging is performed every 12 weeks for first year, every 16 weeks for 2nd year, every 24 weeks for third year and then annually. Primary endpoint will be disease free survival as assessed by investigator with key secondary endpoint of overall survival. The study will enroll 1040 patients to detect a minimum detectable hazard ratio of 0.67 (24 month DFS 84% in experimental arm) with 90% power. Quality of life analysis will compare global quality of life and fatigue between the two arms while imaging and specimens will be banked for future research.

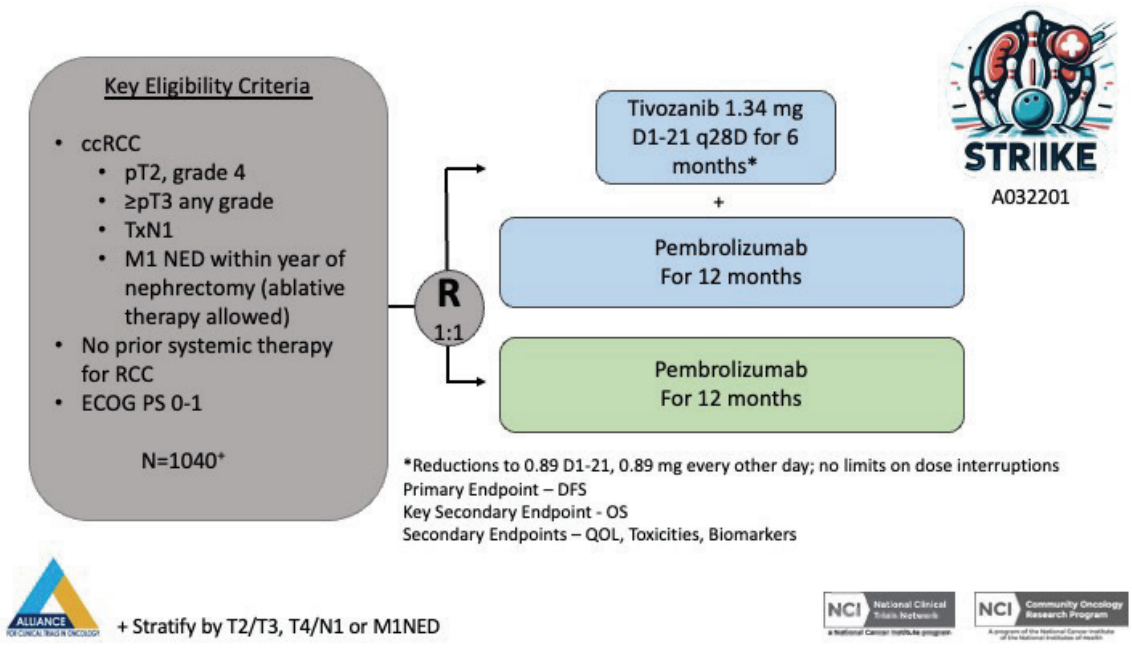
Significance & Vision

STRIKE! is the first trial and only trial to explore the role of adding a VEGF TKI to immunotherapy in the adjuvant setting for resected high risk ccRCC. Correlative analysis will be essential to develop-ment of biomarkers of minimal residual disease and response to therapy.

Keywords

Renal Cell carcinoma, Adjuvant therapy, TKI, Immunotherapy

Trial Schema



Posters

22

Final results of the phase 3 COSMIC-313 study comparing first-line cabozantinib plus nivolumab and ipilimumab with nivolumab plus ipilimumab in patients with advanced renal-cell carcinoma

Laurence Albiges[1], Robert Motzer[2], Sergio Arnoldo Trevino Aguirre[3], Ravindran Kanesvaran[4], Piotr Centkowski[5], Melissa A. Reimers[6], Juan Pablo Sade[7], Damien Pouessel[8], Elisa Biscaldi[9], Emilio Esteban[10], Jose Angel Arranz Arija[11], Scott Tykodi[12], Haijun Ma[13], Lei Zhou[13], Maximiliano van Kooten Losio[14], Andrew Simmons[13], David Braun[15], Toni Choueiri[16], Thomas Powles[17]

[1]Institut Gustave Roussy, [2]Memorial Sloan Kettering Cancer Center, [3]I Can Oncology Center SA De CV, [4]National Cancer Centre Singapore, [5]KO-MED Centra Kliniczne, [6]Washington University in St. Louis, [7]Instituto Alexander Fleming, [8]IUCT Oncopole – Oncopole Claudius Régaud, [9]Istituti Clinici Scientifici Maugeri–IRCCS Pavia, [10]Central Hospital Universitario Central de Asturias, [11]Hospital General Universitario Gregorio Maranon, [12]Fred Hutchinson Cancer Center, [13]Exelixis, Inc., [14]Bristol Myers Squibb, Boudry, Neuchâtel, Switzerland, [15]Yale New Haven Hospital, [16]Dana-Farber Cancer Institute, [17]Barts Cancer Institute, Queen Mary University of London, Barts Health NHS Trust

Background

The randomized, double-blind, phase 3 COSMIC-313 study (ClinicalTrials.gov: NCT03937219) met its primary endpoint, demonstrating significantly improved progression-free survival (PFS) with the combination of cabozantinib plus nivolumab and ipilimumab versus placebo plus nivolumab and ipilimumab in patients with previously untreated advanced renal-cell carcinoma (aRCC) who had intermediate or poor prognostic risk according to International Metastatic RCC Database Consortium (IMDC) categories (Choueiri et al. N Engl J Med. 2023). Here, the secondary endpoint of overall survival (OS) is presented, as well as updated efficacy and safety data and the results of exploratory biomarker analyses.

Methods

In COSMIC-313, patients with previously untreated IMDC intermediate- or poor-risk aRCC were randomized to receive oral cabozantinib 40 mg once daily or placebo. Both groups received nivolumab (3 mg/kg) plus ipilimumab (1 mg/kg) intravenously every 3 weeks for four cycles, followed by nivolumab therapy (480 mg every 4 weeks) for up to 2 years. The primary endpoint (previously reported) was PFS by blinded independent central review per Response Evaluation Criteria in Solid Tumors version 1.1 in the first 550 randomized patients. The secondary endpoint was OS in all randomized patients. Immune subsets (deconvoluted from RNA-sequencing data) associated with improved OS with cabozantinib plus nivolumab and ipilimumab versus placebo plus nivolumab and ipilimumab were identified using a random forest model.

Results

Overall, 855 patients were randomized to cabozantinib plus nivolumab and ipilimumab (n=428) or placebo plus nivolumab and ipilimumab (n=427); of these, 75% had intermediate-risk and 25% had poor-risk disease per IMDC. With a median follow-up of 45.0 months, the improvement in PFS with

Table. Efficacy outcomes with first-line cabozantinib plus nivolumab and ipilimumab versus placebo plus nivolumab and ipilimumab

	Cabozantinib plus nivolumab and ipilimumab (n=428)	Placebo plus nivolumab and ipilimumab (n=427)
Median OS, months (95% CI)	41.9 (34.8–47.9)	42.0 (34.9–53.1)
HR (95% CI); *P*-value	1.02 (0.85–1.23); *P*=0.8366	
ORR, % (95% CI)	46 (41–51)	37 (32–41)
Complete response, %	4	3
Partial response, %	42	33
Stable disease, %	40	36
Progressive disease, %	8	20

CI, confidence interval; HR, hazard ratio; ORR, objective response rate; OS, overall survival.

cabozantinib plus nivolumab and ipilimumab was maintained; median PFS was 16.6 months (95% confidence interval [CI], 14.0–22.6) with cabozantinib plus nivolumab and ipilimumab and 11.2 months (95% CI, 9.3–14.0) with placebo plus nivolumab and ipilimumab (hazard ratio [HR], 0.82 [95% CI, 0.69–0.98]). There was no significant difference in median OS between cabozantinib plus nivolumab and ipilimumab and placebo plus nivolumab and ipilimumab in the intention-to-treat population (Table) or by IMDC risk group. The objective response rate (ORR) was higher with cabozantinib plus nivolumab and ipilimumab, and fewer patients had progressive disease as a best response (Table). Grade 3/4 treatment-emergent adverse events (TEAEs) were reported in 81% of patients treated with cabozantinib plus nivolumab and ipilimumab and 62% of those treated with placebo plus nivolumab and ipilimumab. The most common grade 3/4 TEAEs were increased alanine aminotransferase (27% and 6%, respectively) and increased aspartate aminotransferase (20% and 5%, respectively). Grade 5 treatment-related adverse events occurred in 1% of patients in each group. Exploratory biomarker analyses showed no significant differences in OS according to baseline c-Met or programmed death-ligand 1 levels. A higher abundance of M2 macrophages was observed in patients with poor-risk disease per IMDC, a high baseline sum of target lesions, or visceral metastasis. In patients with higher levels of M2 macrophages, treatment with cabozantinib plus nivolumab and ipilimumab was associated with improved OS versus placebo plus nivolumab and ipilimumab (HR, 0.51 [95% CI, 0.31–0.86]). Further analyses of angiogenic and immune signatures are ongoing.

Conclusions

For patients with intermediate- or poor-risk aRCC, first-line treatment with cabozantinib plus nivolumab and ipilimumab continued to demonstrate PFS and ORR benefits over placebo plus nivolumab and ipilimumab. OS was comparable between the two arms, and there were no new safety signals. Patients with tumors that had high levels of M2 macrophages had improved OS with cabozantinib plus nivolumab and ipilimumab versus placebo plus nivolumab and ipilimumab.

Keywords

Cabozantinib, ipilimumab, nivolumab, phase 3, renal cell carcinoma

23

Molecular Residual Disease (MRD) Guided Adjuvant ThErapy in Renal Cell Carcinoma (RCC) -MRD GATE RCC

Arnab Basu[1], Fady Sidhom[1], Caleb Hwang[2], Nonna Shakhnazaryan[2], Vishruti Pandya[1], James Ferguson[1], Sejong Bae[1], Soroush Rais-Bahrami[1], Deepak Kilari[3], Arpita Desai[2], Mollie Deshazo[1], Joelle Hamilton[1], Charles Peyton[1]

[1]University of Alabama at Birmingham, O'Neal Comprehensive Cancer Center, [2]University of California, San Francisco, Helen Diller Family Comprehensive Cancer Center, [3]Medical College of Wisconsin Cancer Center

Background

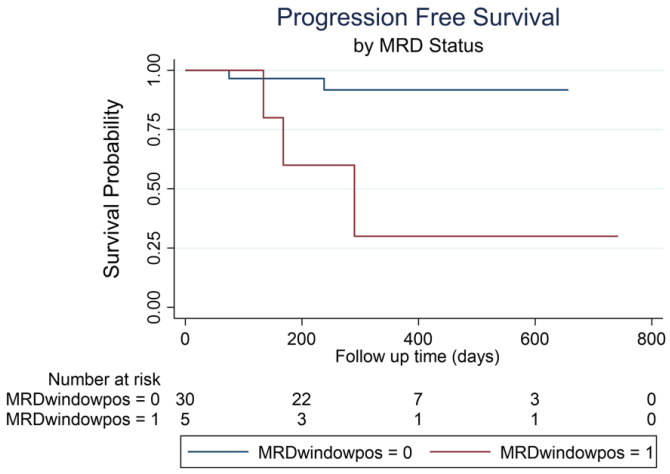
Ultrasensitive ctDNA assays are emerging as a prognostic marker in various tumor types including in renal cell carcinoma (RCC). Pembrolizumab is currently approved for intermediate and high-risk, surgically resected RCC patients based on a survival benefit of approximately 5% at 48 months. There are no currently established biomarkers for treatment selection. We examine a tumor informed MRD-guided approach to the assignment of adjuvant immunotherapy in an ambispective cohort.

Methods

The study was conducted with Institutional Review Board (IRB) approval and obtained informed consent from all prospective participants. Key inclusion criteria included age ≥18 years, clear cell RCC of intermediate to high-risk of recurrence, no prior systemic therapy, Eastern Cooperative Oncology Group (ECOG) performance status 0–2, and availability of tumor sample for development of a tumor informed ctDNA MRD probe. M1 NED (No Evidence of Disease) was an exclusion criteria. In the prospective cohort, patients were assigned to receive pembrolizumab (400mg q6 weeks or 200mg q3 weeks) by intravenous infusion only if found to be ctDNA positive within a MRD surveillance window (<120 days from surgery). A minimum of one MRD test was required but more were allowed. In the retrospective cohort, only patients meeting prospective inclusion criteria and treated concordant to MRD with pembrolizumab were included. Data was analyzed for a period of 1/12/2023 - 2/23/2025. The primary and secondary endpoints were 1-year DFS and OS with an MRD guided approach respectively.

Results

35 patients have been accrued (7 prospective, 28 retrospective), with a median follow up of 11 months. All patients were evaluable for radiologic progression. A median of 3 MRD tests were performed within the 12-week



post-surgical eligibility window (range 1–4). 5 patients were MRD positive (14.28%), of which 3 have had recurred at the time of data cutoff. Among 30 patients who were MRD negative 2 patients progressed at followup (NPV = 93%). MRD guided therapy was associated with a 1-year DFS rate of 85.7% (95% CI: 69.7% – 93.4%) and MRD positivity was associated strongly with relapse risk HR 9.48 95%CI (1.58-57.00) , p = 0.014 [Fig 1]. The median disease free survival in patients who tested positive for MRD was 5.6 months (95% CI 4.5 – 9.7 months). Median DFS was not reached in MRD negative patients. OS follow-up was not mature as no deaths were recorded in the study period.

Conclusions

This analysis of an intermediate-high risk RCC population treated based on serial postoperative MRD monitoring suggests that intensive MRD monitoring may be a valuable approach to better tailor adjuvant therapy for intermediate to high-risk RCC patients

Keywords

MRD, RCC, Adjuvant Therapy

24

TGF-Beta alters CD8+ T cell phenotype and drives resistance to immune checkpoint inhibitors (ICI) in renal cell carcinoma (RCC)

Rishabh Rout[1], Soki Kashima[2], Miya Hugaboom[2], Zhaochen Ye[2], Nicholas Schindler[2], Anasuya Dighe[2], Maxine Sun[3], Gwo-Shu Mary Lee[3], Wenxin (Vincent) Xu[3], Sabina Signoretti[4], Bradley A. McGregor[3], Rana McKay[5], Toni Choueri[3], David Braun[6]

[1]Yale University, [2]Yale Cancer Center, Yale School of Medicine, [3]Dana-Farber Cancer Institute, [4]Brigham and Women's Hospital, [5]University of California, San Diego, [6]Yale New Haven Hospital

Background

The most successful treatments for advanced RCC have been ICI-based combination therapies. However, the vast majority of patients with advanced RCC ultimately have disease progression despite ICI treatment, thus necessitating further analysis of the immunological differences in patients that respond to or are resistant to ICI therapy. CD8+ T cells display tremendous phenotypic diversity and play a critical role in anti-tumor immunity. However, it is unclear what drives different CD8+ T cell phenotypes in the RCC tumor microenvironment (TME), and how individual phenotypes impact ICI response and resistance.

Methods

70 tumor samples from 63 RCC patients were collected, either before (n = 48) or after (n = 22) therapies (VEGFi, n = 9; ICI monotherapy, n = 20; ICI + ICI, n = 17; ICI + VEGFi, n = 9; others, n = 15). 11 samples were also collected from patients without tumors. RCC variants included 59 clear cell and 11 non-clear cell samples. Of these samples, 18 were labeled as clinical benefit (CB, partial or complete response as the best response) and 11 as no-clinical benefit (NCB, progressive disease as the best response). Single-cell RNA sequencing (10x Genomics) was performed on these samples in order to generate a transcriptome of the RCC tumor microenvironment (TME). Graph-based clustering was performed in order to identify cell type populations, which were then annotated using known lineage genes. Non-negative matrix factorization (NMF) was used to identify gene programs within the exhausted CD8+ T cell (Tex) population. The NicheNet algorithm was utilized to predict ligand-target interactions between macrophage cells and the Tex population.

Results

Within the CD8+ T cell population, Tex cells were identified through elevated expression levels of TOX, PDCD1 (PD-1), and HAVCR2 (TIM-3). NMF generated 4 gene programs within Tex cells, which expressed markers relating to immediate early genes, exhaustion/activation, tissue residency, and stress response respectively. The NMF program corresponding to tissue residency within Tex cells was associated with resistance to ICI-based therapy ($p = 0.05$); the stress program was increased in ICI response ($p < 0.002$). NicheNet identified TGF-beta (TGFB1), produced by macrophages in non-responding tumors, as the ligand with the highest regulatory potential that generated the "resistant" tissue residency program in Tex cells. It specifically identified CD69 and IL7R as notable downstream genes, which were shown to be associated with NCB through differential gene expression ($p < 0.001$). Notably, the expression of the TGF-beta receptor (TGFBR2) was significantly higher ($p = 0.01$) in Tex cells from nonresponsive tumors. To further explore the effect of TGF-beta on the tissue resident program, we sorted naïve CD8 T cells from healthy donor peripheral blood mononuclear cells, and cultured them with stimulation under hypoxia (1% O2) or normoxia, and with or without TGFb. CD69/CD103-double positive tissue-resident-like T cells were found to be significantly higher with TGFb under hypoxia ($p = 0.02$). Further, in hypoxic conditions (mimicking the RCC TME), TGF-beta also led to an increase in PD-1 expression on CD8+ T cells ($p = 0.012$).

Conclusions

Through single-cell RNA-seq analysis, we identify an ICI-resistance circuit whereby tumor-associated macrophages produce TGF-beta, which then leads to a tissue residency gene program in Tex cells associated with non-response to immunotherapy. Experimental validation studies demonstrated that TGF-beta and hypoxia are sufficient for the induction of a tissue residency program and PD-1 expression on CD8+ T cells. Overall, this study provides a framework for using scRNA-seq to identify mechanisms of ICI resistance in RCC, and nominates the TGF-beta axis as a potentially targetable pathway to improve CD8 T cell-mediated anti-tumor immunity.

Keywords

Renal cell carcinoma, CD8+ T cells, Immune checkpoint inhibitors

25

Determining the impact of HIF2α inhibition on T cell function in clear cell renal cell carcinoma

Katrine Madsen[1], Hanna Soulati[1], Vivien Mortiz[1], David Braun[2]

[1]Yale Cancer Center, Yale School of Medicine, [2]Yale New Haven Hospital

Background

Immune checkpoint blockade, which is standard-of-care therapy in the high-risk adjuvant and first-line metastatic-clear cell renal cell carcinoma (ccRCC) setting, relies on re-invigorating T cells for anti-tumor immunity. Belzutifan, a HIF2α inhibitor, was recently approved as a treatment for refractory, sporadic advanced RCC, and is under investigation in combination with pembrolizumab in the adjuvant (LITESPARK-022) and first-line metastatic (LITESPARK-012) setting. While preclinical murine studies suggest that HIF signaling enhances $CD8^+$ T cell cytotoxicity, the impact of pharmacologic HIF2α inhibition on human T cell function remains unknown. We aimed to determine how HIF2α inhibition affects human T cell effector function (proliferation and cytokine production) under hypoxic conditions mimicking the RCC tumor microenvironment.

Methods

T cells were isolated from fresh human ccRCC tumors (i.e. tumor-infiltrating lymphocytes) or from healthy donor peripheral blood mononuclear cells (PBMCs) and stimulated with anti-CD3/CD28 beads for 48 hours under normoxic (21% O_2) or hypoxic (1% O_2) conditions. HIF2α knockout (KO) T cells were generated using CRISPR-Cas9 electroporation. RT-qPCR and bulk RNA sequencing were used for transcriptomic analysis. For functional assays, T cells were treated with DMSO (vehicle), tacrolimus (control for effective inhibition of T cell function), or HIF2α inhibitors (belzutifan or PT2399). Cytokine production (IFNγ, IL-2, TNFα) was measured via intracellular flow cytometry, and proliferation was assessed using a flow cytometry-based dye dilution assay (CellTrace Violet).

Results

HIF2α mRNA expression increased ~70-fold in T cells upon stimulation under hypoxic conditions. Differential gene expression analysis of bulk RNA sequencing revealed that IL-2 and IFNγ were among the most significantly downregulated genes in HIF2α knockout T cells, with $\log_2$ fold changes of −4.08 and −2.13, and adjusted p-values of 3.1×10^{-11} and 5.5×10^{-20}, respectively. Despite these transcriptional changes,

pharmacologic treatment with belzutifan or PT2399 did not significantly alter cytokine production at the protein level in CD8⁺ T cells from either healthy donor PBMCs or ccRCC tumor-infiltrating lymphocytes. Similarly, proliferation assays revealed no significant difference in division index upon treatment with belzutifan or PT2399 compared to DMSO control. Of note, hypoxia alone reduced CD8⁺ T cell proliferation ($p = 0.0048$) and enhanced CD4⁺ T cell proliferation ($p = 0.0034$) compared to normoxia, but HIF2α inhibition did not modulate these effects.

Conclusions

Although HIF2α is strongly upregulated under hypoxia and its genetic deletion reduces cytokine gene expression, short-term pharmacologic inhibition does not impair effector cytokine production at the protein level or alter proliferation of human CD8⁺ T cells in vitro. In the settings examined, HIF2α inhibition did not impair T cell function, suggesting that combination with immune checkpoint inhibitors remains a viable therapeutic strategy pending results of ongoing clinical studies. Ongoing laboratory-based assessment will assess the impact of prolonged HIF2α inhibition on T cell phenotype, evaluate its effects on direct cytotoxicity using antigen-specific RCC killing assays, and examine potential synergy with anti–PD-1 therapy.

Keywords

HIF2α, Belzutifan, clear cell renal cell carcinoma, T cell function

26

Subgroup analysis of the efficacy and safety of cabozantinib ± atezolizumab in patients from CONTACT-03 who received first-line treatment with immuno-oncology–based combinations

Bradley A. McGregor[1], Cristina Suarez[2], Toni Choueri[1], Laurence Albiges[3], Martin Voss[4], Omara Khan[5], Denise Williamson[6], Jose Ricardo Perez[6], Tasha Hall[6], Sumanta Pal[7]

[1]Dana-Farber Cancer Institute, [2]Vall d´Hebron Institute of Oncology (VHIO), Hospital Universitari Vall d´Hebron, [3]Institut Gustave Roussy, [4]Memorial Sloan Kettering Cancer Center, [5]Roche Products Ltd., [6]Exelixis, Inc., [7]City of Hope Comprehensive Cancer Center

Background

Cabozantinib, a tyrosine kinase inhibitor (TKI) that targets multiple kinases, including vascular endothelial growth factor receptor, is a preferred treatment option for patients with previously treated advanced renal cell carcinoma (RCC); however, its effectiveness after treatment with first-line immuno-oncology (IO)-based combinations is not fully understood. The efficacy and safety of second-line cabozantinib, with or without atezolizumab, were evaluated in the multicenter, randomized, phase 3 CONTACT-03 study (Pal et al., Lancet 2023; ClinicalTrials.gov: NCT04338269). Here, we report the results of a post hoc analysis of patients from CONTACT-03 who received contemporary IO–IO or IO–TKI combination regimens in the first-line setting.

Methods

In CONTACT-03, adults with metastatic RCC and disease progression on or after IO-based regimens were randomized to oral cabozantinib 60 mg once daily alone or with atezolizumab 1200 mg intravenously every 3 weeks. The current analysis evaluated progression-free survival (PFS) by blinded independent central review (BICR), overall survival (OS), objective response rate (ORR), duration of response (DOR), and safety in the subgroup of patients who received first-line standard-of-care IO–IO (ipilimumab–nivolumab) or IO–TKI (avelumab–axitinib, pembrolizumab–axitinib, or pembrolizumab–lenvatinib) combinations prior to enrolling in CONTACT-03.

Results

Of 522 patients enrolled in CONTACT-03, 107 and 129 in the cabozantinib and cabozantinib plus atezolizumab arms, respectively, received prior treatment with first-line IO–IO or IO–TKI combinations. Efficacy outcomes were comparable between treatments. For cabozantinib and cabozantinib plus atezolizumab, respectively, median PFS by BICR was 10.4 months (95% confidence interval [CI], 7.95–12.45) and 10.2 months (95% CI, 8.34–10.64), and median OS was not estimable (NE; 95% CI, 18.30–NE) and 24.3 months (95% CI, 20.24–NE). The ORR was 36% with cabozantinib and 37% with cabozantinib plus atezolizumab (all partial responses); 50% and 52% of patients had a best response of stable disease, and 10% and 5% had progressive disease, respectively. The median DOR was 15.1 months (95% CI, 10.28–NE) with cabozantinib and 10.5 months (95% CI, 7.95–NE) with cabozantinib plus atezolizumab. Grade 3/4 treatment-related adverse events (TRAEs) were reported in 48% of patients treated with cabozantinib and in 58% of those treated with cabozantinib plus atezolizumab; serious TRAEs were reported in 13% and 25% of patients, respectively. Dose modifications due to adverse events were reported in 87% of patients treated with cabozantinib and in 92% of those treated with cabozantinib plus atezolizumab; discontinuation of treatment due to adverse events occurred in 5% and 17% of patients, respectively.

Conclusions

From this post hoc subgroup analysis of CONTACT-03 can help inform treatment decisions for patients with disease progression on first-line IO-containing combinations. The data suggest that second-line cabozantinib is effective in patients with advanced RCC previously treated with contemporary first-line IO–IO or IO–TKI regimens. Safety outcomes were consistent with the overall study population.

Keywords

Cabozantinib, atezolizumab, immuno-oncology, phase 3, renal cell carcinoma

27

Characterization of aberrant alternative splicing landscape in patients with metastatic renal cell carcinoma

Benjamin Mercier[1], Ameish Govindarajan[2], Nathaniel Hansen[3], Sara Byron[3], Apurva Hegde[3], Kristin Leskoske[3], Neal Chawla[1], Luis Meza[4], Zeynep Zengin[4], Regina Barragan-Carrillo[5], Hedyeh Ebrahimi[1], Daniela Castro[1], Salvador Jaime-Casas[1], Miguel Zugman[1], Nazli Dizman[6], JoAnn Hsu[1], Alexander Chehrazi-Raffle[1], Abhishek Tripathi[1], Nicholas Salgia[7], Sumanta Pal[1], Patrick Pirrotte[8]

[1]City of Hope Comprehensive Cancer Center, [2]Memorial Sloan Kettering Cancer Center, [3]The Translational Genomics Research Institute (TGen), [4]Yale School of Medicine, [5]National Cancer Institute of Mexico, [6]Department of Medical Oncology, MD Anderson Cancer Center, [7]Department of Immunology, Roswell Park Comprehensive Cancer Center, [8]The Translational Genomics Research Institute (TGen)

Background

Errors in alternative splicing (AS) events are recognized as contributors to the tumorigenesis and metastasis of various cancer types. However, the role of aberrant AS events in metastatic renal cell carcinoma (mRCC) remains largely unexplored. We aimed to identify aberrant AS events associated with clinical benefits from immune checkpoint inhibitors (ICIs) and targeted therapies (TTs) in mRCC.

Methods

We conducted a retrospective analysis on 101 patients with mRCC who received systemic therapy and underwent RNA sequencing with sufficient output quality. Patients were categorized into two cohorts based on whether they received ICIs or TTs. Patients were then further subcategorized as responders or non-responders to systemic therapy based on RECIST v1.1 criteria. Differential gene expression and splicing analyses were performed between responders and non-responders for each cohort. Paired-end bulk RNA sequencing, utilized in the analyses of splicing events, was performed as part of the OncoExTra clinical assay. Novel AS events were analyzed for their potential to generate peptide neoantigens through MHC class I binding predictions.

Results

Outlier splicing analysis identified 10 aberrant AS events specific to mRCC. Alternative splicing analysis revealed 409 differentially spliced events between responders and non-responders in the ICI cohort and 231 in the TT cohort, with intron retention enriched as the predominant motif of aberrant AS in responders relative to non-responders. Seven unique AS events were enriched in responders, including PTPN6, ACTN1, and SUN2. Predictive neoantigen analysis identified high MHC class I binding potential in peptides from AS events in IFFO1, ZNF692, and SUN2. A novel splice burden gene set was developed from differentially expressed genes in novel splice burden-high samples. Within both ICI and TT cohorts, this splice burden-high gene set was enriched in responders relative to non-responders. The presence of high splice burden was linked to an immunogenic tumor microenvironment, characterized by enriched antigen processing and adaptive immune responses. Nearly 50 adaptive immune cell pathways were enriched in splice burden-high patients, including CD22-mediated BCR regulation, immunoglobulin production, and humoral immune response.

Conclusions

This study provides a comprehensive analysis of AS events in mRCC, highlighting enrichment of intron retention as potential transcriptomic biomarkers for treatment response. Numerous adaptive immune gene pathways were enriched in mRCC patients with high splice burden, particularly humoral immune responses. Aberrant AS-derived neoantigens may serve as potential targets for adoptive cell therapy strategies.

Keywords

Immunotherapy, alternative splicing, intron retention, neoantigen, biomarker

28

Microbial metabolic pathways to abrogate immunotherapy toxicity and promote anti-tumor response in metastatic renal cell cancer.

Shahla Bari[1], Alicia Darwin[2], Humaira Sarfraz[3], Tarundeep Singh[1], Noha Muzaffar[1], Jameel Muzaffar[1]

[1]Duke University, [2]Stanford University, [3]University of Alabama at Birmingham

Background

Metastatic RCC has a poor prognosis. Despite improvement in treatment outcomes with ICB and targeted therapy, many patients fail to respond to first line therapy and immune mediated adverse events(irAE) remains a major challenge, often leading to treatment discontinuation. Therefore, mitigating irAE without compromising antitumor immunity is a critical unmet need. Tryptophan microbial metabolic pathway is known to play a major role in immune homeostasis through its action on Aryl hydrocarbon receptor (AhR) balancing immune suppresser with immune effector responses. We hypothesize that microbial metabolism of tryptophan to indole metabolites may play a role in ICB resistance as well in irAE , identification of which may help us predict patients most likely to respond , without life threatening toxicity.

Methods

We prospectively collected paired stool and blood samples of treatment naïve metastatic RCC patients, treated with ICB +/- Tyrosine kinase inhibitors (TKI) at treatment initiation and at time of first response assessment (12+/-3 weeks). We evaluated stool metagenomics and untargeted stool and plasma metabolomics among responders (R) and non-responders (NR). We focused on kynurenine/tryptophan and indoles/tryptophan ratio to evaluate differential host and microbial metabolism of tryptophan. A responder was classified as progression free survival (PFS) greater than 6 months while patients with grade 3 or higher irAE was classified as serious IrAE .

Results

Among 120 patients accrued, 49 were treated with combination ICB, while 71 patients were treated with ICB + TKI. Median follow up was 27 months. 28 patients (23%) had a Grade 3 or higher irAE. 3 patients died from complications attributable to irAE. The median duration to development of any irAE was 3.5 months.

Using negative binomial regression model evaluating baseline relative abundance of microbial tryptophan metabolites that were associated both with response as well as serious irAE, we noted significant higher abundance of Indole acetic acid (IAA), indole acetonitrile(ACN), indole acetyl phenylalanine (IAAP)and IAA/kynurenine (Kyn) and lower abundance of tryptophol, indole 3 pyruvic (IPA), (coefficient of 6.4, 1.8, 7.15, 4.6 , 0.04, 0.46, with adj p value < 0.05) with serious irAE as well as ICB resistance (Coefficient-5.42, 1.83, 6.15, 4.05, 0.03, 0.4, $p < 0.05$).

Conclusions

This is one of the first studies evaluating microbial metabolic pathways that may play a role in predicting patients who are more likely to respond with lower likelihood of serious irAE in RCC, thus helping to identify strategies to decouple tumor immunity from autoimmunity to improve ICB outcomes. Further the results can be extrapolated to many other solid tumor treated with immunotherapy, as tryptophan metabolism plays a immune homeostatic role across cancers.

Keywords

Immunotherapy toxicity, Response, Microbial metabolites

29

An artificial intelligence model to predict somatic mutations from histopathology in metastatic renal cell carcinoma

Regina Barragan-Carrillo[1], Mohsen Nabian[2], Chi Wah Wong[2], Miguel Zugman[2], Salvador Jaime-Casas[2], Hedyeh Ebrahimi[2], Sumanta Pal[2], Evita Sadimin[2]

[1]National Cancer Institute Mexico, [2]City of Hope Comprehensive Cancer Center

Background

Metastatic renal cell carcinoma (mRCC) is a molecularly heterogeneous disease commonly driven by somatic mutations in genes such as VHL, PBRM1, and BAP1. Although next-generation sequencing (NGS) is the gold standard for identifying such mutations, it remains costly and logistically challenging. Given that genetic alterations often lead to morphological changes, we hypothesized that an artificial intelligence (AI) model applied to hematoxylin and eosin (H&E)-stained whole-slide images (WSIs) could predict underlying somatic mutations.

Methods

We identified consecutive patients with mRCC who had undergone clinical NGS and had available H&E-stained histopathology slides. Patients with somatic alterations in at

least one target gene were annotated. WSIs were tiled into non-overlapping 256×256-pixel patches. Background tiles were excluded based on brightness. Across 160 total WSIs, 3 slides had no valid tissue tiles and were excluded. The final dataset included 157 slides with usable content. From 69,672 tile attempts, 28,924 tiles (41.5%) passed quality filters and were used for model development. Two modeling pipelines were implemented: (1) slide-level, aggregating global features from WSIs, and (2) tile-level, embedding and classifying each tile with prediction aggregation at the slide level. Embeddings were generated using DINOv2 and the GigaPath foundation model. To evaluate model performance, we used receiver operating characteristic (ROC) curves and computed the area under the curve (AUC) for both slide-level and tile-level pipelines. ROC analysis was applied at both the tile level and the patient-aggregated level. Principal component analysis (PCA) was used for embedding visualization. Violin plots summarized patient-level AUCs across genes.

Results

A total of 157 WSIs (one per patient) were analyzed. The cohort included 83 VHL with pathogenic variants (PV) (52.9%) and 74 VHL-wild type (47.1%), along with PVs in: PBRM1 (48/157, 30.6%), BAP1 (9/157, 5.7%), PTEN (8/157, 5.1%), TSC1 (7/157, 4.5%), KDM5C (14/157, 8.9%), SETD2 (27/157, 17.2%), MTOR (8/157, 5.1%), TERT (19/157, 12.1%), and NF2 (2/157, 1.3%). Slide-level modeling demonstrated limited performance in mutation prediction. However, tile-level modeling substantially improved performance. The ROC curve for tile-level VHL prediction achieved AUC = 0.7206. Other tile-based AUCs included PBRM1 (0.76), PTEN (0.80), BAP1 (0.69), TSC1 (0.70), and NF2 (0.62), while lower performance persisted for MTOR (0.25), TERT (0.46), and KDM5C (0.47). PCA of tile embeddings revealed partial clustering by mutation status, and heatmaps localized high-probability regions consistent with expected histologic features.

Conclusions

Tile-level AI modeling enables accurate, interpretable prediction of somatic mutations in mRCC using H&E-stained WSIs.This approach may offer a scalable and accessible tool for expanding molecular profiling in settings without widespread access to NGS.

Keywords

Artificial Intelligence

30

Meta-analysis of single-cell RNA sequencing of tumor-infiltrating T-cells in clear cell renal cell carcinoma reveals distinct phenotypes and prediction markers of expanded T-cell clonotypes

Yuexin Xu, Chris Miller, Scott Tykodi, Edus Warren

Fred Hutchinson Cancer Center

Background

The recent clinical success of tumor-infiltrating lymphocyte (TIL) therapy in immune checkpoint inhibitor-refractory melanoma has renewed interest in applying this approach to other malignancies. Renal cell carcinoma (RCC) is characterized by prominent $CD8^+$ T-cell infiltration and elevated expression of cytolytic genes, suggesting the presence of tumor-reactive T-cells that could be harnessed for personalized cell therapy. TIL products are polyclonal and may recognize a diverse repertoire of tumor antigens, which could reduce the likelihood of immune escape through antigen loss. Despite this potential, past efforts to implement TIL therapy in RCC have been largely unsuccessful, likely due to the dominance of TILs exhibiting an exhausted phenotype, and the inability to effectively rejuvenate these cells during ex vivo expansion. Thus, the development of strategies that can selectively isolate and expand tumor-specific T-cells with minimal off-target toxicity and durable cytotoxic function will likely be key to the successful development of TIL therapy for RCC. We recently demonstrated that highly expanded clonal $CD8^+$ T-cell populations in RCC tumors exhibit an antigen-experienced phenotype, indicative of chronic stimulation and consistent with tumor antigen recognition. These clonotypes represent a key feature of RCC TIL populations. Based on this, we hypothesize that the selection of non-exhausted, clonally expanded T-cells using specific surface markers will enhance the therapeutic potency and specificity of RCC-derived TIL products.

Methods

To identify surface markers that distinguish non-exhausted, clonally expanded tumor-reactive T-cells, we compiled a comprehensive single-cell RNA sequencing (scRNAseq) and paired TCR sequencing dataset. This includes tumor, normal adjacent tissue (NAT), peripheral blood mononuclear cells (PBMC), and lymph nodes (LN) from 23 clear cell RCC (ccRCC) patients, combining seven published and in-house studies. We are applying both differential gene expression (DGE) analysis and multi-instance-based machine learning (ML) to identify candidate surface markers linked to non-exhausted,

clonally expanded phenotypes. These models are designed to accommodate the inherent noise and sparsity of single-cell data and to uncover combinatorial marker sets.

Results

In RCC tumors, we observed significant clonal expansion of T-cells with a memory-like, antigen-experienced phenotype. Tumor samples showed significantly higher T-cell clonality compared to matched normal tissues. Cells sharing the same TCR clonotype displayed heterogeneous transcriptional states, including both exhausted and non-exhausted phenotypes. Markers of tumor reactivity identified for other cancers (e.g., CD39, CD103) labeled mainly exhausted subsets of expanded clonotypes, suggesting a need for improved marker combinations for RCC. Clonality tended to decline with increasing tumor stage, possibly indicating a link between exhaustion and tumor progression.

DGE analysis revealed several surface markers associated with expanded TCR clonotypes, for which commercial antibodies are available for flow sorting. To overcome limitations of DGE alone, we are applying ML models that integrate gene expression, TCR identity, and clonal frequency to predict tumor reactivity. We successfully trained and validated multiple machine learning models, including scFormer (transformer-based), attention_MIL (attention-based deep multi-instance learning), miBoost (tree-based), and miSVM (support vector classifier), on sparse and heterogeneous scRNAseq data using a local GPU platform. All models showed consistent improvement in validation accuracy during training. Feature analysis revealed gene sets predictive of large versus small clonotypes, offering candidate markers for isolating tumor-reactive, non-exhausted T cells for downstream applications.

Conclusions

T-cells sharing the same T-cell receptor can display both terminally exhausted and progenitor exhausted states. Selecting clonally expanded, non-exhausted T cells may enhance the tumor reactivity of TIL products. Our ongoing analyses, including model hyperparameter optimization and gene pathway comparison, focus on identifying surface markers that are antibody-compatible, broadly expressed across patients, and applicable to $CD8^+$ and $CD4^+$ T-cells while excluding Tregs. These insights will support a refined TIL manufacturing strategy for improved RCC therapy.

Keywords

Tumor-infiltrating lymphocyte (TIL) therapy, single-cell RNA sequencing (scRNAseq), predictive biomarkers of clonal expansion

31

Lymphocyte Heat Shock Signature Predicts Response to Immune Checkpoint Blockade in Renal Cell Carcinoma

Ethan Burns[1], Soki Kashima[2], Rishabh Rout[1], Miya Hugaboom[2], Zhaochen Ye[2], Nicholas Schindler[2], Anasuya Dighe[2], Maxine Sun[3], Gwo-Shu Mary Lee[3], Wenxin (Vincent) Xu[3], Michael B. Atkins4, Sabina Signoretti5, Bradley A. McGregor[3], Rana McKay6, Toni Choueri[3], David Braun[7]

[1]Yale University, [2]Yale Cancer Center, Yale School of Medicine, [3]Dana-Farber Cancer Institute, [4]Georgetown Lombardi Comprehensive Cancer Center, [5]Brigham and Women's Hospital, [6]University of California, San Diego, [7]Yale New Haven Hospital

Background

Immune checkpoint blockade (ICB) therapies have revolutionized treatment for renal cell carcinoma (RCC). Despite this, only a subset of patients respond, and there remains an incomplete understanding of the cellular states that are associated with response. Defining these states may help elucidate potential mechanisms of response and assist in the development of next-generation immune therapies for RCC.

Methods

We utilized an existing tumor single-cell RNA sequencing (scRNA-seq) dataset from our lab of >400,000 cells from 70 donors with RCC, with 49 of them having received ICB therapy (either anti-PD-1 alone or in different combinations). Each donor was also annotated as having benefit (complete or partial response) or non-benefit (progressive disease) after ICB therapy.

Results

In order to find new cell states that may impact response to ICB, we began by sub-clustering the CD4+ T cells, finding 10 clusters that existed. One cluster was strongly enriched in donors who experienced benefit after ICB therapy (Wilcoxon Test, p = 0.0042) and was marked by heat shock protein 70 genes (HSP70) such as HSPA6, HSPA1A, and HSPA1B. Previous work from our group has shown that many of these same HSP70 family genes are associated with response after ICB therapy in CD8+ T cells, so we hypothesized that high expression of these heat shock genes may be able to predict benefit from ICB therapy across diverse lymphocyte subsets (Kashima, ASCO, 2024). In order to test this, we made a module score of the upregulated genes from the CD4+ T cell heat shock cluster and applied it to all lymphocytes. We then calculated the correlation of the heat shock module score rank for each sub-cluster vs. the rank of how strongly each

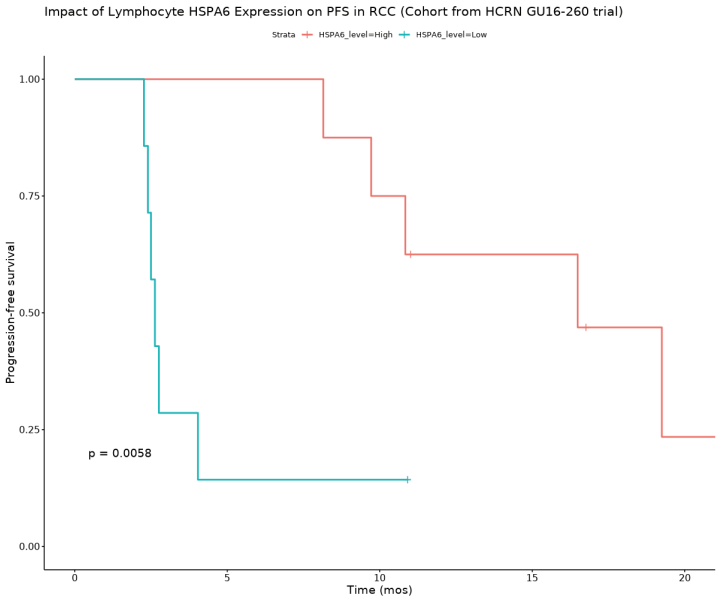
sub-cluster was associated with benefit from ICB. Strikingly, there was a nearly perfect correlation for CD4+ T cells (r = 0.89, p = 0.001), indicating that increased heat shock expression in CD4+ T cell clusters is associated with a better response to ICB. We repeated this test on NK and innate lymphoid cells (r = 0.77, p = 0.005), B cells (r = 0.67, p = 0.00013), and CD8+ T cells (r = 0.3, p = 0.325), finding similar trends each time albeit to varying extents. Next, we calculated the mean heat shock module score for each donor across all lymphocytes and calculated its difference between donors who had benefit vs. non-benefit. We found that there was a significant increase in heat shock score in donors who had benefit from ICB (Wilcoxon Test, p = 0.0031), and this difference was even more pronounced when only the top gene from the module (HSPA6) was used to calculate the mean difference (p = 0.001). To validate our findings, we turned to a pre-existing cohort of 17 donors from the HCRN GU16-260 trial where tumor scRNA-seq was available (Hugaboom et al., Cancer Discovery, 2025). After calculating the mean lymphocyte HSPA6 module score by donor, we discovered that donors who had a score greater than or equal to the median had greatly increased progression free survival (PFS) after ICB therapy (Kaplan-Meier, p = 0.0058; mean PFS of 14.3 months for HSPA6 high vs. 3.9 months for HSPA6 low).

Conclusions

We identified a heat shock signature in lymphocytes that is strongly associated with clinical benefit in RCC after ICB therapy, with the expression of the top gene (HSPA6) predicting PFS in a subset of donors from the HCRN GU16-260 clinical trial. Future studies will mechanistically test whether these genes are responsible for the therapeutic response themselves and uncover the stresses found in the tumor microenvironment that are necessary for their induction.

Keywords

ICB response; immunotherapy; T cell; cell stress



32

Interplay of Tumor-Intrinsic and Microenvironmental Gene Expression Predicts Immune Checkpoint Blockade Response in Metastatic Renal Cell Carcinoma

Nicholas Salgia[1], Eric Kauffman[2], Jason Muhitch[2]

[1]Department of Immunology, Roswell Park Comprehensive Cancer Center, [2]Roswell Park Comprehensive Cancer Center

Background

We previously defined a Genomic Dedifferentiation Signature (GDS) derived from differential gene expression analysis of sarcomatoid renal cell carcinoma (sRCC) tumor clones compared to clear cell RCC (ccRCC; Salgia et al. KCRS. 2024). GDS expression is negatively prognostic across clinical RCC cohorts, yet carries predictive capacity for identifying patients likely to achieve benefit from immune checkpoint blockade (ICB). Furthermore, we have also demonstrated that sRCCs are enriched for expression of tertiary lymphoid structure (TLS) signatures. Crucially, TLS signatures have been associated with response to ICB in ccRCC (Jammihal et al. Nature Cancer. 2025). Therefore, we sought to investigate if an interplay between expression of the GDS – a tumor-intrinsic gene signature – and TLS signatures – characterizing the inflammatory immune microenvironment – could best identify ICB sensitivity in patients with metastatic RCC.

Methods

Transcript-per-million normalized gene expression counts matrices and clinical metadata were collected from three trials of ICB regimens in patients with metastatic RCC: IMmotion 151 (Motzer et al. Cancer Cell. 2020), Javelin101 (Motzer et al. Nature Medicine. 2020), and HCRN-GU16-260 (Hugaboom et al. Cancer Discovery. 2025). Gene expression scores for the GDS and the Imprint TLS signature (Meylan et al. Immunity. 2022) were assigned to cases using single sample gene set enrichment analysis. Correlation between GDS and TLS scores was performed via Spearman's rank-order correlation. Cases were stratified into -high and -low signature expression (TLShigh-GDShigh, TLShigh-GDSlow, TLSlow-GDShigh, and TLSlow-GDSlow) based on median signature expression within trial cohorts. Progression-free survival (PFS) was compared between groups and trial arms within each cohort using Cox proportional hazards models, while objective response rates (ORR) were compared using Fisher's exact tests.

Results

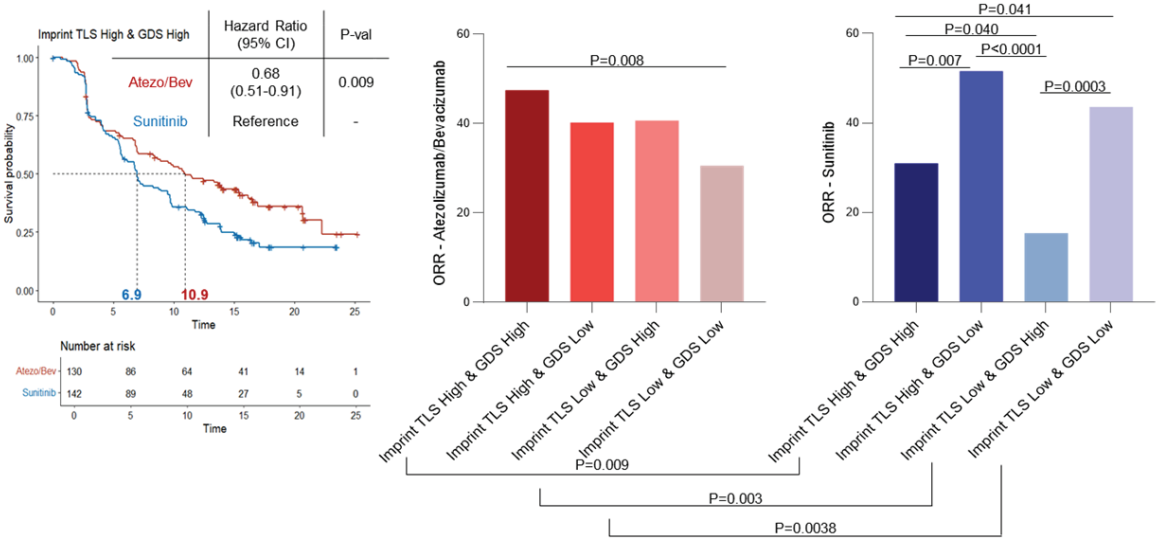
The correlation between GDS & Imprint TLS expression was moderate across IMmotion151 (n=822; R=0.44; p<2.2x10-16), Javelin101 (n=723; R=0.43; p<2.2x10-16) and HCRN-GU16-260 (n=72; R=0.53; p=2.6x10-6). Within IMmotion151, patients classified as TLShigh-GDShigh experienced prolonged PFS with the ICB-containing atezolizumab/bevacizumab regimen (median PFS: 10.9 months) compared to sunitinib (median PFS: 6.9 months; Hazard Ratio [HR]=0.68; p=0.009; Figure 1), whereas no significant differences between atezolizumab/bevacizumab and sunitinib PFS were observed in TLShigh-GDSlow (HR=1.18; p=0.5), TLSlow-GDShigh (HR=0.71; p=0.09), or TLSlow-GDSlow (HR=0.93; p=0.6) subgroups. ORR to atezolizumab/bevacizumab within the TLShigh-GDShigh population (47.5%) was also significantly higher compared to atezolizumab/bevacizumab ORR within the TLSlow-GDSlow population (30.6%; p=0.008) and compared to ORR with sunitinib in the TLShigh-GDShigh population (31.0%; p=0.009). Conversely, ORR with sunitinib (43.6%) was significantly greater than with atezolizumab/bevacizumab (30.6%; p=0.004) in the GDSlow-TLSlow population. Consistent results were observed in Javelin101: the TLShigh-GDShigh population experienced prolonged PFS with the ICB-containing axitinib/avelumab regimen (median PFS: 12.5 months) compared to sunitinib (median PFS: 6.9 months; HR=0.47; p<0.001). Again, no significant differences between axitinib/avelumab and sunitinib PFS were observed in TLShigh-GDSlow (HR=1.04; p=0.9), TLSlow-GDShigh (HR=0.81; p=0.4), or TLSlow-GDSlow (HR=0.81; p=0.3) subgroups. In the HCRN-GU16-260 trial of front-line nivolumab in metastatic RCC, TLShigh-GDShigh status was associated with prolonged PFS, albeit non-significantly, compared to TLShigh-GDSlow (HR=2.02; p=0.10), TLSlow-GDShigh (HR=1.99; p=0.13) and TLSlow-GDSlow (HR=1.72; p=0.09). Additionally, ORR to nivolumab was significantly enriched in the TLShigh-GDShigh cohort (76.9%) compared to those classified as TLShigh-GDSlow (23.1%; p=0.0009), TLSlow-GDShigh (25.0%; p=0.01), and TLSlow-GDSlow (18.5%; p<0.0001) within HCRN-GU16-260.

Conclusions

Across metastatic RCC patient cohorts, simultaneous enrichment of tumor-intrinsic and TLS gene expression best predict response to ICB versus anti-angiogenic therapy. This suggests that a pro-inflammatory milieu is not sufficient for effective immune sensitivity, but that a biologic interplay between tumor cells and their surrounding microenvironment is necessary for effective immune surveillance and ICB responsiveness in RCC.

Keywords

Genomic Dedifferentiation Signature, Immune Checkpoint Blockade, Metastatic RCC, Predictive Biomarker, Tertiary Lymphoid Structures



33

Fusion Derived Oncogenic Programs Shape the Immune Landscape in translocation Renal Cell Carcinoma

Prathyusha Konda[1], Cary Weiss[2], Yantong Cui[2], Jinyu Wang[2], Sayed Matar[3], Yasmin Nabil Laimon[4], Aseman Sheshdeh[4], Riva Deodhar[4], Sabrina Camp[4], Jack Horst[4], Jonathan Hecht[4], David Einstein[4], Anwesha Nag[4], Aaron Thorner[4], Eliezer Van Allen[1], Cheng-Zhong Zhang[1], Sabina Signoretti[4], Toni Choueri[1], Srinivas Viswanathan[1]

[1]Dana-Farber Cancer Institute, [2]Dana-Farber/Boston Children's Cancer and Blood Disorders Center, [3]Yale School of Medicine, [4]Brigham and Women's Hospital

Background

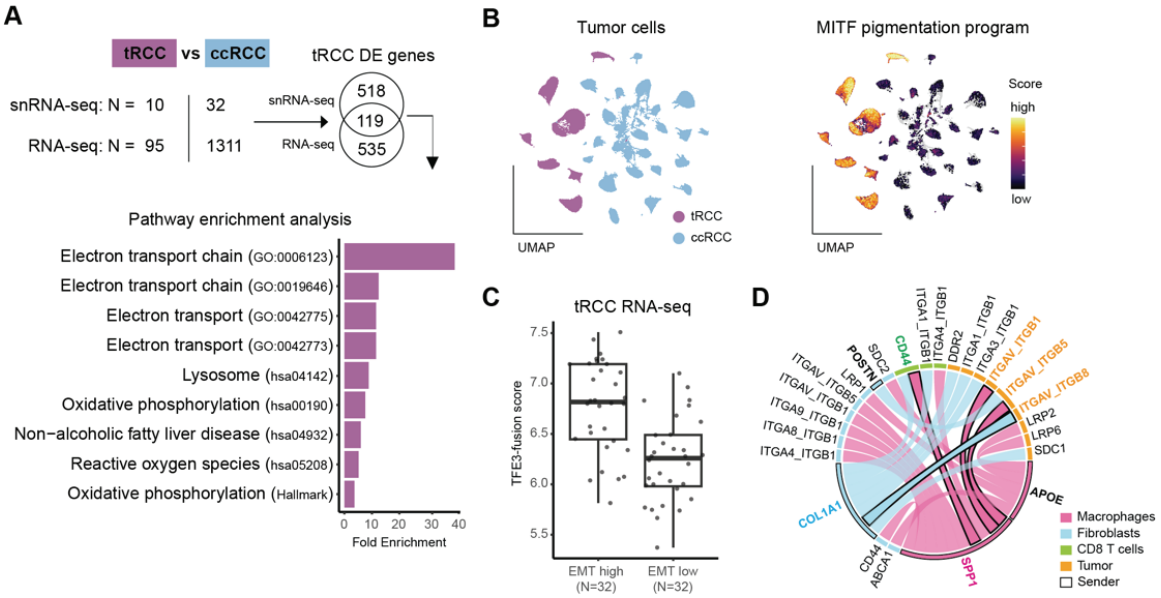
Renal cell carcinoma (RCC) comprises a heterogeneous group of cancers with diverse molecular drivers and clinical behaviors. Despite this diversity, the majority of RCC cases are treated using therapeutic strategies developed for the most common subtype, clear cell RCC (ccRCC), due to limited understanding of subtype-specific biology. Translocation RCC (tRCC) is a rare and clinically aggressive RCC subtype defined by gene fusions involving MiT/TFE family transcription factors, most commonly TFE3. Currently, there are no molecularly tailored treatments for tRCC, and standard-of-care therapies utilized for other RCC subtypes are typically less effective in tRCC. Emerging data suggest that tRCC is molecularly distinct from other RCC subtypes. However, an incomplete understanding of both tumor-intrinsic drivers and the tumor microenvironment (TME) features of tRCC presents barriers to developing effective therapeutics for this cancer.

Methods

The study employed an integrative multi-omics approach to dissect the cellular and molecular landscape of tRCC. The tRCC cohort consisted of 16 tumor samples from 15 patients, analyzed using single-nucleus RNA sequencing (snRNA-seq), single-nucleus ATAC sequencing (snATAC-seq), spatial transcriptomics, and T cell receptor (TCR) sequencing. Comparative analyses were performed against single-cell datasets from ccRCC samples, and bulk RNA-sequencing datasets were integrated for validation. Differential gene expression and chromatin accessibility analyses were conducted to identify tRCC-specific transcriptional programs and regulatory elements. The tumor cell-of-origin was inferred by comparing tumor transcriptomes to a single-cell atlas of normal human kidney tissue. Tumor-intrinsic transcriptional programs and intra-tumoral heterogeneity were delineated using non-negative matrix factorization methods. Finally, we characterized the immune landscape and cellular crosstalk within the TME by integrating snRNA-seq data, immune deconvolution of bulk RNA-seq data, TCR sequencing, and spatial transcriptomics.

Results

Our study revealed that tRCC and ccRCC likely share a common cell of origin in the VCAM1-positive proximal tubule cells but diverge significantly at the molecular level due to their distinct oncogenic drivers. Tumors from tRCC demonstrated profound differences in transcriptional pathways compared to ccRCC, including upregulation of oxidative phosphorylation, respiration, and lysosomal pathways driven by TFE3 fusions (Figure A). Notably, tRCC tumors showed higher activity of a pigmentation-related MITF-like transcriptional program (Figure B). Chromatin accessibility profiling revealed selective enrichment of regulatory elements associated with TFE3 and epithelial-mesenchymal transition (EMT), underscoring the unique epigenomic landscape of tRCC.



Despite the genetically quiescent landscape, we identified six conserved oncogenic meta-programs shared across tRCC tumors, describing the intra-tumoral heterogeneity. Among them, EMT and proximal tubule programs were largely mutually exclusive and modulated by the level of TFE3 activity, with high TFE3 expression driving EMT and suppressing epithelial identity (Figure C).

The tRCC tumor microenvironment was characterized by limited infiltration of cytotoxic $CD8^+$ T cells compared to ccRCC, many of which displayed dysfunctional phenotypes. Additionally, the TME was enriched for immunosuppressive tumor-associated macrophages and matrix-associated fibroblasts. Spatial and ligand-receptor interaction analyses revealed several suppressive cellular interactions, including those involving COL1A1-ITGAV and SPP1-ITGAV axes, which may promote EMT and reinforce local immune suppression (Figure D).

Conclusions

This study defines the fusion-driven oncogenic programs, intratumoral heterogeneity, and a profoundly immunosuppressive TME of tRCC, which likely underlie its poor response to immunotherapy. Our findings provide a framework for rational therapeutic development, including strategies targeting fusion-mediated transcriptional programs and reprogramming the tumor microenvironment to overcome immune resistance.

Keywords

Translocation RCC, tumor microenvironment, immunology, resistance

34

Hypoxia and immune suppression shapes therapeutic outcomes and metastases in clear cell renal cell carcinoma

Lynda Vuong[1], Andrew Cornish[1], Yash Khandwala[1], Hui Jiang[1], Eduardo Mascareno[1], Doris Zheng[1], Phillip Rappold[2], Josef Leibold[2], Erich Sabio[2], Kate Weiss[2], Carlene Gonzalez[2], Nicole Rittenhouse[1], Liangliang Ji[1], Jing Zhang[1], Mojca Adlesic[1], Oguz Akin[1], Jessica Flynn[1], Chirag Krishna[1], Alejandro Sanchez[3], Renzo Di Natale[3], Kyle Blum[3], Paul Russo[1], Jonathan Coleman[1], Ian Frew[1], Diego Chowell[1], Yingbei Chen[1], David Solit[1], Irina Ostrovnaya[1], Robert Motzer[1], Martin Voss[4], Ritesh Kotecha[1], Timothy Chan[1], Fengshen Kuo[1], Ming Li[1], A. Ari Hakimi[1]

[1]Memorial Sloan Kettering Cancer Center, [2]University of Rochester, [3]Huntsman Cancer Institute

Background

Vascular endothelial growth factor receptor-targeting tyrosine kinase inhibitors (VEGFR-TKIs) and aPD1 combinations are effective in multiple solid tumors, particularly in clear cell renal cell carcinoma (ccRCC), due to its characteristic pseudo-hypoxic, hyper-angiogenic state driven by biallelic VHL-loss. However, long-term durability is inferior to dual aPD1/aCTLA4 regimens, yet the mechanisms underlying these differences remain unclear.

Methods

Since tumor-associated macrophages (TAMs) are implicated in therapeutic resistance, we used immunofluorescence staining and scRNAseq (n=37) to investigate TAM evolution following VEGFR-TKI, aPD1 and combined VEGFR-TKI/aPD1 treatment in a genetically engineered (Ksp1.3cre-ERT2Vhlf/fp53f/f Rb1f/f) ccRCC mouse model. We further corroborate our findings in a novel human scRNAseq cohort (n=15) of on-treatment tumor samples from patients who received VEGFR-TKI/aPD1 or aPD1/aCTLA4 therapies and experienced a range of clinical responses before undergoing cytoreductive nephrectomy.

Results

By quantifying hypoxia using pimonidazole in mice, we reveal that VEGFR-TKIs induced severe intratumor hypoxia. This enabled the identification of hypoxia-responsive SPP1+ TAMs that are absent in baseline pseudo-hypoxic ccRCC tumors. This proxy of true hypoxia tracks with successful response to VEGFR-TKI/aPD1 in both mouse and human on-treatment samples, reflecting treatment-induced hypoxic necrosis. Paradoxically, high levels of pretreatment

hypoxic TAM signatures predicted worse outcomes across multiple VEGFR-TKI/aPD1 trials including JAVELIN101 and IMMOTION150/151, as well as an MSKCC real-world data cohort (n=44). Furthermore, extended exposure to hypoxia-inducing VEGFR-TKIs and aPD1 exacerbated metastasis in two syngeneic models of ccRCC.

Conclusions

In conclusion, our study suggests that VEGFR-TKIs induce tumor hypoxia in responsive ccRCC tumors, but preexisting hypoxia renders tumors refractory to VEGFR-TKI/aPD1 therapies. Our data also suggests that chronic therapy-induced hypoxia and inflammation may promote metastatic evolution, thus offering potential mechanistic insight into the poor durability of VEGFR-TKI/aPD1 regimens across multiple cancer types.

Keywords

Hypoxia, tumor associated macrophages, immune checkpoint blockade

35

FGD1 Splice Variant as a Novel Biomarker for Inferior Clinical Outcomes and Development of Brain and Bone Metastasis in Clear Cell Renal Cell Carcinoma.

Alex Soupir[1], Alyssa Obermayer[1], Kapil Avasthi[1], Youngchul Kim[1], Justin Miller[1], Mitchell Hayes[1], Nicholas Abreu[1], Roy Elias[1], Nirmish Singla[2], Michele Churchman[2], Daniel Grass[1], Ahmad Tarhini[1], Paola Ramos-Echevarria[1], Kelly Zea[1], Eric A. Singer[3], Sean Kern[4], Yousef Zakharia[5], Paul Viscuse[6], Patrick Hensley[6], Liang Wang[1], Timothy Shaw[1], Brandon Manley[1]

[1]H Lee Moffitt Cancer Center & Research Institute, [2]Johns Hopkins University School of Medicine, [3]The Ohio State University Comprehensive Cancer Center, [4]Uniformed Services University Murtha Cancer Center and Walter Reed National Military Medical Center, [5]University of Iowa Holden Comprehensive Cancer Center, [6]University of Virginia

Background

Currently, no reliable tissue or blood-based biomarkers exist for clear cell renal cell carcinoma (ccRCC), neither in the localized nor metastatic setting. Two of the most common and morbid sites of metastatic development are brain and bone metastases (B&BM). Existing treatment guidelines do not recommend routine brain or bone directed imaging during surveillance after curative treatment or upon initial staging for metastatic patient in the absence of clinical signs or symptoms. Previously identified recurrent somatic splice variants (SV) in ccRCC may hold promise for novel biomarker development. One such splice variant significantly associated with increased progression and decreased survival among ccRCC patients was FYVE, RhoGEF and PH domain-containing protein 1 (FGD1; Chang et al. Eur Urol, 2022 Oct). Our study aims to validate clinical outcomes for tumors with the FGD1-splice variant (FGD1-SV), investigate metastatic organotropism associated with FGD1-SV and explore the feasibility of plasma-based detection assay for FGD1-SV among ccRCC patients.

Methods

Patient tumor samples from Moffitt Cancer Center and the ORIEN cohort, a data-sharing alliance of 18 NCI-designated cancer centers, were identified. The detection of FGD1-SV was evaluated in a cohort of 105 primary ccRCC tumors from Moffitt patients and 1,037 ccRCC patients from ORIEN, which includes 84 metastatic tumors, using bulk RNA-sequencing. For bulk RNA-sequencing analysis, samples with three or more FGD1-SV reads were classified as positive. Kaplan-Meier curves were used to examine associations with clinical variables. The relationship between FGD1-SV positivity and metastatic site was assessed with Fisher's exact test. Additionally, pre-surgery plasma, post-surgery plasma, and tissue specimens prospectively collected from 64 ccRCC patients undergoing surgery were examined using a novel multiplexed PCR-sequencing assay. Read count from PCR data was log2 transformed and then normalized using housekeeping genes. Batch effect was corrected using COMBAT.

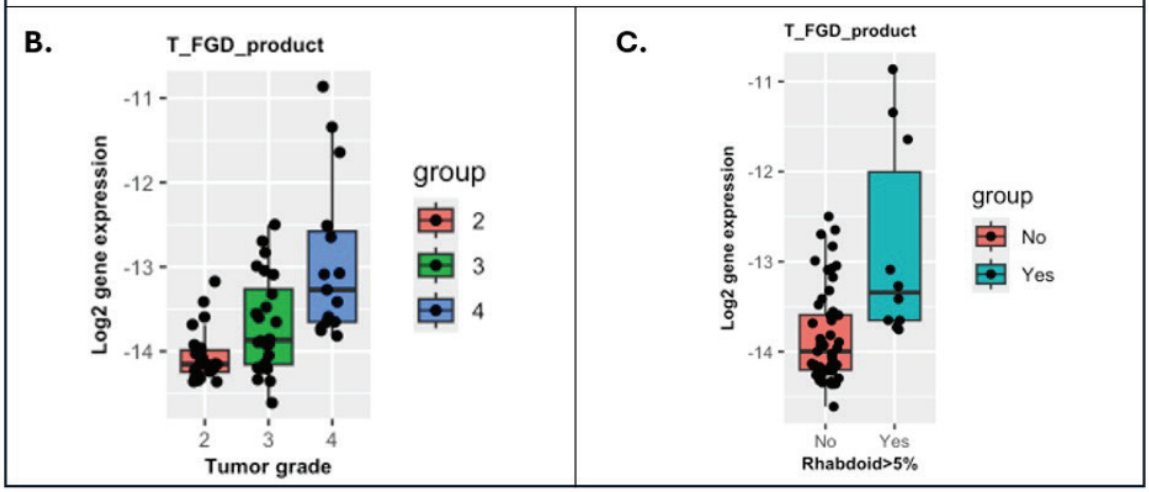
Results

Among 105 Moffitt patients, we detected the FGD1-SV in 15 patients and these patients were at significantly elevated risk for the development of brain metastasis during follow-up compared to those patients without the variant (HR 10.38; 95%CI 2.13-50.6; p=0.004). We then evaluated the presence of FGD1-SV among the 84 metastatic samples from the ORIEN cohort. Here we found B&BM demonstrated the highest FGD1-SV detection rate (50% brain and 44% bone, respectively) and enrichment compared to other sites (Figure 1A). Among 1,008 primary tumors from ORIEN, FGD1-SV positive tumors were validated for their association with inferior overall survival (p=0.0029). Our PCR assay among the prospective cohort (n=64) found a strong association of the FGD1-SV in tumor samples with aggressive histology, including WHO grade (ANOVA p=<0.0001; Figure 1B) and the presence of rhabdoid features (p=0.0001; Figure 1C). Lastly, we found significantly higher FGD1-SV in plasma collected before surgery than plasma collected after surgery (p=0.007.)

A.

	Metastatic Samples							
	Total	Brain	Bone	Adrenal	Pancreas	Lymph Node	Liver	Lung
Total	84	10	16	13	8	14	2	21
FGD1 reads = 0	54	4	7	13	7	10	1	12
FGD1 reads ≤ 2	65	5	9	13	7	12	2	17
FGD1 reads ≥ 3	19	5 (50%)	7 (43.7%)	0 (0%)	1 (12.5%)	2 (14.3%)	0 (0%)	4 (19%)

Table 1: FGD1 splice variant (FGD1-SV) reads identified in bulk RNAseq of ccRCC metastatic sites. Percentages indicate the proportion of samples with FGD1 reads ≥ 3 relative to the total number of samples for each metastatic site.



Conclusions

FGD1-SV is significantly associated with poorer clinical outcomes and increased risk of B&BM in ccRCC patients. Initial studies examining FGD1-SV detection in patient plasma and tumor through a practical PCR-based assay demonstrates feasibility and correlates with important pathological outcomes. Further studies are needed to investigate the integration of FGD1-SV into clinical decision-making, potentially guiding personalized surveillance and staging strategies.

Keywords

Liquid biopsy, FGD1 splice variant, brain and bone metastasis

36

International Neoadjuvant Kidney Cancer Consortium guidelines on assessing pathological response after neoadjuvant therapy in kidney cancer

James Jones[1], James Blackmur[2], Koen van der Mijn[3], Anne Warren[4], Lisa Browning[5], Femke Burgers[3], Michelle S. Hirsch[6], Payal Kapur[7], Rohit Mehra[8], Priya Rao[9], Sabina Signoretti[6], Axel Bex[10], Grant Stewart[11], Maurits van Montfoort[12], On behalf of the INKCC members

[1]University of Cambridge, Department of Oncology, [2]Western General Hospital, Edinburgh, [3]Netherlands Cancer Institute, Department of Oncology, [4]Cambridge University Hospitals NHS Foundation Trust, [5]University of Oxford, [6]Brigham and Women's Hospital, [7]UT Southwestern Medical Center, Department of Pathology, [8]University of Michigan, Department of Pathology, [9]MD Anderson, Department of Pathology, [10]Royal Free London NHS Foundation Trust, UK & The Netherlands Cancer Institute, Netherlands, [11]University of Cambridge, Department of Surgery, [12]Netherlands Cancer Institute, Department of Pathology

Background

Despite effective surgery and adjuvant immunotherapy, 1/3 of patients with initially localised renal cell carcinoma (RCC) will go on to develop relapse. Neoadjuvant therapy might improve outcomes for some of these patients; however, the approach has not been widely adopted due to a lack of prospective randomised trial data. Designing prospective neoadjuvant studies for RCC depends on properly defined clinicopathological endpoints. Pathological response is a surrogate marker of efficacy for neoadjuvant therapy in many non-renal tumour types. However, there are no standard guidelines on pathological response reporting for RCC, and correlation between pathological response following neoadjuvant therapy and survival has not been established. This study aimed to assess the status of pathological response reporting in RCC and develop a recommendation on tissue preparation and reporting for neoadjuvant RCC clinical trials.

Methods

A systematic review of the PubMed and Web of Science databases was conducted to identify manuscripts reporting response to pre-surgical therapy in RCC. Guidelines for tissue preparation and pathological response reporting were reviewed at a workshop of the International Neoadjuvant Kidney Cancer Consortium (INKCC) held at the Netherlands Cancer Institute in October 2024, and further developed through expert discussions involving pathologists, surgeons, oncologists and patient advocates.

Results

119 eligible papers were identified. Of these, 27 were prospective neoadjuvant studies, 81.5% of which included a systematic assessment of pathological response across participants. However, methods varied widely between studies. Across all papers, ypT stage post treatment was reported in 34.5%, grade in 22.7%, and a quantitative assessment of residual tumour in 6.7% of manuscripts. Only 4.2% of papers provided specific methodology on tumour sampling for pathological response assessment.

Key points from the INKCC guideline on pathological response assessment include:

1. One tissue section every 10mm should be submitted for masses with grossly viable tumour, with consideration of increased sampling to identify microscopic residual viable tumour foci in selected cases.

2. Areas of residual viable tumour, fibroinflammatory regression, necrosis, and haemorrhage should be quantified by microscopic assessment and reported in 10% intervals. The largest viable tumour measurement should also be reported.

3. Until prospective evidence is generated, suggested response cut offs for percentage residual viable tumour are: >50% - non-response, <50% - partial response, <10% - major response, 0% - complete response.

4. Extent of viable tumour in venous tumour thrombus and metastatic lesions should be reported separately using the same methods as the primary tumour.

Academic studies assessing neoadjuvant response should report a core set of information including neoadjuvant treatment details, macroscopic and microscopic extent of viable tumour, and linked oncological outcome data. We recommend that sampling for correlative studies is embedded in study design, including comparison to pre-treatment biopsy features, so that we can understand neoadjuvant therapy response and identify the patients that benefit from this approach.

Conclusions

Current reporting of pathological response to neoadjuvant therapy in RCC is highly variable, without defined guidelines. We have provided a standardised method for assessment and reporting pathological response, initially for use in clinical trials or research settings. We anticipate that based on application of this method, a streamlined approach can be developed for use in standard clinical care. Critically, future neoadjuvant trials in RCC should assess whether the degree of pathological response is linked to survival outcomes, to refine the cut-off levels for response and validate pathological response as a surrogate endpoint in RCC.

Keywords

Neoadjuvant, pathological response, clinical trials, pathology, surgery

Version 1. 07.14.2025 © KidneyCAN.

37

Integrative multi-omic characterization of the immune landscape in renal cell carcinoma

Jennifer Pfeil, Shirley Hui, Daniel Stueckmann, Xiaoyu Zhang, Lisa Martin, Jennifer Gorman, Eddy Chen, Somi Afiuni, Jalna Meens, Maria Komisarenko, Stephane Chevrier, Sujana Sivapatham, Julia Szusz, Zhihui Liu, Susan Prendiville, Laurie Ailles, Philip Jonsson, Fred Davis, Cristina Penaranda, Ryan Newton, Nicolas Stransky, Piotr Bielecki, Gromek Smolen, Masoom Haider, Bernd Bodenmiller, Sarah Crome, Gary Bader, Anthony Finelli, Hartland Jackson, Keith Lawson

Lunenfeld-Tanenbaum Research Institute

Background

Renal Cell Carcinoma (RCC) has been characterized as being amongst the most immune infiltrated solid tumors with a highly heterogenous immune landscape. Within spatially organized cellular networks (CNs) of the tumor immune microenvironment (TIME), key immune cell-cell interactions (CCIs) impact immune cell function and organization ultimately impacting the patient's overall response. Multiple studies have observed an association of tertiary lymphoid structures, a commonly observed spatial CN, with positive clinical outcomes in RCC, however additional CNs and the CCIs that control these networks need to be identified to better harness and potentially reprogram immune responses to improve patient outcomes. The recent explosion of interest in the heterogeneity of the immune landscape in RCC has led to numerous publications using the latest technologies in spatial transcriptomics, proteomics, and metabolomics. However, many of these studies use this data in isolation and therefore, may be hindered by the technological biases inherent in each method. Here, we have developed a novel approach to integrate spatial and single cell multi-omic data harnessing the strengths of each technology to better interrogate CNs that exist in the RCC TIME.

Methods

Fresh surgical samples were procured at the University Health Network (Toronto, Canada) through the REnal cancer MicroEnvironment DiscoverY (REMEDY) study. Bulk RNA sequencing (RNA-seq), single cell RNA sequencing (scRNA-seq), single cell suspension mass cytometry (SMC), whole transcriptome digital spatial profiling (DSP), and imaging mass cytometry (IMC) was performed on spatially concordant tumor regions across 54 patients. scRNA-seq enabled the identification of immune, stromal, and malignant high-resolution cell states, which informed a tailored antibody panel design for SMC and IMC and served as a reference framework for harmonized cell-type annotation across modalities. This enabled the integration of our transcriptomic and proteomic data to delineate RCC-specific CNs enriched for defined CCIs across unique biological pathways.

Results

Using this integrative approach, we identified seven high-resolution patient immunophenotypes. To evaluate their prognostic and predictive relevance, we derived representative gene signatures using a linear mixed model (Flash-MM) to interrogate publicly available bulk RNA-seq datasets, including TCGA, JAVELIN, and IMmotion151. This analysis revealed immunophenotype-specific associations with survival following surgery or systemic therapy in univariate models. To explore potential biological mechanisms associated with these divergent clinical outcomes, we incorporated spatial information into traditional CCI analyses and performed pathway analyses to define functional relationships. This revealed that patient subtypes with high lymphoid infiltration exhibit greater spatial heterogeneity, potentially reflecting the coexistence of multiple activated immune pathways. In contrast, patient subtypes with low immune infiltration were enriched in more developmental signaling pathways. In addition to our biological observations, we were also able to assess the technological differences between patient matched samples and compare the ability of each technology to capture inter-patient and intra-patient heterogeneity.

Conclusions

Collectively, this work identifies clinically distinct subgroups defined by CNs and details the interpatient cellular heterogeneity that exists in RCC, providing the foundation for future personalized therapeutic interventions against this disease.

Keywords

Multi-omic, Immunophenotyping, Methods integration

38

Presence of tertiary lymphoid structures and exhausted tissue-resident T cells determines clinical response to PD-1 blockade in renal cell carcinoma

Lena Wirth[1], Miya Hugaboom[2], Kelly Street[2], Neil Ruthen[2], Opeyemi Jegede[2], Nicholas Schindler[2], Valisha Shah[2], Jacob Zaemes[2], Nourhan El Ahmar[3], Sayed Matar[4], Varunika Savla[4], Toni Choueiri[5], Thomas Denize[5], Destiny West[5], David McDermott[6], Elizabeth Plimack[7], Jeffrey A. Sosman[8], Naomi B. Haas[9], Michael Hurwitz[10], Hans J. Hammers[11], Mark N. Stein[12], Robert Alter[12], Mehmet Bilen[13], Sabina Signoretti[3], Michael B. Atkins[14], Catherine Wu[5], David Braun[15]

[1]Yale University, [2]Yale Cancer Center, Yale School of Medicine, [3]Brigham and Women's Hospital, [4]Yale School of Medicine, [5]Dana-Farber Cancer Institute, [6]Beth Israel Deaconess Medical Center, [7]Fox Chase Cancer Center, [8]Northwestern University Feinberg School of Medicine, [9]Hospital of the University of Pennsylvania, [10]Yale Cancer Center, [11]UT Southwestern, [12]Columbia University Medical Center, [13]Emory Winship Cancer Institute, [14]Georgetown Lombardi Comprehensive Cancer Center, [15]Yale New Haven Hospital

Background

Despite the success of immune checkpoint inhibitors (ICI) for the treatment of renal cell carcinoma (RCC), many patients do not receive durable clinical benefit. Therefore, an understanding of resistance to ICIs is critical for the treatment of this disease. Using scRNA-seq, we previously found increased tissue-resident ZNF683+ (Hobit) SLAMF7+ CD8+ exhausted T cells (T-exh-SLAMF7) in human RCC resistant to PD-1 blockade in the HCRN GU16-260 trial. A T-exh-SLAMF7 gene expression signature (GES) was associated with worse clinical outcomes with PD-1 blockade in multiple validation cohorts. Here, through bulk RNA-seq of RCC biospecimens from 90 patients enrolled in this trial, we identified higher tertiary lymphoid structures (TLS) in patients responsive to PD-1 blockade and investigated the interplay between TLS and T-exh-SLAMF7 in shaping therapeutic responses.

Methods

Bulk RNA sequencing was performed on tumor samples from 90 RCC patients enrolled in the HCRN GU16-260 clinical trial. GES scores were calculated for each sample by z-scoring all genes and then computing the average expression of the genes comprising each signature of interest. To validate TLS presence at the protein level, 19 FFPE RCC tumor samples were analyzed using a 7-plex multiplex immunofluorescence panel targeting DAPI, CD20, CD3, CD21, CD4, PD-1, and FOXP3. TLS were manually quantified based on the colocalization of B and T cell markers in organized structures. Patients were stratified by high versus low TLS and T-exh-SLAMF7 GES scores (≥ or < median) for downstream analyses of clinical response and progression-free survival.

Results

Patients with complete/partial response had a higher (≥ median) TLS GES score compared to patients with progressive disease (p=0.0004). Similarly, high TLS signature scores were associated with improved progression-free survival (PFS; HR = 2.08, 95% CI: 1.28–3.4, p=0.0032), indicating significantly higher risk of progression in patients with low TLS scores. We confirmed that tumors with a high TLS GES score had a higher number of TLS detected by multiplex immunofluorescence (p=0.028). Finally, we analyzed the interplay between TLS and tissue-resident exhausted CD8+ T cells. We divided patients into four categories based on median split TLS and T-exh-SLAMF7 GES score values: TLS high SLAMF7 low (n = 28), TLS high SLAMF7 high (n = 15), TLS low SLAMF7 high (n = 28), and TLS low SLAMF7 low (n = 15). Patients with both high TLS and low T-exh-SLAMF7 GES scores had substantially improved PFS compared to all other patients (HR = 0.45, 95% CI: 0.26-0.79, p=0.0052), with 60.7% PFS at 12 months compared to 25.9% in the remaining groups.

Conclusions

These findings support a paradigm where both high TLS and low T-exh-SLAMF7 cells are required for optimal response to PD-1 blockade in RCC. Ongoing studies will use spatial transcriptomics and functional assays to evaluate the interaction between TLS and T-exh-SLAMF7 cells and to define the roles of SLAMF7 and Hobit in regulating CD8+ T cell effector functions within the RCC tumor microenvironment.

Note: Encore Presentation; recently published in Cancer Discovery (PMID: 39992403)

Keywords

TLS, T cells, PD-1 blockade, Immunotherapy

39

Intratumoral Viral Transcriptomic Signatures Stratify Immune Phenotypes and Clinical Outcomes in Renal Cell Carcinoma (RCC)

Mustafa Saleh[1], Eddy Saad[1], Pablo Barrios[1], Marc Machaalani[1], Liliana Ascione[1], Wassim Daoud Khatoun[1], Jad El Masri[1], Razane El Hajj Chehade[1], Marc Eid[1], Rashad Nawfal[1], Karl Semaan[1], Emre Yekeduz[1], Clara Steiner[1], Weiwei Bian[1], Maxine Sun[1], Sabina Signoretti[2], Eliezer Van Allen[1], David Braun[3], Alexander Gusev[1], Toni Choueiri[1]

[1]*Dana-Farber Cancer Institute,* [2]*Brigham and Women's Hospital,* [3]*Yale New Haven Hospital*

Background

Unlike other cancer types the determinants of anti-PD-1 response in clear cell RCC are not well defined; ccRCC exhibits a low mutational burden and CD8+ T cells infiltration is associated with worse prognosis. Cytomegalovirus (CMV) and human papillomavirus (HPV) infections are postulated to modulate the anti-tumor immune responses within the tumor microenvironment. We sought to investigate the clinical and immunologic impact of CMV and HPV viral transcriptomic signatures, as defined by prior studies, in patients with RCC.

Methods

RNA-seq data from three RCC prospetive trials were upper-quartile normalized, log2-transformed (TPM+1), and batch-corrected using ComBat. Transcriptomic scores for CMV (75 genes) and HPV (79 genes) were computed using geometric means (71 and 77 genes were found, respectively). CD8 immunofluorescence (IF) was performed on tumor samples. Overall survival (OS) and progression-free survival (PFS) were assessed using multivariable Cox regression, adjusting for age at therapy start, gender, IMDC risk, sarcomatoid/rhabdoid features, and number of previous lines received.

Results

A high intratumoral CMV transcriptomic score was significantly correlated with T-effector signature (ρ = 0.54, p = 4.8×10^{-6}), IF tumor core $CD8^+$ (ρ = 0.43, p < 0.001), IF tumor margin $CD8^+$ (ρ= 0.41, p < 0.001), and myeloid signature (ρ = 0.40, p < 0.001). The CMV score was significantly higher in infiltrated versus excluded/desert tumors (p = 0.0079).The CMV score was associated with worse OS among patients receiving immune checkpoint blockade (ICB) (HR 4.98, p= 0.039). In contrast, the HPV transcriptomic score showed only a modest correlation with myeloid signature (ρ = 0.24, p = 0.051) and no association was found with OS nor PFS.

Conclusions

In metastatic RCC, a high tumor CMV transcriptomic score was associated with a paradoxical immune landscape, marked by $CD8^+$ infiltration yet co-enriched with suppressive myeloid signatures, that predicts inferior overall survival following ICB. These viral signatures within the complex immune architecture of RCC may help understand immune responsiveness and resistance within distinct genomic and therapeutic contexts.

Keywords

Transcriptome, Genomics, Renal Carcinoma, Cytomegalovirus Infections, Papillomavirus Infections, Immune Checkpoint Inhibitors, Immunologic Memory, Survival Analysis, Therapeutics

Table. Results from multivariable Cox model and Correlation analyses.

	ICB		MTORi	
	HR	P-Value	HR	P-Value
CMV Transcriptomic Score (OS)[1]	4.98 (1.09 – 22.82)	0.039 (*N=74*)	2.21 (0.63 – 7.79)	0.215 (*N=92*)
HPV Transcriptomic Score (OS)[1]	1.71 (0.56 – 5.19)	0.345 (*N=74*)	0.94 (0.33 – 2.64)	0.906 (*N=92*)
CMV Transcriptomic Score (PFS)[1]	1.22 (0.29 – 5.22)	0.788 (*N=74*)	0.98 (0.27 – 3.52)	0.977 (*N=92*)
HPV Transcriptomic Score (PFS)[1]	1.38 (0.49 – 3.92)	0.545 (*N=74*)	2.45 (0.84 – 7.13)	0.101 (*N=92*)
	CMV Transcriptomic Score		HPV Transcriptomic Score	
	Spearman ρ	P-Value	Spearman ρ	P-Value
Myeloid Signature Score	0.40	< 0.001 (*N=64*)	0.24	0.051 (*N=64*)
T-effector Signature Score	0.43	< 0.001 (*N=64*)	0.18	0.150 (*N=64*)
Tumor Margin (TM) CD8 (in %)	0.54	< 0.001 (*N=64*)	0.03	0.790 (*N=64*)
Tumor Core (TC) CD8 (in %)	0.41	< 0.001 (*N=64*)	0.01	0.950 (*N=64*)
TM/TC Ratio	0.01	0.930 (*N=64*)	0.04	0.740 (*N=64*)

[1]Adjusted for Age at Therapy Start, Gender, IMDC Risk, Sarcomatoid/Rhabdoid Feature, Previous Number of Lines Received (< 2/ ≥ 2).

Abbreviations: ICB: Immune Checkpoint Blockade; MTORi: mTOR (mammalian target of rapamycin) inhibitors; OS: Overall Survival; PFS: Progression-Free Survival; CMV: Cytomegalovirus; HPV: Human Papillomaviruses.

40

Investigating the determinants of immunotherapy response in the primary tumor of clear cell renal cell carcinoma (RCC)

Cerise Tang[1], Deepak Poduval[1], Rishabh Rout[1], Suzanna Lee[2], Justine Panian[2], Ava Saidian[3], Rana McKay[2], David Braun[4]

[1]Yale University, [2]University of California, San Diego, [3]University of Tennessee, [4]Yale New Haven Hospital

Background

While previous studies have examined the determinants of a patient's overall response to immune checkpoint inhibitor (ICI) in advanced RCC, the factors that specifically influence ICI response in the primary tumor remain poorly defined. This is of particular importance in the current era, where cytoreductive nephrectomy is less commonly performed, and many patients with metastatic disease still have the primary RCC tumor in place. To deepen our understanding of ICI response in the primary tumor and to understand the evolution of RCC on ICI, we conducted a comprehensive genomic analysis of paired pre- and post-treatment primary RCC tumors treated with ICI.

Methods

46 RCC tissue samples comprised of 15 pre-treatment (biopsy of kidney) and 31 post-treatment nephrectomy samples (n=33 patients, n=13 with paired samples) were analyzed. 17 samples were from responders (>30% radiographic shrinkage or ypT0, n=4 pre-treatment, n=13 post-treatment) and 29 samples were from non-responders (<30% shrinkage, n=11 pre-treatment, n=18 post-treatment). Whole-exome and RNA-seq were performed at Caris Life Science. Wilcoxon rank-sum test was used to compare total mutation burden (TMB), loss of heterozygosity (LOH), and HLA evolutionary divergence (HED). Fisher's exact test was used to assess the prevalence of driver genes for genes mutated in more than 3 samples. Comparisons were made between pre- and post-treatment specimens, and between response and nonresponse in pre-treatment samples. Ranked gene set enrichment analysis (GSEA) was performed using the 50 hallmark gene sets. Published immune signatures were quantified using single-sample GSEA. P-values were FDR adjusted, with a significance threshold at < 0.05.

Results

Pre-treatment tumors that responded to ICI were significantly enriched for gene expression signatures of immune response, including interferon-alpha and interferon-gamma. Conversely, pre-treatment tumors resistant to ICI were significantly enriched for pathways associated with hypoxia, epithelial-to-mesenchymal transition, and metabolic activity. Further, pre-treatment responder biopsies are enriched for immune-related gene programs, including B cell and tertiary lymphoid structure (TLS) signatures compared to non-responder biopsies.

Longitudinal analysis of paired samples reveals that immune pathways decline in responders and increase in non-responders post-treatment, suggesting divergent remodeling of the tumor microenvironment. These findings highlight the value of primary tumor profiling in understanding ICI response dynamics in RCC.

Conclusions

This study has important implications for understanding ICI response and resistance in the metastatic context, especially where the primary tumor remains in place, and in the neoadjuvant setting. Our findings suggest that that both the baseline immune landscape and treatment-induced transcriptional remodeling shape ICI response in primary RCC, and that the primary tumor provides a valuable window into these dynamics.

Keywords

Immune checkpoint inhibitors, tumor microenvironment, genomic analysis

41

Single-cell dissection of immunosuppressive myeloid subclusters driving resistance to immune checkpoint therapy in renal cell carcinoma (RCC)

Soki Kashima[1], Rishabh Rout[2], Miya Hugaboom[1], Zhaochen Ye[1], Nicholas Schindler[1], Anasuya Dighe[1], Maxine Sun[3], Gwo-Shu Mary Lee[3], Wenxin (Vincent) Xu[3], Sabina Signoretti[4], Bradley A. McGregor[3], Rana McKay[5], Toni Choueri[3], David Braun[6]

[1]Yale Cancer Center, Yale School of Medicine, [2]Yale University, [3]Dana-Farber Cancer Institute, [4]Brigham and Women's Hospital, [5]University of California, San Diego, [6]Yale New Haven Hospital

Background

With immune checkpoint inhibitors (ICIs) now widely used as a primary treatment for metastatic RCC, understanding the composition and function of the tumor microenvironment (TME) has become more important. Numerous studies have focused on T cells to explain both treatment response and

resistance, and single-cell RNA sequencing (scRNA-seq) has revealed the complex heterogeneity of T cell states. However, the contribution of myeloid cells (particularly tumor-associated macrophages (TAMs), which are known to suppress antitumor immunity) remains incompletely understood in the context of ICI therapy. In this study, we aimed to investigate TAM populations associated with ICI resistance in RCC using single-cell transcriptomic profiling.

Methods

We analyzed 70 tumor samples (58 clear cell and 12 non-clear cell) obtained from 63 patients with advanced RCC. The cohort included 9 untreated patients, 10 who received non-ICI systemic therapies, and 44 who were treated with ICI-based regimens. From the ICI-based therapy group, we excluded 17 patients who had stable disease and focused on 29 tumor samples from 27 patients with either pre-treatment (n = 15) or post-treatment (n = 14) samples. These patients received various ICI regimens, including mono-ICI (n = 11), ICI plus ICI (n = 11), ICI plus VEGF inhibitor (n = 6), and ICI plus IDO1 inhibitor (n = 1). We performed scRNA-seq (10x Genomics) on all samples and applied non-negative matrix factorization (NMF) to identify transcriptional programs within TAMs. We then compared these programs between responders (n = 18, complete or partial response) and non-responders (n = 11, progressive disease) based on RECIST criteria. Statistical significance was assessed using the Wilcoxon signed-rank test.

Results

A total of 443,337 high-quality viable cells were analyzed and classified into major cell types, including lymphoid, myeloid, tumor, endothelial, and fibroblast compartments. Within the TAM compartment, NMF uncovered 8 gene expression programs, such as “antigen presentation”, “S100A8/9 inflammation”, “stress response”, “C1Q /APOE/TREM2 signaling”, “CD163/MRC1-M2-like”, “hypoxia-related signaling”, “interferon-stimulated response”, and a distinct “LILRB/SIGLEC10” immunosuppressive program. This LILRB/SIGLEC10-enriched TAM subcluster was significantly more abundant in non-responders than in responders ($p = 0.005$). Importantly, this difference was also observed in pre-treatment samples alone ($p = 0.014$), suggesting it may be involved in primary resistance. These TAMs expressed higher expression levels of immunosuppressive LILRB1/2/3 genes, the inhibitory receptor SIGLEC10 (a recently characterized “don’t eat me” signal), and the immune checkpoint molecule VISTA, compared to other TAM subclusters ($p < 2.22E-16$ for each gene).

Conclusions

Our scRNA-seq-based analysis identified a distinct population of TAMs characterized by immunosuppressive transcriptional programs associated with poor response to ICI therapy in RCC. These findings provide insight into potential mechanisms of resistance and suggest that targeting this TAM subset may improve therapeutic efficacy. This study also demonstrates the utility of single-cell transcriptomics for uncovering key immunoregulatory populations in large clinical cohorts.

Keywords

Renal cell carcinoma, Tumor-associated macrophages, Immune checkpoint inhibitors

42

The Impact of Belzutifan on Tumor Reduction Procedures and Healthcare Resource Utilization in Von Hippel–Lindau (VHL) Disease

Rimas V. Lukas[1], Vivek K. Narayan[2], Jonathan Freimark[3], Yan Song[3], Zhuo Chen[3], Joanne Chukwueke[3], Murali Sundaram[4], Rodolfo Perini[4], Reshma Shinde[4]

[1]Northwestern University, Department of Neurology, [2]University of Pennsylvania, Perelman School of Medicine, [3]Analysis Group, Inc., [4]Merck & Co., Inc.

Background

Belzutifan, a hypoxia-inducible factor 2 alpha inhibitor, was approved in the United States in August 2021 to treat VHL-associated renal cell carcinoma (RCC), central nervous system hemangioblastomas (CNS-Hb), and pancreatic neuroendocrine tumors (pNETs). Given belzutifan’s relatively recent market approval, real-world data on its clinical and healthcare resource utilization (HRU) outcomes remain limited. This study aimed to evaluate the impact of belzutifan on clinical procedures and HRU among patients with VHL treated with belzutifan.

Methods

This retrospective cohort study selected adult patients with evidence of a VHL diagnosis who initiated belzutifan on or after August 13, 2021, using administrative claims data from the Komodo Research Data (KRD+) database (January 1, 2016 to December 31, 2023). Evidence of VHL disease was identified using diagnosis codes, supplemented by a claims-based algorithm. The index date for each patient was defined as the date of their first belzutifan prescription in their claims history. Patient characteristics and comorbidity profile were summarized during the baseline period of 6 months before the index date, during which patients were continuously covered by healthcare insurance. Incidence rate ratios (IRRs) for tumor reduction procedures (TRPs), HRU, VHL monitoring procedures, and analgesic use were estimated

using generalized linear mixed models with random effects to compare the monthly incidence rates during the 2-year pre- and post-index periods surrounding belzutifan initiation. All models were adjusted for age, sex, geographic region and insurance plan.

Results

The analysis included 140 VHL patients treated with belzutifan, with a mean (standard deviation [SD]) age of 41.1 (14.2) years at the index date, and an equal distribution of males and females. Most patients were white (52.1%) and enrolled in commercial insurance plans (81.4%). Compared to the pre-index period, the monthly incidence rate of any TRP was significantly reduced by 60% (IRR [95% CI] =0.4 [0.3, 0.6], p<0.01) over the 2 years following belzutifan initiation (Figure 1a). Most notably, surgical removal of cerebellar and spinal hemangioblastomas and retinal laser therapy was significantly reduced by 70% (0.3 [0.1, 0.9], p <0.05) and 50% (0.5 [0.3, 1.0], p <0.05) respectively. During the post-index period, the use of ultrasound increased by 50% (1.5 [1.0, 2.2], p<0.05), while no significant differences were found in other imaging or monitoring procedures (1.1 [1.0, 1.2], p=0.14), or analgesic use (1.1 [1.0, 1.3], p=0.11) (Figure 1b). Additionally, all-cause inpatient (IP) admissions significantly declined by 40% (0.6 [0.4, 0.9], p<0.05), while outpatient (OP) visits significantly increased by 50% (1.5 [1.4, 1.5], p<0.01) (Figure 1c).

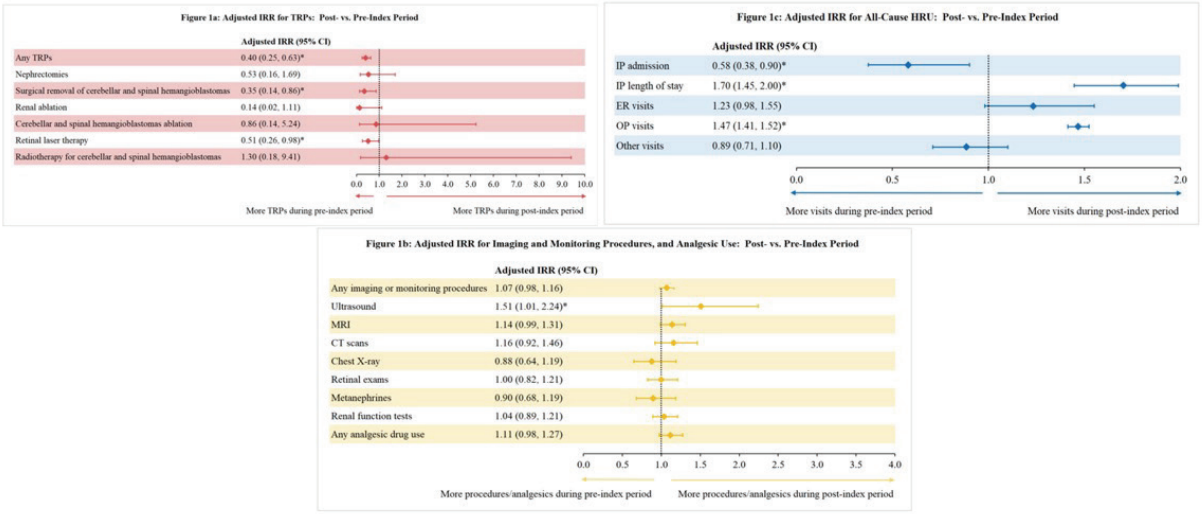
Conclusions

Belzutifan use was associated with significant reduction in TRP burden and fewer hospitalizations, alongside stable analgesic use, suggesting potential real-world clinical benefit in managing VHL disease. The increase in ultrasound utilization, along with a shift from IP to OP care, suggests a transition toward lower-intensity, surveillance-focused management following belzutifan initiation. These findings provide real-world evidence of belzutifan's impact on clinical management in patients with VHL.

Keywords

Von Hippel–Lindau disease, Belzutifan, Renal cell carcinoma, Healthcare resource utilization, Tumor reduction procedures

Figure 1. Pre-Post Belzutifan Initiation Comparison of TRPs, Monitoring Procedures, Analgesic Use, and HRU among VHL Patients



* indicates p-value<0.05.

Notes:

[1] Any TRPs included nephrectomies; surgical removal of cerebellar and spinal hemangioblastomas, adrenal pheochromocytomas and paragangliomas, endolymphatic sac tumors, epididymal cystadenomas, broad ligament cystadenomas, pancreatic neuroendocrine tumors, and retinal hemangioblastomas; adrenal, renal, cerebellar and spinal hemangioblastoma, inner ear, and pancreatic ablations; as well as retinal laser therapy and radiotherapy for cerebellar and spinal hemangioblastomas.

[2] Any imaging or monitoring procedures included ultrasound, magnetic resonance imaging, CI scans, chest X-ray, retinal exams, metanephrines, and renal function tests.

[3] Any analgesic drug included opioids, non-steroidal anti-inflammatory drugs (NSAIDS), corticosteroids, cannabinoids, muscle relaxant (carbamazepine), anti-epileptics, anti-depressants, alpha-2 adrenergic agonists, and botulinum toxin.

43

AURKA Connects NSD1 and SETD2 in an Epigenetic Axis Governing Mitotic Fidelity in ccRCC

Ruhee Dere[1,3], Manga Motrapu[1], Ashley Boice[1], Richard Han[1], Xiaoli Wang[1], Pratim Chowdhury[1], Sung Jung[2], B.V. Venkata Prasad[2]

[1]Center for Precision Environmental Health, Baylor College of Medicine, [2]Department of Biochemistry and Molecular Pharmacology, Baylor College of Medicine, [3]Department of Medicine, Baylor College of Medicine

Background

Chromothripsis-driven 3p deletion and 5q amplification are early, clonal events in clear cell renal cell carcinoma (ccRCC). These lesions respectively target the epigenetic regulators SETD2 and NSD1. Paradoxically, although NSD1 is amplified on 5q, it is frequently hypermethylated and transcriptionally silenced, suggesting functional inactivation is selected for. The mechanistic implications of NSD1 and SETD2 loss in mitotic control remain poorly understood.

Methods

We employed a multifaceted approach integrating in vitro kinase and methyltransferase assays, mass spectrometry, and molecular modeling to investigate the regulatory relationship between NSD1, AURKA, and SETD2. CRISPR/Cas9-engineered cell lines were generated to model genetic loss of NSD1, while pharmacologic inhibitors were used to perturb NSD1 and AURKA activity. Protein-protein interactions and post-translational modifications were characterized via co-immunoprecipitation, immunoblotting, fluorescence microscopy, and quantitative mass spectrometry. Functional outcomes were assessed in cell-based systems, and the impact on tumor growth was evaluated in xenograft models examining AURKA-mediated regulation of SETD2 in vivo.

Results

We identified NSD1 as a methyltransferase that directly methylates AURKA, serving as a negative regulator of its kinase activity and subcellular dynamics during mitosis. Loss of NSD1, through genetic deletion or pharmacologic inhibition, led to AURKA hyperactivation, defective spindle architecture, chromosome missegregation, and increased micronuclei formation. Unexpectedly, we found that AURKA phosphorylates SETD2, functionally linking these two epigenetic regulators. This phosphorylation selectively regulated SETD2's cytoskeletal activity without affecting its chromatin-associated roles. Disruption of this modification—via AURKA inhibition or mutation of the phosphorylation site—compromised mitotic fidelity and enhanced genomic instability. Importantly, phosphorylation-deficient SETD2 mutants were incapable of sustaining tumor growth in xenograft models, underscoring the oncogenic relevance of this post-translational modification. Moreover, SETD2 loss sensitized ccRCC cells to AURKA inhibition, revealing a potential therapeutic vulnerability.

Conclusions

Our findings reveal a novel regulatory pathway in which NSD1-mediated methylation suppresses AURKA, while AURKA phosphorylation regulates SETD2 activity on the cytoskeleton, linking these two tumor suppressors altered in early ccRCC. Disruption of this NSD1-AURKA-SETD2 axis creates a state of mitotic vulnerability, opening the door for therapeutic intervention using AURKA inhibitors in genetically defined subsets of ccRCC.

Keywords

Epigenetics, NSD1, SETD2, Aurora kinase A

44

Overview of Tivozanib (Tivo) safety in phase 3 clinical trials in patients with metastatic renal cell carcinoma (mRCC)

Pedro C. Barata[1], Brian Rini[2], Toni Choueri[3], Sumanta Pal[4], Philippe Barthelemy[5], Roberto Iacovelli[6], Bradley A. McGregor[3], Laurence Albiges[7], Javier Molina-Cerrillo[8], Benjamin Garmezy[9], Ralph Hauke[10], Sheela Tejwani[11], Arnab Basu[12], Helen Moon[13], Katy Beckermann[14], Moshe Ornstein[15], Rana McKay[16], Claudia Lebedinsky[17], Edgar E. Braendle[17], Robert Motzer[18]

[1]University Hospitals Seidman Cancer Center, [2]Division of Hematology and Oncology, Department of Medicine, Vanderbilt University Medical Center, [3]Dana-Farber Cancer Institute, [4]City of Hope Comprehensive Cancer Center, [5]Institut de Cancerologie Strasbourg Europe, [6]Comprehensive Cancer Center, Oncology Unit, Fondazione Policlinico Universitario "A. Gemelli" IRCCS, [7]Institut Gustave Roussy, [8]Hospital Universitario Ramon y Cajal, [9]Sarah Cannon Research Institute, [10]Nebraska Cancer Specialists, [11]Henry Ford Hospital, [12]University of Alabama at Birmingham, [13]Kaiser Permanente, [14]Tennessee Oncology, [15]Cleveland Clinic, [16]University of California, San Diego, [17]AVEO Oncology, [18]Memorial Sloan Kettering Cancer Center

Background

Tivo is a potent and highly selective VEGFR inhibitor designed to optimize VEGF blockade and minimize off-target toxicities. In TiNivo-2, patients with mRCC who had previous exposure to ICI, were randomized to receive study treatment as 2L or

3L with Tivo alone at 1.34 mg, or at 0.89 mg in combination with the ICI nivolumab (nivo).[1] The addition of nivo to tivo in second line (2L) or third-line treatment (3L) did not improve outcomes, and tivo monotherapy showed activity as a 2L treatment in the post ICI setting. In TIVO-3, randomized patients had at least two previous systemic treatments and received tivo or sorafenib. We carried out a safety review of tivozanib monotherapy in these 2 randomized trials in the context of populations that had been previously exposed to VEGFR-TKI and ICI treatment.

Methods

The safety profile of tivo monotherapy was evaluated in these two phase 3 trial cohorts that consisted of the tivo monotherapy arms of TiNivo-2 (N=171), and TIVO-3 (N=173).[2]

Results

Patient baseline characteristics of the two tivo monotherapy cohorts showed some differences, most notably in the distribution of previous exposure to VEGFR target therapy and ICIs: in TIVO-3, exposure to two prior VEGFR-TKI was 45%, to prior ICI plus VEGFR-TKI was 27%, and to a prior VEGFR-TKI plus other agent was 28%. Whereas inTiNivo-2, exposure to prior ICI was 100% (71% as the most recent line of therapy), while exposure to VEGFR-TKI was: none 31%, one 56% and two 13%. Additionally, 94% of TIVO-3 participants were white, compared with 62% of those in TiNivo-2. The incidence of grade 3-4 TEAEs and serious AEs was lower in TiNivo-2, however there was consistency in the incidence of any cause TEAEs, as well as those leading to death or treatment modifications in both cohorts (Table 1).

Table 1 TEAEs in tivo monotherapy cohorts

Event	Incidence %	
	TiNivo-2	TIVO-3
Tivozanib-related TEAEs	84.2	84.4
Deaths due to treatment-related AEs	0.6	0.6
Related Serious AE	8.8	11.6
Related AE Grade 3 or 4	35.1	45.7
TEAEs Leading to Dose Reductions	22.2	25.4
TEAEs Leading to Dose Interruption	54.4	50.3
TEAEs Leading to Withdrawal	19.3	19.3
Event ≥Grade 3 affecting ≥2% patients		
Hypertension	22.2	21.4
Asthenia	4.7	7.5
Fatigue	4.7	4.6
Decreased Appetite	2.3	4.6
Back Pain	2.9	1.2
Dyspnea	1.2	2.9
Diarrhea	2.3	1.7
Arthralgia	2.3	1.7
Anemia	1.8	2.3

For TEAEs ≥Grade 3, hypertension was the most common, occurring in approximately 20% of patients in each cohort; while the incidence of all other TEAEs ≥Grade 3 was lower, they also occurred at similar rates in each cohort (Table 1).

Conclusions

Here, results show that tivo has a manageable safety profile across phase 3 trials. The better tolerability of tivo in the TiNivo-2 study vs TIVO-3 is driven in part by more patients enrolled in the earlier lines of treatment (2L).

1. Choueiri et al. Lancet 2024
2. Rini et al. Lancet Oncol 2020

Keywords

Tivozanib, VEGFR-TKI, adverse event, second-line, first-line

45

Tumor matrix directed IL12/A3 fusion cytokine secreted by CD70-CAR NK cells markedly enhances anti-ccRCC responses with limited systemic exposure

Fuguo Liu, Xinyu Deng, Maily Nguyen, Mubin Tarannum, Shaobo Yang, Remy Dulery, Jianzhu Chen, Wenxin (Vincent) Xu, Toni Choueri, Rizwan Romee

Dana-Farber Cancer Institute

Background

Despite recent advances, metastatic clear cell renal cell carcinoma (ccRCC) remains largely incurable in most patients, and novel immunotherapeutic strategies to address checkpoint inhibitor refractory renal cell carcinoma are needed. Natural killer (NK) cells are immune effector lymphocytes that are specialized in the cytotoxic elimination of cancer cells. Chimeric antigen receptor (CAR) NK cells have also shown promising effects in clinical trials. IL-12 is a potent cytokine that mediates type 1 immunity and antitumor responses but with systemic toxicity. We hypothesize that IL-12 secreted by CD70-CAR NK cells will allow "tumor-directed" IL-12 delivery and with the incorporation of a novel motif, collagen-binding domain A3, we will further minimize toxicity.

Methods

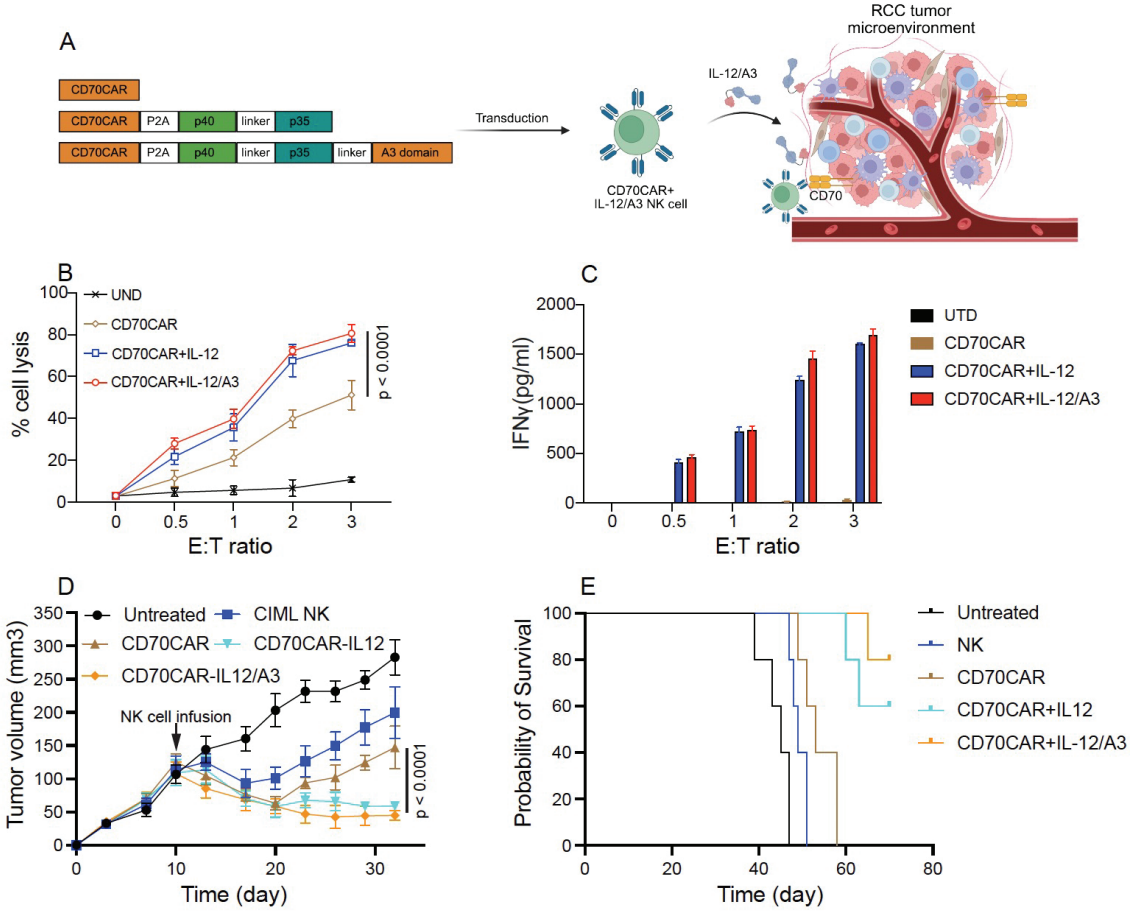
We engineered lentivectors to express CD70-CAR, CD70-CAR+IL-12, and CD70-CAR+IL-12/A3, and evaluated their transduction efficiencies in human NK cells. The phenotypes

of IL-12-secreting CD70-CAR NK cells were analyzed using flow cytometry and bulk RNA sequencing. Untransduced (UTD) and modified NK cells were cocultured with ccRCC tumor cell lines (A498 and ACHN) at various effector to target (E:T) ratios to assess target cell lysis. NK cell activation was determined by measuring degranulation (CD107a) and IFNγ expression. IFNγ secretion was quantified from coculture supernatants. The killing of ccRCC PDXs was similarly evaluated. In vivo, the therapeutic efficacy of CD70-CAR+IL-12/A3 NK cells was tested using ccRCC xenograft models using A498 cells injected subcutaneously into NSG mice. The mice were divided into five groups: no treatment (PBS), NK cell, CD70-CAR NK cell, CD70-CAR+IL-12 NK cell, and CD70-CAR+IL-12/A3 NK cell. When tumors reached ~100 mm^3, 1x10^6 NK cells were administered intravenously. Tumor volumes and mouse survival were monitored. For safety evaluation, the animals were closely monitored for their weight and wellbeing and plasma collected on day 7 post CAR NK cell injection to evaluate the production of IL-12 and other key inflammatory cytokines including IL-1β, IL-2, IL-6, IFNγ, IL-18 and GM-CSF that are associated with cytokine release syndrome (CRS).

Results

High transduction efficiency was achieved in the NK cells with all three CAR constructs (50–85%). IL-12-engineered CD70-CAR NK cells exhibited significantly increased surface expression of CD25, LFA1, CXCR4, and sLex compared to regular CD70-CAR NK cells. Gene expression analysis revealed upregulation of IL12A, IL12B, IFNG, GZMB, IRF1, SOCS3, and ABCA1, alongside downregulation of CISH. These cells also displayed enhanced metabolic fitness, with an increased oxygen consumption rate (OCAR).

CD70-CAR NK cells that secrete IL-12 and IL-12/A3 exhibited significantly increased cytotoxicity in vitro against ccRCC tumor cell lines A498 and ACHN, as well as CD70+ ccRCC patient-derived xenografts (PDXs). The presence of IL-12 and IL-12/A3 effectively stimulated NK cell degranulation and IFNγ production following coculture with ccRCC tumor cells. In vivo studies showed that CD70-CAR NK cells secreting IL-12 and IL-12/A3 achieved notably better control of ccRCC tumors compared to CD70-CAR NK cells alone. Mice treated with CD70-CAR+IL-12/A3 NK cells demonstrated better survival rates than those treated with CD70-CAR+IL-12



NK cells or other constructs (Fig. 1). Additionally, CD70-CAR+IL-12/A3 NK cells resulted in significantly lower systemic levels of IL-12 7 days after CAR NK cell infusion compared to CD70-CAR+IL-12 NK cells, suggesting that fusing IL-12 to a collagen binding domain can reduce systemic IL-12 exposure.

Conclusions

Incorporating IL-12/A3 into CAR NK cells is feasible, safe, and significantly enhances their cytotoxicity against ccRCC tumor cells in vitro and in vivo. These findings provide strong rationale for further clinical evaluation of CD70-CAR+IL-12/A3 NK cells in patients with advanced ccRCC.

Keywords

ccRCC, IL-12, CD70-CAR NK

46

Integrated Efficacy and Safety Exposure Response (ER) Analysis of Tivozanib (TIVO) for the Treatment of Renal Cell Cancer (RCC)

Bradley A. McGregor[1], Toni Choueri[1], Laurence Albiges[2], Katy Beckermann[3], Philippe Barthelemy[4], Roberto Iacovelli[5], Sheik Emambux[6], Javier Molina-Cerrillo[7], Benjamin Garmezy[8], Pedro C. Barata[9], Rana McKay[10], Alexander Chehrazi-Raffle[11], Hans J. Hammers[12], Daniel Yick Chin Heng[13], Klaas Prins[14], Bo Jin[15], Monette Cotreau[16], Edgar E. Braendle[15], Claudia Lebedinsky[15], Robert Motzer[17]

[1]Dana-Farber Cancer Institute, [2]Institut Gustave Roussy, [3]Tennessee Oncology, [4]Institut de Cancerologie Strasbourg Europe, [5]Comprehensive Cancer Center, Oncology Unit, Fondazione Policlinico Universitario "A. Gemelli" IRCCS, [6]Centre Hospitalier Universitaire de Poitiers, [7]Hospital Universitario Ramon y Cajal, [8]Sarah Cannon Research Institute, [9]University Hospitals Seidman Cancer Center, [10]University of California, San Diego, [11]City of Hope Comprehensive Cancer Center, [12]UT Southwestern, [13]Tom Baker Cancer Centre, [14]qPharmetra, [15]AVEO Oncology, [16]MMC Biopartners, [17]Memorial Sloan Kettering Cancer Center

Background

Tivo is an oral vascular endothelial growth factor receptor (VEGFR) tyrosine kinase inhibitor (TKI) approved in the US for treatment of patients with RCC following ≥2 prior systemic therapies. The approved Tivo monotherapy starting dose is 1.34 mg once daily on days (D) 1-21 Q28D, with allowable dose modifications to manage adverse events. In the randomized TiNivo-2 trial, the addition of Nivo 480 mg to Tivo 0.89 mg D1-21 Q28D (lower dose of Tivo was studied given assumed risk of hypertension [HTN]) did not improve outcomes compared with Tivo 1.34 mg D1-21 Q28D. There was a trend toward worse progression-free survival (PFS) in the combination arm.

Methods

Using a predeveloped population pharmacokinetic (PK) model, existing ER models based on TIVO-1 and TIVO-3 studies were augmented to characterize the relationship between Tivo at clinically relevant exposures and central reviewer-based PFS, tumor size (TS) reduction, and safety endpoints. TiNivo-2 trial results were integrated to update the PK and ER models for PFS (Cox proportional hazard), TS (sum of longest diameters longitudinal model), and HTN (logistic regression) and to simulate the ER-based risk/benefit profile of Tivo.

Results

The visual predictive check of the PK model on TiNivo-2 PK data confirmed that the dose-proportional Tivo PK is unaffected by concurrent Nivo. The PFS range of 5.6-9.7 months and TS reduction models, with a range of - 7.02% to -23.8%, showed a significant relationship with Tivo exposure (Table). Concurrent Nivo did not add discernible benefit to Tivo at the dose of 0.89 mg. An ER modeling analysis between maximum concentration and HTN showed that the predicted HTN incidence was similar between Tivo 1.34 mg and Tivo 0.89 mg (41.3% vs 38.8% for any-grade HTN; 23.8% vs 21.5% for grade ≥3 HTN). An effect term for Nivo in the ER model for HTN was nonsignificant.

Efficacy endpoint	Tivo average concentration, ng/mL	n	Observed value, combined studies (range)
PFS	13.9-38.4	192	5.6 months
PFS	38.4-47.9	191	7.3 months
PFS	47.9-62.0	191	9.1 months
PFS	62.0-177	191	9.7 months
CFBTS	13.9-38.4	176	-7.02% (-16% to 1.93%)
CFBTS	38.4-47.9	173	-11.7% (-21.3% to -2.05%)
CFBTS	47.9-62.0	185	-17.3% (-26.4% to -8.27%)
CFBTS	62.0-177	183	-23.8% (-33.5% to -14.1%)

CFB, change from baseline.

Conclusions

The efficacy ER models predicted that Tivo 1.34 mg would provide greater antitumor activity than the 0.89-mg dose, while the predicted HTN incidence (any grade and grade ≥3) was comparable at the 0.89- and 1.34-mg doses. The Tivo monotherapy dose selection of 1.34 mg is important, based on the ER analysis and its safety profile. The results from the TiNivo-2 data set further confirmed that re-challenge with immunotherapy does not add benefit and optimal dosing of TKI provides the highest clinical benefit.

Keywords

Tivozanib, VEGFR-TKI, dose, exposure response

47

TCF1⁺ CD4⁺T Cells Mediate Response to Anti-CTLA-4 Therapy in a Sarcomatoid RCC Mouse Model

Hui Jiang[1], Lynda Vuong[1], Fengshen Kuo[1], Doris Zheng[1], Alex Penson[1], Jing Zhang[1], Shengyu Gao[1], Ankur Eduardo Mascareno[1], Yingbei Chen[1], Yash Khandwala[1], Daniel Barbakoff[1], Andrea Lopez Sanmiguel[1], G. Luca Gusella[2], Ming Li[1], A. Ari Hakimi[1]

[1]Memorial Sloan Kettering Cancer Center, [2]Icahn School of Medicine at Mount Sinai

Background

Dual immune checkpoint blockade (IO/IO) has significantly improved overall survival in renal cell carcinoma (RCC), but only ~50% of patients initially respond to treatment. Understanding the mechanisms underlying primary response and resistance is critical to improving therapeutic outcomes.

Methods

We developed a novel mouse model of sarcomatoid RCC (sRCC) by targeting Vhl, Bap1, and Cdkn2a/b, recapitulating the genomic and histological features and tumor microenvironment of human sRCC. Mice were treated with anti-CTLA-4 antibody. Tumor-infiltrating immune populations were analyzed using single-cell RNA sequencing and flow cytometry to evaluate T cell subsets and cytotoxic function.

Results

Anti-CTLA-4 treatment led to Treg depletion and an increase in activated Th1 cells. Importantly, only responder mice exhibited a selective expansion of TCF1⁺ CD4⁺ T cells. This was accompanied by increased granzyme B and perforin expression in effector CD8⁺ T cells, indicating enhanced cytotoxic activity. In contrast, non-responder mice lacked this TCF1⁺ CD4⁺ population and associated cytotoxic CD8⁺ responses.

Conclusions

Our findings reveal that Treg-depleting anti-CTLA-4 therapy promotes anti-tumor immunity by expanding a TCF1⁺ CD4⁺ T cell population that orchestrates CD8⁺ T cell responses. This mechanism offers a novel insight into immune modulation in sRCC and identifies a potential target to improve immunotherapy efficacy in RCC patients.

Keywords

Immunotherapy, response, mouse model, T cells

48

Immunotherapy Response Correlates in Metastatic Clear Cell Renal Cell Carcinoma from Circulating Cell-Free Epigenomes

Razane El Hajj Chehade[1], Karl Semaan[1], Ze Zhang[1], Noa Phillips[1], John Canniff1, Hunter Savignano[1], Rashad Nawfal[1], Marc Eid[1], Lexi Grisham[2], Rebecca Prather[3], Katy Beckermann[2], Ulka Vaishampayan[4], Naomi Haas[5], Hans Hammers[6], David McDermott[7], Lauren Wood[8], Travis Solley[8], Brian Rini[2], Eric Jonasch[8], Toni K. Choueiri[1], Matthew L. Freedman[1], Scott M. Haake[2], Sylvan C. Baca[1], Jacob E. Berchuck[9]

[1]Dana-Farber Cancer Institute, [2]Vanderbilt University Medical Center, [3]Gadsden Regional Medical Center, [4]University of Michigan, [5]University of Pennsylvania, [6]UT Southwestern, [7]Beth Israel Deaconess Medical Center, [8]MD Anderson Cancer Center, [9]Emory Winship Cancer Institute

Background

Immune checkpoint inhibitors (ICIs) are a mainstay of treatment for metastatic clear cell renal cell carcinoma (mccRCC). With a growing number of treatment options for mccRCC, biomarkers are needed to guide treatment selection by predicting benefit from ICIs. Cell-free DNA (cfDNA)-based assays that measure tumor DNA in plasma are promising biomarkers for treatment response in several cancers, but their role in RCC remains unclear. Here, we tested whether epigenomic profiling of cell-free DNA can identify or predict radiographic responses to immunotherapy in mccRCC.

Methods

Plasma samples were obtained from 180 patients (400 total samples collected, up to 4 samples per patient) with mccRCC enrolled in the DOD-funded Kidney Cancer Research Consortium ctDNA study (NCT04883827). Patients received an immune checkpoint inhibitor and were categorized as non-responders or responders based on CT scan results obtained at 3- or 6-months following treatment initiation. Cell-free chromatin immunoprecipitation sequencing (cfChIP-seq) was performed on patient plasma to profile H3K4me3, a histone modification associated with active gene promoters. DNA methylation was profiled with cell-free methylated DNA immunoprecipitation sequencing (cfMeDIP-seq). H3K4me3 signal at the promoters of ccRCC-associated genes variation between pre-treatment and on-treatment timepoints was assessed for non-responders and responders. We calculated changes in H3K4me3 signal for on- and pre-treatment plasma draws. We then compared these changes between non-responders and responders using the Wilcoxon sum-rank test.

The immune cell types contributing to cfDNA were inferred from cfMeDIP-seq data.

Results

Comparing pre- and on-treatment timepoints drawn between 1-5 months after starting therapy, cfDNA promoter H3K4me3 at RCC-associated genes was concordant with radiographic response in 10 of 11 patients (91%), with signal increasing from pre- to on-treatment samples in 6 of 7 non-responders (86%) and decreasing in 4 of 4 responders (100%). The median change in H3K4me3 differed significantly for non-responders and responders ($p = 0.02$). Analysis of cfDNA methylation profiles identified a higher proportion of memory CD8 T cell-derived cfDNA in non-responders compared to responders in pre-treatment samples ($p = 0.003$).

Conclusions

This pilot study suggests that epigenomic profiling of cfDNA may identify pre-treatment and on-treatment biomarkers of ICI response. Profiling of larger cohorts is underway to test the generalizability of these findings.

Keywords

Epigenetics, cfDNA, clear cell Renal cell carcinoma

49

Preclinical efficacy of combined CDK4/6 and mTORC1 inhibition in translocation renal cell carcinoma

Shikha Gupta

Dana-Farber Cancer Institute

Background

Translocation renal cell carcinoma (tRCC) is an aggressive subtype of RCC driven by a gene fusion involving a transcription factor in the MiT/TFE gene family, most commonly TFE3. There are currently no approved therapeutic agents specific to tRCC and this subtype of kidney cancer represents a major unmet medical need.

Methods

We utilized integrative genomic approaches associated with activation of the cyclin- dependent kinase 4/6 (CDK4/6) and mammalian target of rapamycin complex 1 (mTORC1) signaling in tRCC. We tested the activity of CDK4/6 inhibitors (CDK4/6i), alone or in combination with mTORC1-selective inhibition, using in vitro and in vivo models of tRCC.

Results

Our work shows that tRCC tumors harbor multiple genomic and transcriptional features associated with activation of the CDK4/6 and mTORC1 signaling pathways. Pharmacological inhibition of CDK4/6 activity using palbociclib or abemaciclib, causes cell cycle arrest which was also recapitulated upon genetic knockout of CDK4/6 using CRISPR-Cas9. This was further accompanied by impaired cell growth in long-term culture in presence of palbociclib with a rapid cell regrowth observed upon drug withdrawal.

CDK4/6 proteins regulate G1-S cell cycle progression by combining with CyclinD1, the expression of which is significantly reduced upon treatment with mTORC1-selective inhibitor, RMC-5552. Combined treatment with the CDK4/6 inhibitor, palbociclib, and RMC-5552 resulted in synergistic suppression of tRCC cell viability and increased markers of apoptosis in vitro. The combination of palbociclib and RMC-5552 in a tRCC xenograft model showed greater efficacy than either single agent while also being well-tolerated.

Conclusions

Our work suggests that combined inhibition of CDK4/6 and mTORC1 activity has therapeutic potential in tRCC. This work may offer rationale for molecularly directed therapies in tRCC, which currently lacks any standard of care.

Keywords

CDK4/6, Translocation RCC, mTORC1, combination therapy, preclinical research

50

Clinical characteristics, determinants and subsequent therapy of primary refractory metastatic renal cell carcinoma (mRCC): An International Metastatic Database Consortium (IMDC) study

Marc Eid[1] , Karl Semaan[1], Wanling Xie[1], Razane El Hajj Chehade[1], Liliana Ascione1, David Maj[2], Martin Zarba[2], J. Connor Wells[3], Laura Wood[4], Ben Tran[5], Martin Angel[6], Sumanta K Pal[7], Jae-Lyun Lee[8], Kosuke Takemura[9], Christian K Kollmannsberger[10], Arnoud J Templeton[11], Georg A Bjarnason[12], Jose Manuel Ruiz[13], Daniel Heng[2], Toni K. Choueiri[1]

[1]Dana-Farber Cancer Institute, [2]Arthur J.E. Child Comprehensive Cancer Centre, [3]Barts Cancer Institute, Queen Mary University of London, [4]University of Michigan, [5]Peter MacCallum Cancer Centre, [6]Instituto Alexander Fleming, [7]City of Hope Comprehensive Cancer Center, [8]Asan Medical Center, University of Ulsan College of Medicine, [9]Cancer Institute Hospital, Japanese Foundation for Cancer Research, [10] BC Cancer--Vancouver Cancer Center, University of British Columbia, [11]St. Claraspital Basel and Faculty of Medicine, University of Basel, [12]Sunnybrook Odette Cancer Centre, [13]Fundación Clínica Médica Sur

Background

Immune checkpoint inhibitor (ICI)-based regimens, represent the current standard of care for first line (1L) metastatic renal cell carcinoma (mRCC). A subset of patients (pts) experience progressive disease (PD) on first restaging and are considered "primary refractory." Herein, we characterize this patient population and examine practice patterns and outcomes of subsequent second line (2L) therapy.

Methods

Data from pts with mRCC treated with 1L ICI-based regimens with available data on their best response to 1L were collected from the IMDC. Pts were categorized as primary refractory (PD as best response) and non-primary refractory (stable disease or partial/complete response as best response). Logistic regression was used to identify independent factors associated with primary refractory mRCC. Overall survival (OS) and time to treatment failure (TTF) were calculated from initiation of 2L therapy; their distributions were estimated by the Kaplan Meier methodology.

Results

In total, 2001 pts were included in this study, of which 1301 (65%) were treated with dual ICI combination, and 701 (35%) with ICI + VEGF combination. Of 2001 pts, 494 (24%) had PD as best response. Primary refractory and non-primary refractory groups did not differ by age or gender. The primary refractory group had a higher rate of pts treated with dual ICI combination (76 vs. 62%), higher rate of pts with poor IMDC risk group (39 vs. 25%), more pts with non-clear cell RCC (16 vs. 10%; all p<0.001). The primary refractory group had lower KPS (median: 80 vs. 90), higher percentage of anemia (61% vs. 47%), neutrophilia (19% vs. 12%), and thrombocytosis (23 vs 16%; all p<0.001). The primary refractory group had more liver (24 vs. 15%; p<0.001), bone (39 vs 31%; p=0.001) and lymph nodes metastasis (52 vs. 46%; p=0.03) at the start of the 1L treatment. On multivariate analysis, factors that were independently associated with primary refractory RCC were anemia (Odds Ratio (OR)=1.32, 95% confidence interval (CI) 1.01-1.74, p=0.04),KPS <80% (OR = 1.92, CI 1.38-2.66, p <0.001), neutrophilia (OR= 1.5, 95% CI 1.03-2.17, p=0.03), non-clear cell histology (OR=1.55, 95% CI 1.07-2.26, p=0.02), and the presence of liver metastasis (OR=2.03, 95% CI 1.5-2.75, p<0.001). Dual-ICI combination was associated with a 1.8-fold increase of primary refractory mRCC (OR =1.86, 95% CI: 1.39 – 2.49, p<0.001). 356 (72%) pts with primary refractory mRCC went on to receive subsequent 2L therapy.

Table. Summary of outcomes of patients with primary refractory mRCC receiving 2ndline (2L) therapies.

	ORR		TTF (mos)		OS (mos)*	
	N	No. of response (%)	No.of events/ Evaluable N	Median (95% CI)	No.of events/ Evaluable N	Median (95% CI)
Overall	356	61 (17.1)	239/338	5.5(4.3-6.2)	181/350	14.5(13.0-19.0)
Type of 2L treatment*						
2L Cabozantinib (1L ICI + VEGF)	53	11 (20.8)	30/49	6.5(4.6-11.1)	25/53	13.5(9.2-25.8)
2L Cabozantinib (1L dual ICI)	84	17 (20.2)	56/81	6.8(4.6-9.5)	44/82	15.1(10.5-21.5)
2L Pazopanib	37	6 (16.2)	30/35	2.8(1.5-3.4)	21/36	15.3(5.5-38.9)
2L Sunitinib	115	12 (10.4)	84/109	4.1(3.0-5.6)	67/113	10.7(7.0-15.6)
IMDC risk group at start of 2L						
Favorable	20	7 (35.0)	15/20	6.0(3.3-19.1)	7/20	46.0(9.9-NR)
Intermediate	125	24 (19.2)	81/121	8.4(5.2-9.7)	60/125	19.3(15.4-28.1)
Poor	114	18 (15.8)	82/111	3.3(2.8-5.6)	68/110	7.5(4.6-10.8)

*Median follow-up from 2L initiation was 18.8 months.

The most common regimens in the 2L setting included: cabozantinib (n=137; 38%); sunitinib (n= 115; 32%), and pazopanib (n=37; 10%). 22% of patients had IMDC poor risk at initiation of 2L. Median follow-up from 2L initiation was 18.8 months. Median OS was 14.5 months, and the median TTF was 5.5 months for the whole cohort. The outcomes of patients with primary refractory mRCC receiving 2L therapies are summarized in Table.

Conclusions

In this large multicenter cohort of pts with mRCC, the presence of liver metastasis, the receipt of dual ICI combination therapy, and a KPS<80 are independent risk factors for primary refractory disease. Cabozantinib is the most frequently used regimen as 2L therapy in this patient population and demonstrates favorable clinical outcomes. Biomarker evaluation is needed to explore the mechanism of primary resistance and novel therapeutic strategies for this group.

Keywords

Renal Cell Carcinoma, Primary Refractory, Immunotherapy

51

Antioxidant dependencies in fumarate hydratase–deficient kidney cancer

Blake Wilde[1], Heather R. Christofk[2]

[1]*Department of Urology, Roswell Park Comprehensive Cancer Center,* [2]*University of California, Los Angeles*

Background

Fumarate hydratase (FH)-deficient renal cell carcinoma (RCC), associated with hereditary leiomyomatosis and RCC (HLRCC), is a highly aggressive kidney cancer with limited treatment options. FH loss leads to accumulation of the oncometabolite fumarate, which drives tumor progression not only by inhibiting key enzymes but also by covalently modifying cysteine residues on proteins (succination). Fumarate accumulation leads to persistent oxidative stress, disrupting redox homeostasis and contributing to DNA damage, metabolic reprogramming, and immune evasion. Yet how FH-deficient tumors survive this oxidative pressure—and whether these adaptations reveal druggable vulnerabilities—remains unclear. To address this, we previously functionally characterized FH variants of uncertain significance, generating a panel of RCC cell lines with graded FH activity and fumarate accumulation. This system enables precise dissection of fumarate-driven metabolic rewiring and the identification of therapeutic targets.

Methods

We employed an integrated approach combining transcriptomic profiling of FH-deficient RCC tumors, metabolomics, isotope tracing, and CRISPR-based functional genomics. Using our FH-VUS cell line panel to model increasing intracellular fumarate, we examined antioxidant pathway activation, glutathione (GSH) metabolism, and redox balance. Targeted CRISPR dropout screens were used to identify metabolic dependencies, with a focus on nutrient transporters. Liquid chromatography-mass spectrometry (LC-MS) and stable isotope tracing were used to quantify antioxidant metabolite levels and map substrate utilization.

Results

Both FH-deficient tumors and high-fumarate cell lines showed robust upregulation of NRF2 target genes, particularly those involved in GSH and thioredoxin metabolism—two key antioxidant systems. CRISPR-mediated knockout of NRF2 resulted in rapid cell death in FH-deficient cells, confirming its essential role in counteracting fumarate-induced oxidative stress. Although intracellular GSH levels were markedly elevated in high-fumarate cells, the GSH:GSSG ratio remained unchanged, suggesting that these cells maintain redox balance through enhanced antioxidant capacity rather than by altering the redox potential itself.

Stable isotope tracing revealed that most of the cysteine in FH-deficient cells is diverted to GSH synthesis. Re-expression of wild-type FH reversed this effect, reducing cysteine incorporation into GSH. A focused CRISPR screen identified SLC7A11 as a selective dependency in FH-deficient cells. Finally, cystine deprivation triggered irreversible cell death, indicating that these tumors are metabolically addicted to cystine import to sustain their antioxidant defenses.

Conclusions

Our findings define a central redox adaptation in FH-deficient RCC: sustained activation of NRF2-dependent antioxidant programs and a reliance on cystine import to fuel glutathione synthesis. This cystine addiction creates a metabolic vulnerability that may be therapeutically exploited using SLC7A11 inhibitors or cystine-lowering strategies. By leveraging a tunable FH-VUS cell line model, we directly linked fumarate accumulation to redox rewiring and nutrient dependency. These insights uncover actionable metabolic liabilities in FH-deficient RCC and provide a framework for targeting redox adaptations in malignancies with high oxidative stress.

Keywords

Fumarate hydratase, redox stress, cystine addiction, glutathione, NRF2

52

Spatial Transcriptomic Mapping Reveals Immune-inflamed Niches in Sarcomatoid Chromophobe Renal Cell Carcinoma

Yan Tang[1], Tiegang Han[2], Hadi Mansour[2], Michelle S. Hirsch[2], Katrina Collins[3], Elizabeth P. Henske[2]

[1]Brigham and Women's Hospital of Harvard Medical School, [2]Brigham and Women's Hospital, [3]Indiana University

Background

Chromophobe renal cell carcinoma (ChRCC) is the second most common non-clear cell renal cell carcinoma (ncRCC). A series of 496 ChRCC from Memorial Sloan Kettering Cancer Center demonstrated that sarcomatoid features, which were present in about 1.2% of the cases, are strongly correlated with metastatic disease and reduced overall survival. Little is known about the biological and immunological characteristics of the sarcomatoid variant of ChRCC and how it differs from its classic, non-sarcomatoid form.

Methods

Eight ChRCC tumor samples containing both classic and sarcomatoid components were selected. Xenium Prime 5K assay (5,000 curated genes related to oncoimmunology) was used for high-resolution spatial transcriptomic profiling. Data were analyzed using Seurat and custom scripts to annotate cell types and conduct detailed phenotypic analysis. Pathway enrichment and transcription factor regulatory networks were analyzed using the SENIC package. Cell-cell communication was inferred using CellChat, and spatial proximity of immune and tumor cells ("cellular neighborhoods") was analyzed, which model spatial gene expression patterns and intercellular distances.

Results

Spatial transcriptomic analyses revealed a significantly more immune-inflamed tumor microenvironment in sarcomatoid regions compared to their classic counterparts. We identified distinct spatial immune "neighborhoods" in sarcomatoid areas that were enriched in CD8+ T cells, polarized macrophages, and dendritic cells. These neighborhoods exhibited organized proximity to tumor cells expressing immune evasion markers such as PD-L1. In contrast, classic regions were relatively immune-deserted. Analysis of transcription factor activity showed upregulation of IRF1 and STAT1-related programs in the immune infiltrates of sarcomatoid regions, consistent with inflammatory activation. Importantly, comparison of matched sarcomatoid and classic regions within the same tumors enabled us to define a "sarcomatoid-enriched gene signature" composed of immune-related, pro-metastatic, and epithelial-to-mesenchymal transition (EMT) genes. This signature was validated in bulk RNA-seq data from The Cancer Genome Atlas (TCGA), where it correlated with poor prognosis in ChRCC patients.

Conclusions

This study presents the first spatial transcriptomic atlas of sarcomatoid ChRCC in comparison to matched non-sarcomatoid (classic) from the same patient. Profound immune microenvironmental differences were identified between tumor compartments. The sarcomatoid variant exhibits hallmarks of an immune-inflamed but potentially immune-evasive phenotype, including enriched immune infiltration, pro-inflammatory signaling, and EMT-associated transcriptional programs. These findings highlight the biological differences between sarcomatoid and classic ChRCC and uncover specific immune pathways and spatial cell-cell interactions that may be targeted in future immunotherapeutic strategies. Our work also establishes a foundational spatial map for ChRCC that offers new insight into the disease heterogeneity and progression.

Keywords

Chromophobe renal cell carcinoma (ChRCC), sarcomatoid variant, single cell spatial analysis, tumor immune microenvironment

53

Microenvironmental characteristics of disease relapse after nephrectomy in clear cell renal cell carcinoma

Yu Fujiwara[1], Nicholas Salgia[2], Adil Khan[1], Spencer Rosario[1], Jason Muhitch[1]

[1]Roswell Park Comprehensive Cancer Center, [2]Department of Immunology, Roswell Park Comprehensive Cancer Center

Background

Localized renal cell carcinoma (RCC) is primarily treated with nephrectomy, but approximately 30% of patients with localized RCC eventually develop local recurrence or distant metastasis. The KEYNOTE-564 trial demonstrated overall survival benefit with adjuvant pembrolizumab for high-risk RCC after nephrectomy. However, the survival at 48 months in patients without adjuvant therapy was 86.0%, suggesting that a large proportion of high-risk patients can be spared adjuvant immunotherapy. However, factors at a molecular

level to predict disease relapse, and ultimately, who requires adjuvant immunotherapy, in RCC remain undetermined. Therefore, we sought to elucidate the microenvironmental characteristics of disease relapse after nephrectomy in patients with clear cell RCC (ccRCC).

Methods

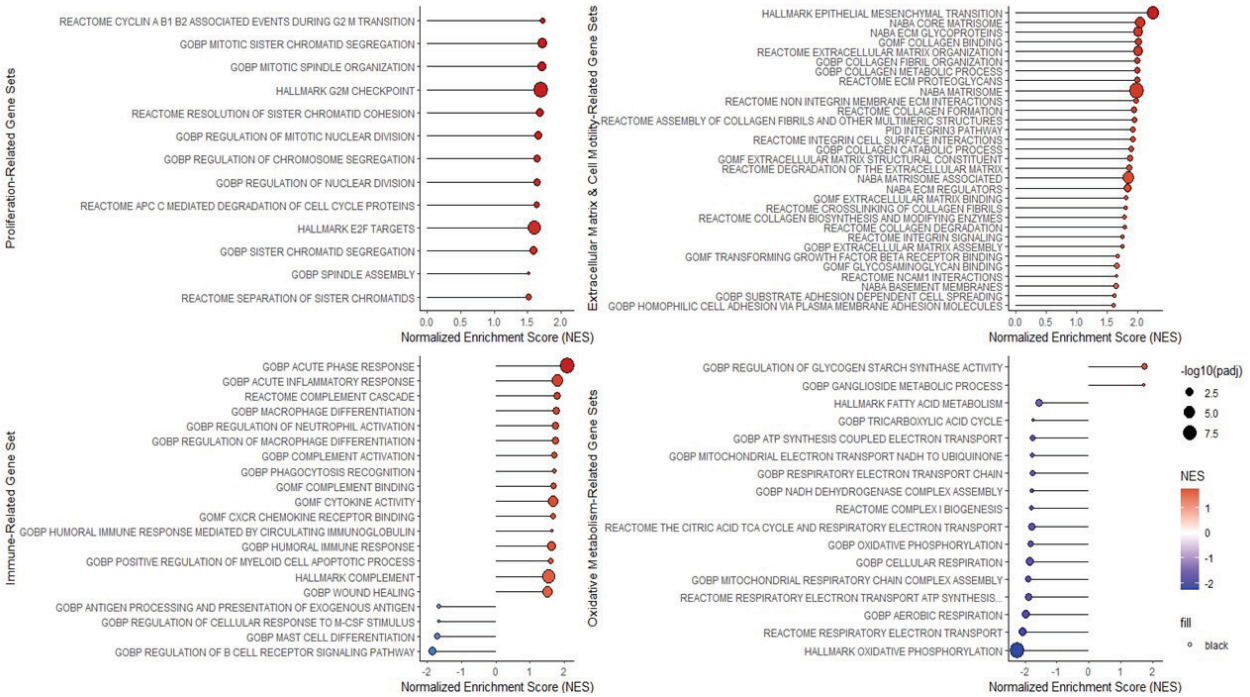
Gene expression matrices and associated metadata from The Oncology Research Information Exchange Network (ORIEN) as a discovery cohort, and The Cancer Genome Atlas Kidney Renal Clear Cell Carcinoma (TCGA-KIRC) and Clinical Proteomic Tumor Analysis Consortium (CPTAC) ccRCC as validation cohorts, were obtained. Patients with no adjuvant immunotherapy exposure were classified into one of two groups: Relapse (R) – patients who had disease relapse within 5 years after nephrectomy – or Non-Relapse (NR) – those without relapse for at least 5 years (3 years for CPTAC ccRCC) after nephrectomy. Patients with metastatic disease at the time of ccRCC diagnosis/nephrectomy were excluded. Clinical characteristics were summarized and compared between the two groups using Fisher's exact test. Single sample gene set enrichment analysis (ssGSEA) scores of Hallmark, IMmotion, and tertiary lymphoid structure signatures were assigned to cases utilizing TPM-normalized gene expression. GSEA of Hallmark, Reactome, and Gene Ontology pathways was performed on transcriptomic datasets. xCell immune deconvolution was also performed on normalized counts. Enrichment of gene set signature and deconvolution scores was compared via the Wilcoxon rank sum test between R versus NR groups. All analyses were performed with R version 4.4.2.

Results

In total, 152 (R: 66; NR: 86) patients in the ORIEN cohort, 166 (R: 91; NR 75) in TCGA-KIRC and 55 (R: 19; NR: 36) in CPTAC ccRCC were included. Higher T stage was more frequently seen in R than NR in all cohorts ($p<0.05$). When assessed by ssGSEA in the ORIEN cohort, the epithelial mesenchymal transition (EMT) ($p<0.05$) Hallmark pathway and IMmotion-derived complement cascade ($p<0.01$), and FAS pentose phosphate ($p<0.05$) molecular subset signatures were enriched in R, and these findings were all validated in the TCGA and CPTAC datasets. Immune-related (such as acute inflammatory response, macrophage differentiation, neutrophil activation, humoral immune response, and complement pathways), proliferation-related, and extracellular matrix/cell motility-related gene sets, including EMT, were significantly enriched in R, whereas oxidative metabolism-related gene sets were more enriched in NR (Figure). No difference in tertiary lymphoid structure signature expression was observed between R and NR. Immune deconvolution analysis revealed enrichment of NK T cells in R and eosinophils in NR in the ORIEN and TCGA datasets ($p<0.05$).

Conclusions

These findings suggest that programs associated with tumor aggression such as EMT and proliferation, IMmotion-derived complement cascade and FAS pentose phosphate pathways, alongside numerous inflammatory signals are contributing processes to disease relapse after nephrectomy in ccRCC. Such characteristics may have use as biomarkers for the identification of disease relapse, as well as



potential therapeutic targets for (neo)adjuvant strategies in patients with high-risk localized ccRCC. Ongoing work comparing immune cell compositions will further elucidate the immunological determinants of ccRCC disease fate following nephrectomy, creating avenues for the tailoring of perioperative therapy strategies.

Keywords

Clear cell renal cell carcinoma, relapse, RNA sequencing, adjuvant, neoadjuvant

54

Allogeneic HSPC-engineered CD70-directed CAR-NKT cells for renal cell carcinoma targeting tumor, microenvironment, and alloreactive T cells

Yan-ruide Li, Junhui Hu, Lili Yang, Lily Wu, Arnold I. Chin

University of California Los Angeles

Background

Renal cell carcinoma (RCC), originating from renal epithelium, is the most prevalent type of kidney cancer, accounting for over 90% of all cases. Although targeted therapies such as vascular endothelial growth factor (VEGF) and mammalian target of rapamycin (mTOR) inhibitors have improved clinical outcomes, approximately 33% of patients still progress to metastatic disease, with a 5-year survival of only 12%. These limitations highlight the urgent need for more effective and Innovative treatment options. Chimeric antigen receptor (CAR)-engineered T (CAR-T) cell therapy targeting CD70 is emerging as an attractive approach for RCC. Clinical trials investigating CD70-directed CAR-T (CAR70-T) cell therapies in RCC are currently underway. Despite their therapeutic potential, current CAR70-T cell therapies face several key limitations. Clinical responses have been modest, likely due to the inherent challenges posed by solid tumors, including antigen heterogeneity and a highly immunosuppressive tumor microenvironment (TME). To overcome these limitations, the development of potent, off-the-shelf CAR70-based cell therapies that can address RCC tumor immune evasion and TME-associated suppression is critically needed.

Methods

To address these challenges, we employed our previously established hematopoietic stem and progenitor cell (HSPC) gene engineering technology and a clinically guided culture method to generate allogeneic CD70-directed CAR-engineered invariant natural killer T (AlloCAR70-NKT) cells for the treatment of RCC. Through the use of a comprehensive array of experimental models, including primary RCC patient samples, patient-derived tumor cell lines, in vitro functional assays, and both orthotopic and metastatic in vivo xenograft models, we comprehensively evaluated the AlloCAR70-NKT cells, including their manufacturing, in vitro and in vivo antitumor efficacy, mechanism of action, pharmacodynamics and pharmacokinetics, safety, and immunogenicity.

Results

In this study, we characterize primary RCC patient samples and identify a distinct opportunity to leverage CAR-NKT cells for therapeutic intervention. Utilizing a clinically guided culture method, we successfully generated AlloCAR70-NKT cells from hematopoietic stem and progenitor cells, with high purity, robust expansion, and no fratricide risk. These cells demonstrated multimodal targeting capabilities, including potent cytotoxicity against orthotopic and metastatic RCCs via both CAR- and NK receptor-mediated mechanisms, as well as selective engagement of the immunosuppressive TME through TCR recognition. Notably, host alloreactive T cells express elevated levels of CD70 and can be efficiently targeted by AlloCAR70-NKT cells, leading to enhanced in vivo persistence of therapeutic cells.

Conclusions

Taken together, our findings support the therapeutic potential of AlloCAR70-NKT cells as a next-generation, off-the-shelf immunotherapy with dual tumor- and TME-targeting functionality, and the added advantage of alloreactive T cell elimination, offering a compelling strategy for treating RCC.

Keywords

Renal cell carcinoma (RCC); CD70; CD27; invariant natural killer T (NKT) cell; CAR-NKT cell; hematopoietic stem and progenitor cell (HSPC); clinically guided culture method; tumor microenvironment; alloreactive T cell; patient-derived xenograft (PDX) model; multimodal tumor killing

55

The Prognostic Role of Circulating Tumor DNA (ctDNA) Clearance as a Biomarker in Localized and Metastatic Renal Cell Carcinoma (RCC): A Single-Center Experience

Adanma Ayanambakkam[1], Rana McKay[2], Arnab Basu[3]

[1]Stephenson Cancer Center, University of Oklahoma Health Sciences Center, [2]University of California, San Diego, [3]University of Alabama at Birmingham

Background

The use of ctDNA-based molecular residual disease detection represents a promising prognostic biomarker in multiple solid tumors, yet limited data exist in RCC. This study aims to prospectively assess the utility of longitudinal ctDNA monitoring in localized and metastatic RCC.

Methods

We conducted a retrospective analysis on the use of longitudinal ctDNA testing in a single academic center for patients with RCC from 2022 - 2024. We used a clinically validated, personalized, tumor-informed, multiple PCR-NGS assay (Signatera, Natera, Inc.) to detect and quantify ctDNA. A total of 229 plasma samples from 69 patients were analyzed. Clinical data were collected on pathologic subtype, tumor stage and grade including the presence of sarcomatoid/rhabdoid features and type of treatment. ctDNA dynamics were categorized as follows : clearance, decrease, or increase in ctDNA levels. Treating physicians were not blinded to ctDNA results, no treatment decisions were made based on ctDNA dynamics.

Results

A total of 69 patients (mean age = 62, 23% female) with RCC were included in the analysis, (median: 3 samples/patient), with 33 (48%) having localized RCC and 36 (52%) having metastatic RCC (mRCC). Clear cell RCC was the predominant subtype, present in 61 (88%) patients. Among 33 patients with localized disease, 8 (24%) patients were on surveillance, and 25 (76%) patients received adjuvant pembrolizumab. Among 36 patients with mRCC, 32 (89%) patients were on systemic therapy and 4 (11%) patients were on surveillance. Among those with localized RCC, 1 (3%) patient was ctDNA positive 12 months after nephrectomy and, subsequently developed metastatic disease 1 month from ctDNA detection. Thirty-two (97%) patients with localized RCC and ctDNA negative results remained relapse-free with a median follow-up of 9 months. Among patients with mRCC, 22 (61%) patients were ctDNA positive, 12 (55%) achieved ctDNA clearance (10 after systemic therapy and 2 spontaneously on surveillance). Of these, 10 (83%) remained progression-free at a median follow-up of 11.5 months, while 2 had rise in ctDNA levels after clearance, correlating with disease progression. At median follow-up of 15 months (range 2 to 70 months), all 4 patients with radiographic progression had rising ctDNA levels (median lead time 4 weeks). One patient had rising ctDNA without evidence of radiographic progression.

Conclusions

Our findings highlight the potential of ctDNA detection and dynamics as a valuable prognostic biomarker for patients with both localized and metastatic RCC. These results support further prospective studies to establish the clinical utility of ctDNA clearance as a predictive marker in metastatic RCC

Keywords

Renal Cell Carcinoma, Circulating Tumor DNA

56

NPRL2 loss enhances DNA damage while isolating cGAS-STING pathway and conferring immunotherapy resistance

Xiande Liu, Muhammed Onel, Hongchao He, Xuesong Zhang, Yanting Zhang, Anh Hoang, Guang Peng, Eric Jonasch

MD Anderson Cancer Center

Background

Unrepaired DNA damage leads to the accumulation of cytosolic DNA and the activation of cGAS-STING-mediated inflammatory response, which modulates the tumor immune microenvironment and immunotherapy response. NPRL2 (NPR2 like, GATOR1 complex subunit) is located on chromosome 3p. Deep deletion of NPRL2 was identified in 10% of ccRCC, and is often mutually exclusive with loss of PBRM1, SETD2, and BAP1. However, it remains unclear whether NPRL2 loss independently influences DNA damage and anti-cancer immunity in ccRCC.

Methods

Both lentiviral shRNA-mediated knockdown and CRISPR/Cas9-mediated knockout were performed in human and murine RCC cell lines to suppress NPRL2 expression. The immunocompetent Renca-Balb/c murine RCC model was used to evaluate therapy response. The tumor immune microenvironment was analyzed using gene expression-based inference and immunohistochemistry (IHC).

Immunofluorescence, western blotting and real-time PCR were used for molecular studies.

Results

Guided by our reverse phase protein array (RPPA) results, we first found that NPRL2 loss activated the ATM-CHK2 DNA damage response pathway and led to the accumulation of cytosolic DNA. The lysosome is known to play important roles in DNA repair and cytosolic DNA degradation. We further found that NPRL2 loss promoted the phosphorylation of TFEB, the master regulator of lysosome biogenesis, and thus prevented its translocation to the nucleus. Pharmacologic activation of TFEB with ML-SA1 reduced ATM phosphorylation and cytosolic DNA accumulation, and lysosomal inhibition by chloroquine or bafilomycin A1 yielded the opposite results. However, genetic inhibition of autophagy by knocking down ATG5, ATG7, BECN1, or p62 had no apparent impact.

The increased cytosolic DNA led us to hypothesize that NPRL2 deficiency would consequently activate the cGAS-STING pathway. Unexpectedly, NPRL2 deficiency suppressed the cGAS-STING-mediated inflammatory response, as evidenced by dramatic decreases in TBK1 and IRF3 phosphorylation, and in downstream gene expression (e.g. CCL5, CXCL10 and IFNB1). To investigate the underlying mechanism, we first analyzed the expression of the key molecules that are involved in the cGAS-STING pathway. It turned out that NPRL2 loss reduced the expression of STING at both mRNA and protein levels.

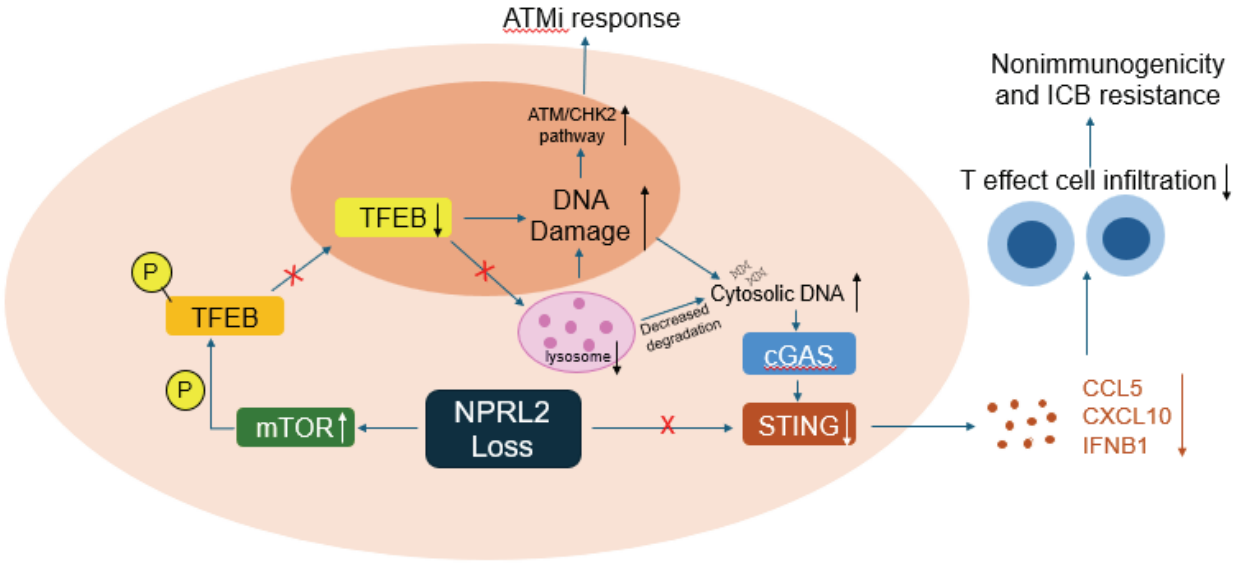
By analyzing the KIRC TCGA dataset, we found that low NPRL2 expression was associated with reduced T cell infiltration and immune checkpoint (CTLA4 and PDCD1) expression, reflecting an immunologically cold tumor microenvironment, which may respond poorly to immunotherapy. To test this hypothesis, we knocked down the expression of Nprl2 in Renca cells and found that Nprl2 loss reduced the complete response rate to anti-PD1 therapy in a syngeneic tumor model. However, NPRL2/Nprl2 loss sensitized RCC cells and Renca tumors to the ATM inhibitor KU60019, while the combination of KU60019 and anti-PD1 therapy showed no evidence of synergistic effect.

Conclusions

These results indicate that NPRL2 loss regulates DNA damage and cytosolic DNA accumulation via lysosomal but not canonical autophagic inhibition, and on the other hand, silences cytosolic DNA response by suppressing STING expression. NPRL2 loss defines a genomically unstable but nonimmunogenic tumor phenotype associated with checkpoint inhibitor resistance in RCC.

Keywords

RCC, NRPL2, DNA damage, cGAS, immunotherapy



57

VHL and TP53 mutation status are not associated with response or progression-free survival in metastatic renal cell carcinoma treated with VEGF-targeted therapies

Daniela Castro[1], Miguel Zugman[1], Peter Zang[1], Koral Shah[1], Hedyeh Ebrahimi[1], Regina Barragan-Carrillo[2], Salvador Jaime-Casas[1], Benjamin Mercier[1], Nazli Dizman[3], Nicholas Salgia[4], JoAnn Hsu[1], Charles Nguyen[1], Wesley Yip[1], Alexander Chehrazi-Raffle[1], Abhishek Tripathi[1], Sumanta Pal[1]

[1]City of Hope Comprehensive Cancer Center, [2]National Cancer Institute of Mexico, [3]Department of Medical Oncology, University of Texas MD Anderson Cancer Center, [4]Department of Immunology, Roswell Park Comprehensive Cancer Center

Background

VHL is the most commonly altered gene in clear cell renal cell carcinoma (ccRCC), but its value as a predictive biomarker for vascular endothelial growth factor (VEGF)-targeted therapies remains uncertain. Prior studies (e.g., Choueiri et al., 2017) found no association between VHL status and clinical outcomes in patients treated with early-generation VEGF inhibitors. Similarly, TP53 mutations have been associated with poor prognosis in RCC, though their relevance in the context of modern VEGF-directed therapy remains unclear. This study examined the relationship between circulating tumor DNA (ctDNA)-detected VHL and TP53 mutations and outcomes with VEGF-targeted therapies in patients with metastatic RCC (mRCC).

Methods

We retrospectively identified patients with mRCC who underwent Guardant360 ctDNA testing and subsequently received VEGF-targeted therapy. Patients were excluded if they did not receive a VEGF-targeted regimen after ctDNA testing. VEGF-targeted therapy was defined broadly to include newer generation vascular endothelial growth factor tyrosine kinase inhibitors (VEGF-TKIs; excluding agents like sunitinib), belzutifan, and VEGF-TKI–based combinations with immunotherapy or everolimus. Demographic and clinical characteristics—including age, sex, histology, best overall response (BOR), current treatment, and line of therapy—were summarized by mutation subgroup. Progression-free survival (PFS) was defined as the time from the start of VEGF-targeted therapy to radiographic progression, clinical deterioration, last follow-up, or death. Survival curves were estimated using the Kaplan–Meier method and compared using the log-rank test. Objective response rate (ORR), defined as complete or partial response (CR/PR), was stratified by mutation status and compared using Fisher's exact test. All analyses were performed using R (version 4.3.2).

Results

Among the 32 patients included, 87.5% had clear cell histology. The most common VEGF-targeted therapies were cabozantinib, lenvatinib, axitinib, and tivozanib, frequently administered in combination with immunotherapy or everolimus. VHL mutations were detected in 8 patients (25%) and TP53 mutations in 8 patients (25%). The difference in proportion of responders to non-responders in patients with VHL alterations was non-significant (44.0% responders in the VHL non-mutated cohort vs. 28.6% in the VHL mutated cohort, p = 0.671). This was also seen in the TP53 mutated vs non-mutated cohort (47.8% responders in the TP53 non-mutated cohort vs. 22.2% in the TP53 mutated cohort, p = 0.249). There was no significant difference in the PFS based on VHL mutation status or TP53 mutation status (8.0 months vs 4.2 months, p = 0.58 and 8.0 months vs. 4.1 months, p = 0.46 respectively).

Conclusions

In this ctDNA-based analysis of patients with mRCC treated with VEGF-targeted therapies, neither VHL nor TP53 mutation status was associated with meaningful differences in clinical outcomes. These findings align with prior reports and suggest that mutation status alone may not predict efficacy of VEGF-targeted regimens, even in the context of combination therapies.

Keywords

Biomarkers, ctDNA analysis

58

Dissecting the Interplay between Bap1 and Pbrm1 in Renal Cell Carcinoma

Bingqing Xie[1], Akhilesh Mishra[2], Ming Gao[2], James Brugarolas[1]

[1]UT Southwestern Medical Center, [2]National Institute of Technology Rourkela

Background

Polybromo 1 (PBRM1) and BRCA1-associated protein 1 (BAP1) are tumor suppressor genes frequently mutated in clear cell renal cell carcinoma (ccRCC) with distinct contributions to tumor grade and aggressiveness that are mutually exclusive. Interestingly, rare double-mutant tumors are particularly aggressive and associated with worse prognosis.

Methods

To understand the effects of simultaneous inactivation of PBRM1 and BAP1 we generated conditional double mutant mouse models. We introduced variant LoxP sites flanking essential Bap1 sequences in Pbrm1F/F zygotes using CRISPR/Cas9 overcoming thereby barriers associated with genetic linkage. We then investigated the developmental and oncogenic consequences of Bap1/Pbrm1 co-inactivation using different Cre drivers. Next, we evaluated the impact of simultaneous inactivation of Bap1 and Pbrm1 in the kidney using a Pax8-Cre driver (double knockout [DKO mice]). To further explore the role of Bap1 and Pbrm1 in ccRCC development, we generated mice with simultaneous inactivation of the von Hippel-Lindau (Vhl) gene (triple knockout [TKO mice]). To probe ccRCC pathogenesis, we performed both RNA-seq and GeoMx spatial transcriptomic profiling in DKO and TKO mice.

Results

In the embryonic model, simultaneous inactivation of Bap1 and Pbrm1 in embryos using a CAG-Cre accelerated embryonic lethality. Developmental defects were observed as early as E7.5, compared to the previous established developmental defects for Bap1 and Pbrm1 loss at E8.5 and E11.5, respectively. This finding supports the idea that simultaneous inactivation of Bap1 and Pbrm1 accentuates developmental phenotypes.

Using Pax8-Cre driver, compared to Bap1F/F and Pbrm1F/F mice, we found that kidneys of DKO mice developed cystic tumors, suggesting that loss of Bap1 and Pbrm1 alone is sufficient for tumorigenesis. Interestingly, TKO mice developed aggressive ccRCC tumors that differed from those observed in DKO mice.

Interestingly, we observed that tumor grade was a more important driver of gene expression than genotype. In addition, while Pbrm1-deficient tumors exhibited a metabolic shift from oxidative phosphorylation to glycolysis (consistent with the Warburg effect), Bap1 loss was associated with immune cell activation and mesenchymal features. GeoMx spatial transcriptomic analyses showed that DKO tumors were enriched for T-effector and complement cascade signatures, while TKO tumors showed increased angiogenesis and fatty acid metabolism.

Conclusions

Together, our results suggest that BAP1 and PBRM1 are infrequently mutated together because of developmental synthetic lethality, but when co-occurring with VHL loss, can drive aggressive tumor phenotypes. This study highlights the genetic crosstalk between key tumor suppressors in shaping RCC evolution and heterogeneity.

Keywords

Clear cell renal cell carcinoma, PBRM1 and BAP1 double mutant, genetic engineered mouse model, spatial transcriptomic

59

Real-World Efficacy and Safety of Belzutifan in Sporadic Metastatic Renal Cell Carcinoma: A Multicenter Study from The City of Hope Enterprise

Charles Nguyen, Kim Nguyen, Hedyeh Ebrahimi, Miguel Zugman, Peter Zang, Evan Pisick, Sudarsan Kollimuttathuillam, Nilesh Mehta, Sandy Liu, Abhishek Tripathi, Alexander Chehrazi-Raffle, Bamidele Adesunloye, Alan Bryce, Tanya Dorff, Sumanta Pal

City of Hope Comprehensive Cancer Center

Background

Belzutifan is a novel HIF-2α inhibitor approved for use in Von Hippel-Lindau (VHL)-associated tumors and sporadic clear cell metastatic renal cell carcinoma (mRCC) following prior treatment with immune checkpoint inhibitor (IO) and tyrosine kinase inhibitor (TKI). However, real-world data on its efficacy and safety in patients with mRCC not represented in clinical trial remains limited.

Methods

We conducted a multicenter, retrospective study of patients with sporadic mRCC treated with belzutifan across the City of Hope Cancer Center enterprise in the United States. Clinical information and disease characteristics were abstracted from electronic medical records. Data were analyzed for objective response rate (ORR), disease control rate, progression-free survival (PFS), and overall survival (OS). Adverse events (AEs) were also recorded and graded per CTCAE v5.0.

Results

Between 2023 and 2025, 43 patients with sporadic mRCC received belzutifan. Among them, 26% were Hispanic and 70% identified as male. Median age at therapy initiation was 67 years (range 21-86). Clear cell histology was the most common (91%); one patient had mixed clear cell and papillary RCC; one patient had chromophobe histology with somatic VHL mutation; one patient had unclassified RCC. Sarcomatoid and rhabdoid features were present in 19% and 12%, respectively. At the start of therapy, baseline liver

metastases and peritoneal disease were present in 33% and 19% of patients, respectively; 30% had bone metastases. The median number of prior lines of therapy in the metastatic setting was 3 (range 0-6), with the majority of whom received prior IO (95%) and prior TKI (88%). A total of 79% of patients previously had a nephrectomy, of whom 12% had prior adjuvant therapy. Among the 36 patients with available interval imaging after starting belzutifan, the ORR was 25% (9/36) with 9 patients having a partial response and no complete responses; 15 patients had stable disease and 13 had disease progression. The disease control rate was 64%. The median OS was 6.93 months (95% CI: 3.75-12.58). The median PFS was 3.09 months (95% CI 2.53-5.72). AEs of any grade were reported in 93% of patients. The most common all-grade AEs were anemia (79%), fatigue (30%), hypoxia (14%), and dyspnea (9%). Frequent grade 3-5 AEs included anemia (68%) and hypoxia (16%). Treatment interruption and dose reduction occurred in 16% and 26% of patients, respectively. Belzutifan discontinuation due to AEs occurred in 12%.

Conclusions

In this diverse and heavily pretreated cohort of patients with sporadic mRCC and higher frequency of visceral metastases, belzutifan had similar ORR but shorter OS and PFS compared to prior clinical trial observations. The safety profile remained consistent with previous reports. A key limitation of this study is that belzutifan was frequently initiated late in the disease course which may have limited observed efficacy.

Keywords

Belzutifan, real-world data, kidney cancer

60

Systemically Administered Oncolytic Vaccinia Virus Enhances the In Vivo Antitumor Effects of RTKI and Anti-PD-1 Based Therapies in an Immunocompetent Renal Cancer Model

Ngoc Huong Giang Tran[1], Carolina Merchan Mendes[1], Valery Chavez[1], Melissa Montero[1], Wieder Eric[1], Jaime Merchan[2]

[1]University of Miami, [2]University of Miami Leonard M. Miller School of Medicine

Background

While significant advances have been made in the treatment of metastatic renal cell carcinoma (RCC), most patients develop treatment resistance and succumb to progressive disease. Limited options exist for patients checkpoint inhibitor (CPI) and/or receptor tyrosine kinase inhibitor (RTKI) based therapies, underscoring the urgent need to develop novel strategies for RCC. The oncolytic vaccinia virus (VV) is a promising antitumor agent undergoing clinical development in RCC and other cancers. The objectives of this study are to characterize the in vivo effects and mechanisms of oncolytic VV in combination with RTKIs and checkpoint inhibitors in RCC.

Methods

The oncolytic effects of VV expressing human (JX-594) or murine (mJX-594) GMCSF, on human and murine renal cancer cell lines were assessed (xCELLigence). The effects of VV on human RCC hypoxia, metabolism, and survival pathways were assessed by RPPA analysis. The effects of mJX-594 on the tumor immune microenvironment were investigated in the immunocompetent RENCA murine model through transcriptomic analyses and imaging mass cytometry to delineate immune cell infiltration and gene expression signatures. The effects of VV in combination with the RTKI Cabozantinib (C) on viral oncolysis and replication were determined. The in vivo anti-tumor effects of mJX-594, Cabozantinib and anti-PD-1 antibodies alone and in combination (doublets vs. triplet) were determined in the RENCA model. Tumor correlative studies were performed to characterize the mechanisms of VV-Cabozantinib-anti-PD-1 combinations.

Results

Potent in vitro oncolysis and efficient viral replication were observed in human and murine RCC cells after VV infection. Viral oncolysis was associated with significant modulation of metabolism, survival and hypoxia pathways. Mass cytometry analysis showed a significant increase in immune cell infiltrates, especially neutrophils, after VV treatment. NanoString gene expression data confirmed VV-induced regulation of immune pathways, with strong increases in neutrophils, T cells, and cytotoxic T cells. In vitro, Cabozantinib did not interfere with vaccinia viral replication or with viral oncolysis in human or murine RCC cell lines. In vivo, while Cabozantinib, and treatment doublets had enhanced antitumor activity compared to single agents, the mJX-594, Cabozantinib and anti-PD-1 antibody combination was associated with more profound and prolonged antitumor activity and survival. Correlative tumor studies showed enhanced VV tumor penetration by Cabozantinib, decreased tumor angiogenesis and enhanced apoptosis by VV.

Conclusions

This is the first report demonstrating that the oncolytic VV significantly enhances the in vivo antitumor effects of RTKI+CPI combination therapy in an immunocompetent renal cancer model. The non-overlapping mechanisms of VV

oncolysis, as well as cabozantinib enhancement of VV tumor penetration, leading to enhanced apoptosis may explain the effects of the virus-drug combination. The superiority of the triplet compared to doublets (C+VV or C+anti-PD-1) suggests that oncolytic viruses, in particular oncolytic VV can synergize with current anti-RCC therapies.

Keywords

Renal cell carcinoma, oncolytic vaccinia virus, tumor microenvironment

61

Predicting Immunotherapy Response in ccRCC using Deep Learning on Histopathological Slides

Satwik Rajaram, Averi Perny, Jay Jasti, Vipul Jarmale, Hua Zhong, Alana Christie, James Brugarolas, Payal Kapur

UT Southwestern Medical Center

Background

Immune checkpoint inhibitors (ICI) are a cornerstone of treatment for metastatic clear cell renal cell carcinoma (mccRCC), yet a significant proportion of patients do not achieve durable responses, while often experiencing immune-related adverse events. There are currently no robust, validated biomarkers to guide therapy selection in the clinic. Retrospective analysis of clinical trial data (e.g. IMmotion150/151 and Javelin) suggest RNA based readouts of immune activity can predict response to ICI. While RNA-based signatures of immune activity have shown promise in research settings for predicting ICI response, their clinical adoption is hampered by high costs and standardization challenges. Furthermore, these bulk assays typically fail to capture crucial spatial information regarding immune cell infiltration and are susceptible to intra-tumor heterogeneity, which may contribute to their variable predictive performance across clinical trials.

Methods

To address these limitations, we developed a deep learning (DL) approach to quantify immune infiltration directly from routinely processed hematoxylin and eosin (H&E) stained histopathology slides, offering a cost-effective and spatially resolved alternative. We build upon an H&E based strategy previously validated by our group, where our prediction of an RNA angiogenesis score by identifying tumor vasculature matched the RNA score's performance for Sunitinib response prediction in the IMmotion150 trial. Our method involves a DL model trained to classify individual nuclei as tumor, endothelial, immune (CD8+ as a key subset), or other, utilizing immunohistochemistry (PAX8 for tumor, ERG for endothelial, CD8 for cytotoxic T-cells) as ground truth for supervised learning. A separate segmentation model delineated tumor regions. We derived an 'H&E DL Immune Score' based on the proportion of immune cells within these tumor regions and validated its correlation with a previously established RNA T-effector signature score. Furthermore, we evaluated the prognostic significance of the H&E DL Immune Score for predicting time to next treatment (TNT) in a real-world cohort of mccRCC patients treated with first-line ipilimumab-nivolumab (Ipi-Nivo) at our institution. We also investigated whether incorporating information from multiple slides per patient and the spatial proximity of immune cells to tumor regions could enhance predictive accuracy.

Results

The H&E DL Immune Score showed a strong correlation (Spearman r = 0.77) with the RNA T-effector score in a validation cohort. The H&E DL Immune Score (derived from tumor areas) predicted TNT with a concordance index (C-index) of 0.60. Notably, the predictive performance improved to 0.75 upon incorporating immune cells within a 0.5mm radius of the tumor regions for patients with multiple slides.

Conclusions

DL-based H&E analysis provides a cost-effective and readily implementable proxy for RNA-based immune signatures. The achieved C-index values (up to 0.75) are comparable to or exceed those reported for other investigational biomarkers for ICI response in mccRCC. Thus, our H&E DL Immune Score shows significant promise for predicting response to ICI therapy in mccRCC patients, with the potential to be developed into a clinically valuable biomarker to be evaluated prospectively in clinical trials.

Keywords

ccRCC, Immunotherapy Biomarkers, Histopathology, Machine Learning

62

The SLC1A1/EAAT3 Dicarboxylic Amino Acid Transporter is an Epigenetically Dysregulated Nutrient Carrier that Sustains Oncogenic Metabolic Programs

Treg Grubb[1], Pooneh Koochaki[1], Sayed Matar[2], Fatme Ghandour[2], Marc Machaalani[3], Eddy Saad[3], Cerise Tang[4], Eduard Reznik[5], Jesminara Khatun[5], Carleigh Salem[5], Noah Dubasik[6], David A. Orlando[6], Matthew G. Guenther[6], Gyanu Parajuli[6], Raghvendra M. Srivastava[6], Steven R. Martinez[6], Jesse Coker[1], Ritesh Kotecha[5], A. Ari Hakimi[5], John Asara[7], Timothy Chan[7], Sakari Vanharanta[7], Shaun Stauffer[1], William G. Kaelin Jr.[8], Sabina Signoretti[9], Toni Choueri[3], Abhishek Chakraborty[6]

[1]Cleveland Clinic, [2]Yale School of Medicine, [3]Dana-Farber Cancer Institute, [4]Yale University, [5]Memorial Sloan Kettering Cancer Center, [6]Cleveland Clinic & Case Western Reserve University, [7]Beth Israel Deaconess Medical Center, Harvard Medical School, [8]Dana-Farber Cancer Institute, Harvard Medical School, [9]Brigham and Women's Hospital

Background

Epigenetic dysregulation, including accumulation of Histone H3 lysine 27 acetylation (H3K27ac), is a hallmark of pVHL-deficient clear cell Renal Cell Carcinomas (ccRCCs). H3K27ac is associated with transcriptional activation and its accumulation at cis-regulatory elements (e.g., promoters and enhancers/super-enhancers) marks key oncogenes and regulators of cellular identity in many cancers. In ccRCC, specific alterations in H3K27ac have been linked to tumorigenesis and metastatic progression. Importantly, these earlier studies largely relied on the HIF2α-dependent 786-O cells (or their metastatic derivatives), perhaps, missing the importance of HIF-independent epigenetic programs. Altogether, we hypothesized that H3K27ac marks critical genes in pVHL-deficient ccRCCs that sustain tumorigenic and metastatic programs via both HIF-dependent and independent mechanisms.

Methods

Using an in vivo positive selection ORF screen in poorly tumorigenic pVHL-proficient cells and cell-based mechanistic studies in pVHL-deficient cells, we discovered that the aspartate (Asp) and glutamate (Glu) transporter, SLC1A1/EAAT3, is a metabolic oncogenic dependency in ccRCC.

Results

pVHL loss promotes HIF-independent SLC1A1 expression via H3K27ac dysregulation. SLC1A1 inactivation, using either genetic or pharmacological approaches, depletes Asp/Glu-derived metabolites [e.g., Tricarboxylic acid (TCA) cycle and nucleotide intermediates], impedes ccRCC growth, and sensitizes ccRCCs to anti-metabolite drugs (e.g., glutaminase blockers). In human tumors, higher SLC1A1 expression is associated with reduced immune infiltration, oncogenic metabolic programs, and advanced stage/metastatic disease. Finally, in ccRCC animal models, SLC1A1 inactivation diminishes lung metastasis and the outgrowth of established renal tumors.

Conclusions

Altogether, our studies credential SLC1A1 as a novel, actionable, HIF-independent, metabolic dependency in pVHL-deficient ccRCCs.

Keywords

Metabolism, H3K27ac, HIF-independent

63

Plasma Proteomic Profiling Reveals Distinct Mitochondrial Signatures in Chromophobe Renal Cell Carcinoma

Clara Steiner[1], Hadi Mansour[2], Wafaa Bzeih[2], Tiegang Han[2], Eddy Saad[1], Jessica F. Williams[2], Michelle S. Hirsch[2], Yehonatan Elon[3], Adam P. Dicker[4], Toni Choueri[1], Elizabeth P. Henske[2], Wenxin (Vincent) Xu[1]

[1]Dana-Farber Cancer Institute, [2]Brigham and Women's Hospital, [3]Oncohost, Binyamina-Giv'at Ada, Israel, [4]Thomas Jefferson University

Background

Chromophobe renal cell carcinoma (chRCC) is a rare kidney cancer subtype that can be challenging to differentiate histologically. Improved molecular classification is essential for accurate diagnosis and potential therapeutic targeting. SomaScan, a high-throughput aptamer-based proteomic platform, enables quantification of thousands of proteins in plasma and offers a promising approach to identify clinically relevant biomarkers for chRCC.

Methods

We analyzed plasma proteomic profiles from 215 patients with renal cell carcinoma using SomaScan, including 18 chRCC and 197 clear cell renal cell carcinoma (ccRCC) samples. After

identifying proteins significantly upregulated in chRCC (log_2 fold change > 1 and adjusted p-value < 0.05), a reproducibility-focused feature selection strategy was employed to prioritize proteins most consistently associated with chRCC. These upregulated proteins were used as input features for the Least Absolute Shrinkage and Selection Operator (LASSO) machine learning algorithm. To enhance the stability and reproducibility of feature selection, we implemented a bootstrap strategy: 100 bootstrap datasets were created by randomly sampling the rows of the upregulated protein matrix with replacement. In each of 100 bootstrap replicates, we randomly sampled with replacement to create a training set, performed LASSO logistic regression for feature selection and model fitting, and evaluated the resulting model on the out-of-bag (OOB) test samples.

Results

Of 7,289 proteins measured, 215 were significantly upregulated in chRCC compared to ccRCC. Unsupervised clustering revealed that the majority of chRCC samples formed a distinct group, suggesting a unique proteomic signature. Notably, chRCC plasma showed strong enrichment of mitochondrial and metabolic proteins, reflecting the tumor's distinct bioenergetic profile.

Several mitochondrial enzymes were among the most upregulated proteins in chRCC. These included ECH1 (log_2FC = 1.81) and ECI1 (log_2FC = 1.66), involved in fatty acid β-oxidation, as well as ALDH6A1 (log_2FC = 2.33), which participates in valine and pyrimidine catabolism. Elevated expression of PCK2 (log_2FC = 1.06), a gluconeogenesis enzyme, and creatine metabolism enzymes such as CKMT1A (log_2FC = 1.07) and GATM (log_2FC = 2.24) could further highlight the distinctive metabolic profile of chRCC. Upregulation of MRPL14 (log_2FC = 1.06), a mitochondrial ribosomal protein, suggests increased mitochondrial biogenesis and translational activity. These findings underscore a bioenergetic program in chRCC that contrasts with the glycolytic phenotype characteristic of ccRCC.

In addition to mitochondrial proteins, we observed differential expression of proteins involved in intracellular trafficking and extracellular matrix remodeling. ARL15 (log_2FC = 1.24), a GTPase involved in vesicle transport and metabolic regulation, was upregulated in chRCC. KLK15 (log_2FC = 1.52), a kallikrein family protease, may play a role in extracellular matrix remodeling.

Conclusions

Plasma proteomic profiling revealed a distinct mitochondrial-based signature in chRCC, offering novel insights into its biology and supporting accurate diagnostic classification. The identified proteins reflect key biological processes such as oxidative metabolism and metabolic adaptation —features that distinguish chRCC from ccRCC and may inform future diagnostic and therapeutic strategies.

Keywords

Chromophobe renal cell carcinoma, non-clear cell RCC, biomarker

64

Defining Cancer Initiating Cells and their Vulnerabilities in Renal Cell Carcinoma

Zohreh Mehrjoo[1], Hellen Kuasne[2], Ariel Madrigal Aguirre[1], Ali Shahini[1], Matthew G Annis[2], Anne-Marie Norah Fortier[2], Tianyuan Lu[3], Larisa Morales Soto[1], Hong Zhao[2], Dongmei Zuo[2], Virginie Pilon[2], Matthew Dankner[2], Tamiko Nishimura[1], Kevin Petrecca[4], Jonathan Spicer[5], Peter Siegel[2], Simon Tanguay[6], Hamed Shateri Najafabadi[1], Morag Park[2], Yasser Riazalhosseini[1]

[1]Department of Human Genetics, McGill University, Victor Dahdaleh Institute of Genomic Medicine, [2]Rosalind and Morris Goodman Cancer Research Institute, McGill University, [3]Lady Davis Institute for Medical Research, [4]Montreal Neurological Institute and Hospital, McGill University, [5]Cancer Research Program, Research Institute of the McGill University Health Centre, [6]Department of Surgery, Division of Urology, McGill University Health Center, McGill University

Background

Clear cell renal cell carcinoma (ccRCC) is the most common form of kidney cancer, leading to 179,000 cancer-related deaths annually. ccRCC initiating cells (CICs) are thought to drive tumor initiation, growth, therapy resistance, and metastasis, yet their molecular characteristics remain poorly defined. This study aims to identify putative CICs and their essential genes using a cell marker-agnostic strategy.

Methods

We performed a comprehensive analysis of ccRCC transcriptomes at single-cell resolution, developed patient-derived xenograft (PDX) and 3D patient-derived organoids (PDO) models of ccRCC, and conducted functional examinations in these models to investigate our findings.

Results

Computational modeling of tumor formation using single-cell RNA velocity analysis of five primary and metastatic ccRCC-PDXs revealed a minor cell population as the origin

of other tumor cells, representing putative CICs. Pathway and network analyses suggested that a core network of proteins, conventionally known to regulate mitosis, are highly active in CICs and may be essential for their function. These proteins were expressed in PDOs and PDX-derived spheroids established following a CIC enrichment protocol. Spheroid cells exhibited higher tumorigenicity and colony formation ability than parental tumor cells, as confirmed by in-vivo injection in nude mice and in-vitro colony formation assays. Successive in vivo passaging confirmed the self-renewal capacity of spheroid-derived tumors. Pharmacological blockade of candidate proteins elicited dose-dependent inhibitory effect on spheroid and colony formation, with in-vivo validation showing that blocking these proteins significantly delayed tumor growth and more efficiently prevented tumor formation in mice. These results highlight the importance of these proteins in the cancer-initiating abilities of malignant cells. Interestingly, our results suggest that the identified target proteins may elicit their CIC-related function independently from their mitosis regulatory roles.

Conclusions

We identified and validated essential proteins in RCC-CICs, supported by single-cell transcriptome data and RCC spheroids and PDX models. Targeting the vulnerabilities of RCC-CICs, given their role in tumor initiation, progression, and therapy resistance, offers significant potential for developing new anti-cancer therapies.

Keywords

Cancer Initiating Cells, Single Cell RNA Sequencing, Spheroids, Organoids, PDX

65

Treatment Patterns and Attrition Rates for Metastatic Non-Clear Cell Renal Cell Carcinoma in the US

Zeynep Irem Ozay[1], Yeonjung Jo[1], Chadi Hage Chehade[1], Micah Ostrowski[1], Georges Gebrael[1], Nicolas Sayegh[1], Ayana Srivastava[1], Richard Ji[1], Diya Garg[1], Tanner Hardy[1], Edwin Lin[1], Neeraj Agarwal[1], Benjamin Maughan[1], Haoran Li[2], Umang Swami[1]

[1]Huntsman Cancer Institute at the University of Utah, [2]University of Kansas Cancer Center

Background

Non-clear cell renal cell carcinoma (nccRCC) represents 25% of subtypes of kidney cancer and portends a poor prognosis [PMID: 37823185]. Given their rarity, clinical trial data to guide systemic therapy for metastatic disease are limited, and they are often treated similarly to clear cell RCC. Herein, we sought to assess treatment patterns and attrition rates of patients with metastatic nccRCC in a real-world nationwide database.

Methods

We utilized the nationwide Flatiron Health electronic health record (EHR)-derived de-identified database. Eligibility: patients diagnosed with metastatic nccRCC (chromophobe, papillary, not otherwise specified [NOS]). Patients treated on clinical trials or with non-recommended chemotherapy regimens were excluded. Treatment patterns by line (L) of therapy and attrition rates by nccRCC subtype were collected.

Results

Of 13,909 patients diagnosed with metastatic RCC from 1/1/2011 to 10/16/2024, 2,607 patients had metastatic nccRCC, received eligible 1L therapy, and were included in our analysis (chromophobe 166 [6.4%]; papillary 740 [28.4%]; NOS 1,701 [65.2%]). Treatment patterns and attrition rates by histological subtype are summarized in Table. Of 166 patients with chromophobe RCC, 57.2% received 2L and 34.3% of patients received 3L. Tyrosine kinase inhibitors (TKIs) were the most common treatment in 1L (50%) and 2L (38.9%), while both TKI and single-agent PD-1 inhibitors (PD-1i) were used similarly in 3L (26.3%, each). Of 740 patients with papillary RCC who received 1L, 59.7% received 2L and 28.9% received 3L. TKIs were the most common treatment in 1L (48.4%), 2L (36.7%), and 3L (34.6%). Of 1701 patients with NOS, 41.3% received 2L, and 17.6% received 3L. TKIs again were the most common treatment in 1L (48.7%), 2L (34.7%), and 3L (41.5%).

Table. Treatment patterns by line (L) of therapy in metastatic non-clear cell renal cell carcinoma

	Chromophobe			Papillary			NOS		
Treatment, n (%)	1L N=166	2L N=95	3L N=57	1L N=740	2L N=442	3L N=214	1L N=1701	2L N=703	3L N=299
TKI	83 (50)	37 (38.9)	15 (26.3)	358 (48.4)	162 (36.7)	74 (34.6)	828 (48.7)	244 (34.7)	124 (41.5)
PD-1i	9 (5.4)	19 (20)	15 (26.3)	86 (11.6)	109 (24.7)	47 (22)	154 (9.1)	181 (25.7)	51 (17.1)
PD-1i + CTLA4i / PD-1i + TKI	17 (10.2) / 18 (10.8)	8 (8.4) / 6 (6.3)	1 (1.8) / 7 (12.3)	81 (10.9)/ 114 (15.4)	26 (5.9)/ 47 (10.6)	13 (6.1)/ 26 (12.1)	301 (17.7)/ 229 (13.5)	28 (4) 94 (13.4)	9 (3)/ 29 (9.7)
Bevacizumab	1 (0.6)	1 (1.1)	4 (7)	4 (0.5)	18 (4.1)	4 (1.9)	13 (0.8)	12 (1.7)	11 (3.7)
Bevacizumab+erlotinib / Bevacizumab+everolimus	0 / 2 (1.2)	0 / 1 (1.1)	0 / 1 (1.8)	8 (1.1)/ 0	7 (1.6)/ 0	6 (2.8)/ 0	0/ 0	0/ 1 (0.1)	0/ 0
Everolimus	11 (6.6)	9 (9.5)	7 (12.3)	17 (2.3)	26 (5.9)	16 (7.5)	26 (1.5)	64 (9.1)	16 (5.4)
Lenvatinib + everolimus	11 (6.6)	5 (5.3)	4 (7)	4 (0.5)	14 (3.2)	11 (5.1)	5 (0.3)	17 (2.4)	25 (8.4)
Other	14 (8.4)	9 (9.5)	3 (5.3)	68 (9.2)	33 (7.5)	17 (7.9)	145 (8.5)	62 (8.8)	34 (11.4)

(i = inhibitor)

Conclusions

In one of the largest real-world studies evaluating treatment patterns and attrition rates in patients with metastatic nccRCC, TKI was the most commonly used treatment across chromophobe, papillary, and NOS subtypes. These data could help guide clinical trial design.

Keywords

Non-clear cell renal cell carcinoma, treatment trends, attrition trends

66

Patient Perceptions of Biomarker Testing in Kidney Cancer (KC) from the International Kidney Cancer Coalition (IKCC) Global Patient Survey (GPS)

Eric Jonasch[1], Michael Jewett[2], Laurence Albiges[3], Stênio de Cássio Zequi[4], Axel Bex[5], Margaret Hickey[6], Christine Collins[7], Karin Kastrati[8], Jyoti Patel Shah[9], Deborah Maskens[6]

[1]MD Anderson Cancer Center, [2]Princess Margaret Cancer Centre and University of Toronto, [3]Institut Gustave Roussy, [4]A.C. Camargo Cancer Ctr & Nat'l Inst for Science & Tech. in Oncogenomics & Ther Innovation, Brazil, [5]Royal Free London NHS Foundation Trust, UK & The Netherlands Cancer Institute, Netherlands, [6]International Kidney Cancer Coalition (IKCC), Netherlands, [7]Kidney Cancer Canada, Ontario, Canada, [8]Nierenkrebs-Netzwerk Deutschland e.V., Germany, [9]V Care Foundation, India

Background

Recent advancements in kidney cancer research have focused on developing and validating new biomarkers for earlier diagnosis, improved prognosis, and personalized treatment strategies. Patient reception of biomarkers can be complex, influenced by factors like familiarity with the testing, health literacy, and communication with healthcare providers. Since 2018 through a biennial GPS, IKCC & its network has captured insights on the pt experience with diagnosis, management and the burden of kidney cancer to identify unmet needs & country variances to help guide development

of action recommendations. We present here the findings related to patient perceptions on the use of biomarker testing to determine treatment selection in the future.

Methods

The survey, designed by an IKCC steering committee of patient advocates, medical experts and the Picker Institute, targeted KC patients and carers. It was cognitively tested, translated into 16 languages, and hosted online. Countries with historic response rates greater than 100 were provided an opportunity to ask five additional questions unique to their local needs of the respondents in their country. Data analysis used cross-tabulations.

Results

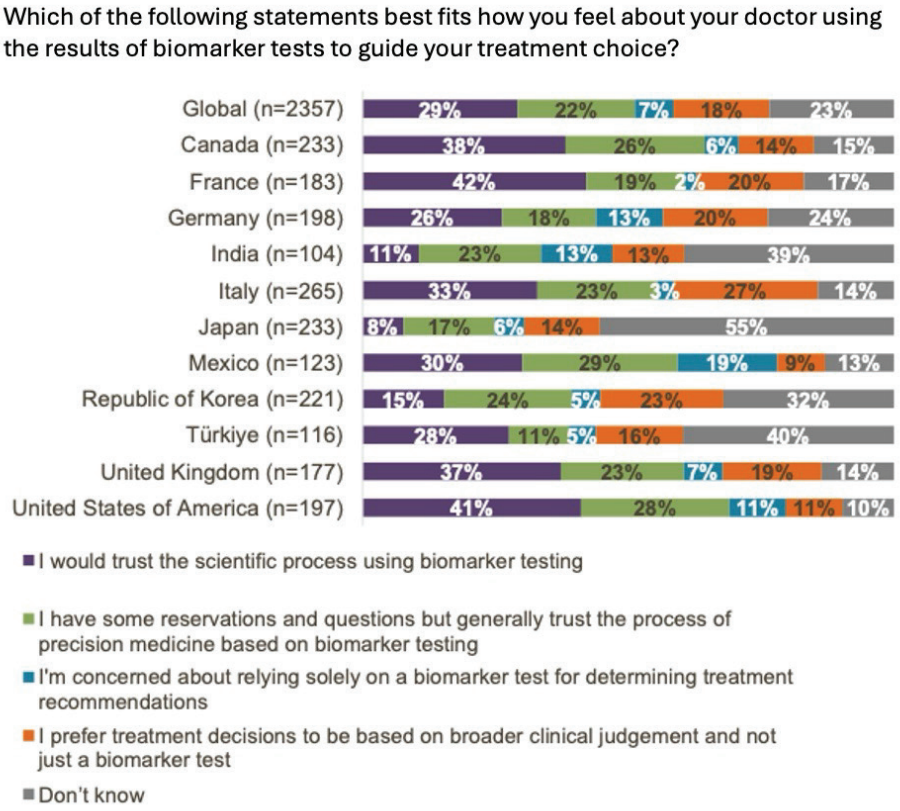
2677 responses (2049 patients, 628 carers) from 46 countries were collected between September 24 and November 15, 2024. Respondents: 54% male; 80% aged 46–80; 62% ccRCC; 19% stage 4 at diagnosis; 52% were diagnosed in the past four years. Globally, when asked how they would feel about their doctor using the results of potential future biomarker tests to guide their treatment choice, 29% would trust biomarker testing, 22% have some reservations and questions but generally trust the process, 25% were concerned about relying only on a biomarker test and (23%, n=552) did not know. These results vary significantly by country, but variances were noted by age, sex, and stage of disease. In the USA (n=220) additional questions specific to US respondents were asked probing patient involvement and interest in personalized treatment strategies, circulating tumor cells and genomic testing. Circulating Tumor Cells: 13% were offered the test with 12% being tested, 63% were not offered testing but would like to have had it offered. Genomic Testing: 27% were offered the test and were tested, 53% were not offered testing but would like to have been.

Conclusions

IKCC GPS is the only worldwide KC survey measuring the experiences of people affected by KC and captured feedback from a record number of respondents. Most patients have some reservations about the use of biomarkers to guide treatment decisions in the future which can be addressed with appropriate education in the shared decision-making process. In the USA, most patients were receptive to circulating tumor cells and/or genomic testing. Patient education addressing the role of biomarkers is essential for clinical research studies and KC care in the future to ensure patients can make informed decisions. Questions about the willingness to pay for potential biomarker tests when available, and the bioethical concerns of positive germline genetic testing should be considered in future surveys.

Keywords

Kidney cancer, Patient Survey, Biomarkers, Patient Education



67

Generating Syngeneic NF2 models of Unclassified Renal Cell Carcinoma

Nicole Rittenhouse[1], Amrita Nargund Mangalvedhekar[1], Samir Zaidi[2], A. Ari Hakimi[1]

[1]*Memorial Sloan Kettering Cancer Center*, [2]*Yale Cancer Center*

Background

Renal cell carcinoma (RCC) comprises of several histological subtypes, with clear cell RCC (~75%), papillary RCC (~15%), and chromophobe RCC (~5%) being the most prevalent. Unclassified RCC (uRCC) accounts for 4–5% of cases that do not align with these major subtypes and is typically aggressive with recurrent mutations in tumor suppressor genes such as NF2, SETD2, CDKN2A, and BAP1. A subset of uRCC defined by NF2 loss exhibits dysregulation of the Hippo–YAP pathway and is associated with poor clinical outcomes. NF2-deficient RCC show limited response to standard therapies, including immune checkpoint inhibitors and VEGFR tyrosine kinase inhibitors. Prior studies using CRISPR-Cas9–based genetically engineered mouse models (GEMMs) have demonstrated that combined loss of CDKN2A/B, NF2, and SETD2 drives tumorigenesis and metastasis. However, the immunologic landscape and therapeutic vulnerabilities of NF2-mutant RCC remain largely uncharacterized.

Methods

To address this, we developed a versatile and transplantable organoid system on a pure C57BL/6 (B6) background that enables rapid genetic manipulation and faithfully models NF2-deficient RCC. LTL+ proximal tubule cells were isolated from microdissected B6 mouse kidney cortex via flow sorting and used to generate kidney organoids. Using RNP–based CRISPR editing, we engineered sequential knockout lines: CDKN2A/B, CDKN2A/B + SetD2, CDKN2A/B +SetD2 +NF2 with and without c-myc. Bulk–RNA sequencing were performed to confirm the cell of origin. Organoids were orthotopically injected into immunocompetent B6 mice to assess for tumor formation in immunocompetent hosts. In parallel, Ex vivo and in-vivo CRISPR–screens are underway to identify therapeutic vulnerabiltiies in the context of NF2 loss.

Results

Wild–type B6 kidney organoids demonstrated robust expression of proximal tubule markers and established their transcriptomic fidelity. Efficient gene targeting in organoids was confirmed using CRISPRseq and western blot. Mutant organoid lines exhibited accelerated growth rates compared to WT controls. Bulk RNA–sequencing of mutant organoid demonstrated NF2 and Setd2 specific transcriptional perturbations. Orthotopically injected organoids are being monitored longitudally for tumor formation via ultrasound imaging.

Conclusions

We have established a tractable, immunocompetent, and transplantable murine organoid-based model of RCC harboring clinically relevant tumor suppressor mutations. This platform enables high-throughput interrogation of NF2-deficient RCC and offers a foundation for discovery of genotype-specific therapeutic targets. Ongoing work includes the completion of customized CRISPR dropout screens—guided by bulk RNA-seq data from both murine organoids and human tumors—to uncover lineage- and mutation-specific dependencies. Hits from these screens will inform downstream therapeutic strategies and be validated through histologic, immunohistochemical, and tumor microenvironmental analyses of harvested tumors and derived organoids.

Keywords

NF2, organoids, RCC, CDKN2A/B

68

Targeting the BBOX1-TBK1-mTORC1 Axis in Clear Cell Renal Cell Carcinoma

Chengheng Liao, Qing Zhang

UT Southwestern Medical Center

Background

Clear cell renal cell carcinoma (ccRCC), a metabolic disease originating from renal proximal convoluted tubule (PCT) epithelial cells, remains incompletely understood regarding its initiating signaling events.

Methods

We use clinical data-driven analysis, combined with pathological validations to identify γ-butyrobetaine hydroxylase 1 (BBOX1), a key enzyme in carnitine synthesis predominantly expressed in PCT cells, as a tumor suppressor in ccRCC. We also conducted substantial in vitro and in vivo functional studies to understand the role of BBOX1 in ccRCC tumorigenesis. In terms of mechanistic studies, we combined a variety of methods, including transcriptomics, metabolomics, and IP-mass spectrometry, to uncover the underlying mechanisms of BBOX1 in regulating metabolism and ccRCC development.

Results

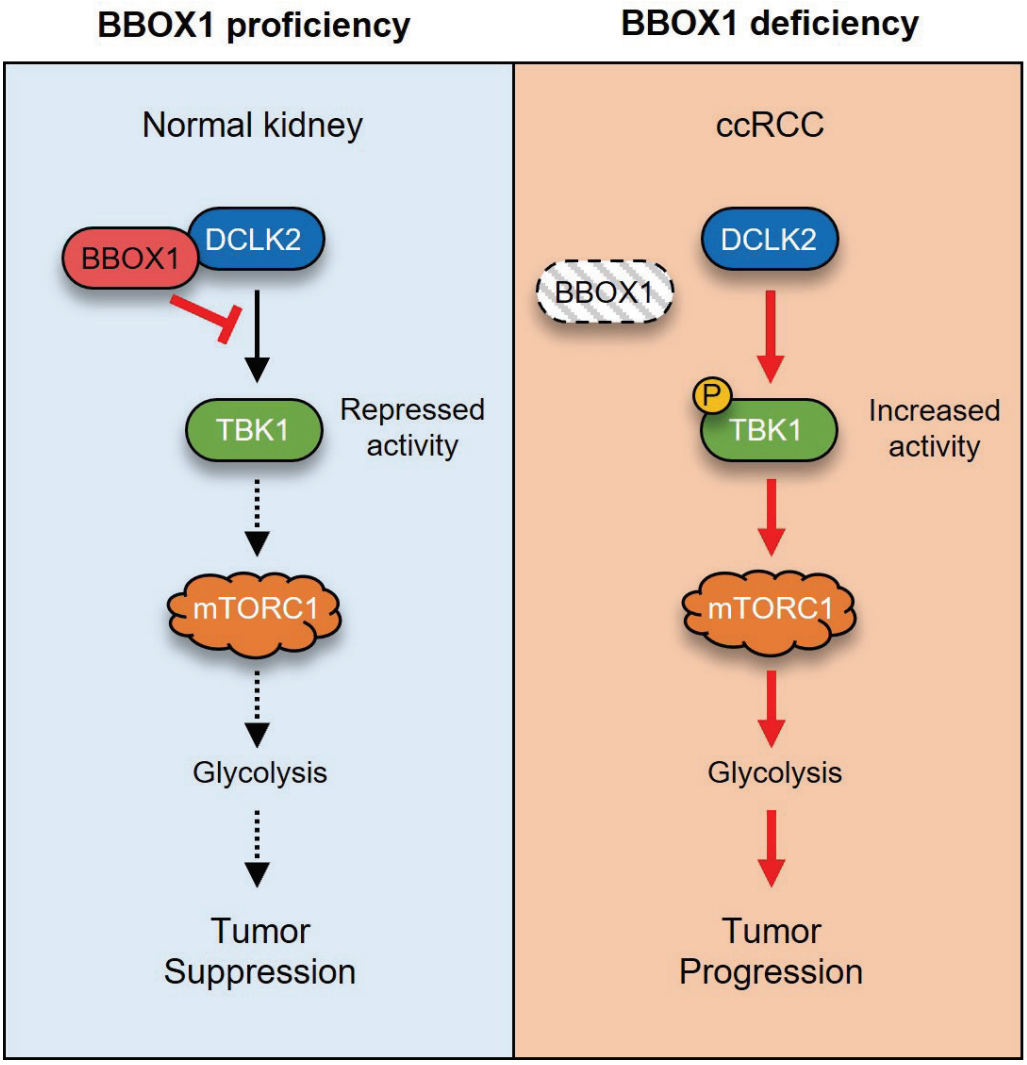
BBOX1 expression is lost during ccRCC malignant transformation, and its restoration reduces cell viability in physiological medium and inhibits xenograft tumor growth. Transcriptomic analyses reveal that BBOX1 suppresses critical metabolic pathways, including mTORC1 signaling and glycolysis in ccRCC. Further, we identify TANK-binding kinase 1 (TBK1) as an essential mediator of mTORC1 and glycolysis activation and as a target of BBOX1-mediated tumor suppression. Mechanistically, BBOX1 disrupts TBK1 activation by preventing its interaction with the upstream activator doublecortin-like kinase 2 (DCLK2). In a therapeutic approach, we developed a novel TBK1 Proteolysis-targeting chimera (PROTAC) to target ccRCC tumorigenesis.

Conclusions

This BBOX1-TBK1-mTORC1 axis unveils a previously uncharacterized mechanism in ccRCC metabolic dysregulation and highlights potential therapeutic strategies.

Keywords

ccRCC, mTORC1, glycolysis, TBK1, BBOX1



Trials in Progress Posters

69

Testing Cabozantinib with or without Atezolizumab in Patients with Advanced Papillary Kidney Cancer (NCT05411081)

Benjamin Maughan[1], Melissa Plets[2], Sumanta Pal[3], Yasser Ged[4], Cathryn Tangen[2], Ulka Vaishampayan[5], Seth Lerner[6], Arpita Desai[7]

[1]Huntsman Cancer Institute at the University of Utah, [2]SWOG Cancer Research Network, [3]City of Hope Comprehensive Cancer Center, [4]Johns Hopkins, [5]University of Michigan, [6]Baylor College of Medicine, [7]University of California, San Francisco, Helen Diller Family Comprehensive Cancer Center

Background

The role of combination immune therapy is not fully established in PRCC. The S1500 (PAPMET) clinical trial established single-agent cabozantinib as the standard of care for PRCC [PMID 33592176] with a median progression-free survival (PFS) of 9.0 months compared to 5.6 months with sunitinib. Additionally, trials have shown activity of PD-(L)1 antagonists as monotherapy [PMID 33529058] or in combination with targeted therapy [PMID 34491815]. In a single-arm study of cabozantinib/nivolumab the median PFS was 12.5 months [PMID 35298296]. In contrast, some data from retrospective studies suggest no benefit with combination therapy [PMID 36610815] over sequential single agent studies. Importantly no prior randomized studies of immune therapy in PRCC have compared sequential therapy versus upfront combination therapy. Toxicity is higher with combination therapy suggesting some equipoise and rationale for testing combinations in PRCC. We hypothesize that the combination will have higher clinical activity than single-agent cabozantinib while maintaining a reasonable quality of life.

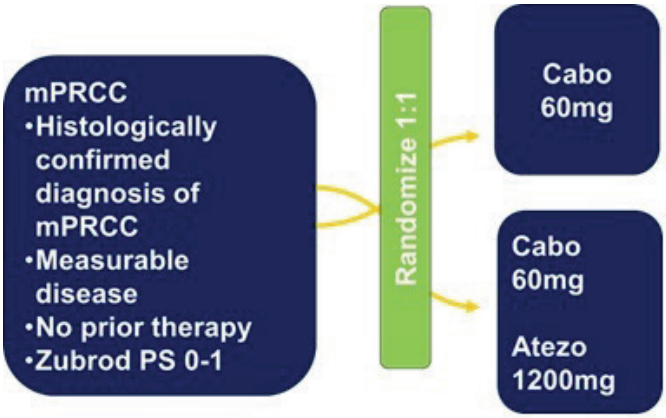
Methods

This is a prospective randomized phase II clinical trial conducted through the NCTN and led by SWOG. The primary endpoint is a comparison of PFS between cabozantinib and cabozantinib/atezolizumab. Secondary endpoints include comparison of objective response rate, overall survival and safety. Patients are treated with cabozantinib 60mg/day versus cabozantinib 60mg/day + atezolizumab 1200 mg q3 weeks. Dose reductions of cabozantinib are allowed. Dose delays of either treatment are allowed. The sample size is planned for 200 patients to be enrolled and randomized 1:1 to each treatment arm. Treatment is allowed to continue even with discontinuation of the second agent in the combination arm.

Significance & Vision

Current clinical practice for patients with PRCC is defined by the approved treatment methods for clear cell RCC. It is unclear if combination strategies are as successful for PRCC as ccRCC. Additionally, the long-term follow up of prior TKI/IO studies in ccRCC do not demonstrate immunologic synergy suggesting that combination approaches might lead to increased toxicity without significant clinical benefit is many patients. Here we aim to establish the true clinical value of combination therapy for this disease. Additionally a rich biobank of liquid samples, soft-tissue tumor samples and stool samples will be collected in order to further basic scientific research with the aim of developing disease specific treatments for patients with PRCC.

Trial Schema



Keywords

Papillary, Kidney cancer, cabozantinib, atezolizumab

70

A Phase 1 Clinical Trial of the Farnesyltransferase Inhibitor KO-2806 in Combination with Cabozantinib in Renal Cell Carcinoma

Adanma Ayanambakkam[1], Lee S. Rosen[2], Benjamin Garmezy[3], Meredith Pelster[3], Glenn J. Hanna[4], Jacob Thomas[5], Manish R. Patel[3,6], Nawal Bendris[7], Paria Mahboub Johnson[7], Stephen Dale[7], Andrew Saunders[7], JC Kuan[7], Binaifer Balsara[7], Jabed Seraj[7], Adam E. Singer[2]

[1]Stephenson Cancer Center, University of Oklahoma Health Sciences Center, [2]Division of Hematology-Oncology, University of California Los Angeles Medical Center, [3]Sarah Cannon Research Institute, [4]Center for Head and Neck Oncology, Dana-Farber Cancer Institute, [5]Department of Medicine, University of Southern California, Norris Comprehensive Cancer Center, [6]Florida Cancer Specialists, [7]Kura Oncology, Inc.

Background

Farnesyltransferase inhibitors (FTIs) block post-translational modification of RAS and other farnesylated proteins. HRAS-driven tumors are highly sensitive to FTI treatment. Recent clinical trials (NCT03719690, NCT02383927) of the FTI tipifarnib in patients with HRAS-mutant (HRAS-m) head and neck squamous cell carcinoma harboring high variant allele frequency mutations (VAF ≥20%) showed objective response rates of up to 50% and favorable long-term outcomes. KO-2806 is a next-generation FTI that has increased potency and improved pharmacokinetic properties. Furthermore, in preclinical studies, KO-2806 has been shown to enhance tumor growth inhibition of tyrosine kinase inhibitors, including cabozantinib, in multiple clear cell (cc) renal cell carcinoma (RCC) cell line- and patient-derived xenograft models. These preclinical data support clinical investigation of KO-2806 in combination with cabozantinib in RCC.

Methods

FIT-001 is an ongoing first-in-human, multicenter, open-label Phase 1a/b clinical trial evaluating the safety, tolerability, pharmacokinetics, pharmacodynamics (PD), and preliminary antitumor activity of KO-2806 as monotherapy or in combination therapy in advanced solid tumors (NCT06026410; Figure). Up to 270 patients will be enrolled in Phase 1a and Phase 1b combined across approximately 50 sites. Phase 1a has separate monotherapy and combination dose-escalation arms. KO-2806 in combination with cabozantinib is being evaluated in RCC. Patients with advanced or metastatic ccRCC who progressed on ≥1 prior line of immunotherapy-based systemic therapy and patients with non-ccRCC who are treatment-naïve or who received any prior systemic therapy are eligible. On the basis of emerging data from Phase 1a, two PD cohorts (n≤12) with mandatory pre- and on-treatment tumor biopsies may be enrolled. In Phase 1b dose expansion, patients will receive the recommended phase 2 dose (RP2D) of KO-2806 with cabozantinib or will be randomized by dose if two potential KO-2806 RP2Ds are identified for the combination. The study began accrual in October 2023, and recruitment is ongoing.

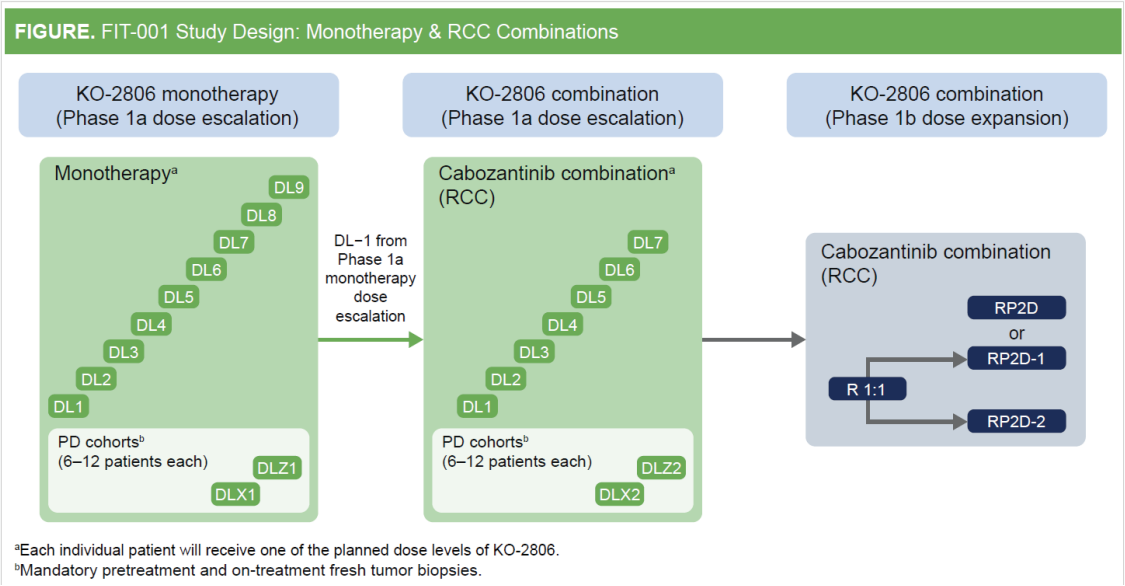
Significance & Vision

FIT-001 is assessing the safety, tolerability, pharmacokinetics, PD, and preliminary antitumor activity of KO-2806 in combination with cabozantinib in patients with ccRCC and non-ccRCC.

Keywords

Renal cell carcinoma, RCC, KO-2806, farnesyltransferase inhibitor, cabozantinib

Trial Schema



71

Educational Video Intervention to Enhance Latinx Participation in Genitourinary Oncology Clinical Trials: A Randomized Study

Regina Barragan-Carrillo[1], Sumanta Pal[2], Rana McKay[3]

[1]National Cancer Institute Mexico, [2]City of Hope Comprehensive Cancer Center, [3]University of California, San Diego

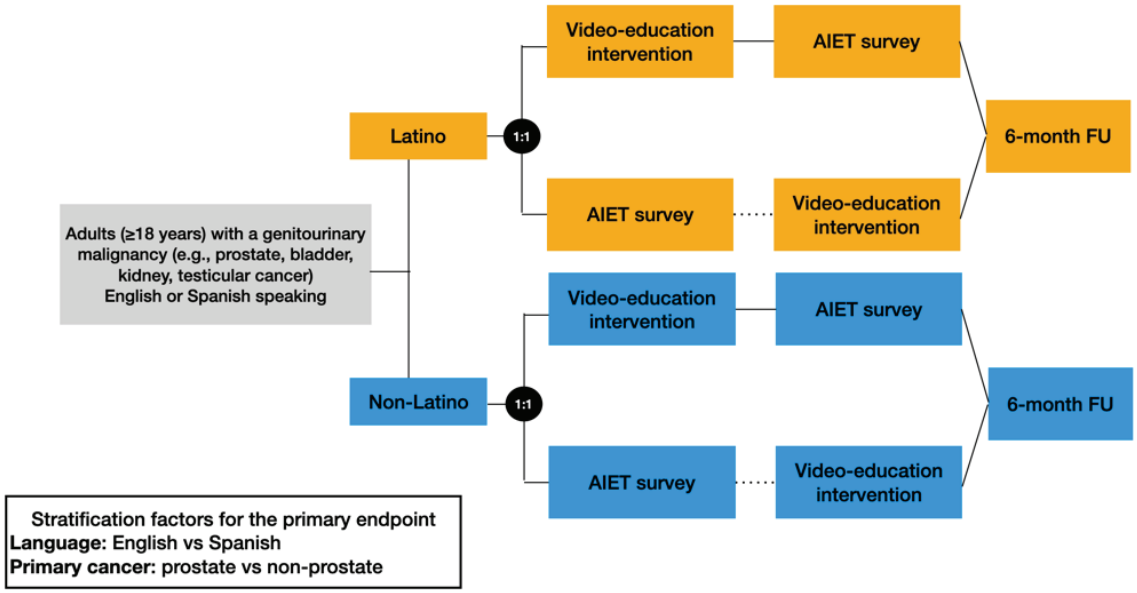
Background

The Hispanic and Latinx population comprises over 60 million individuals in the United States, representing approximately 18 percent of the total population. Cancer is the leading cause of death in this group. Despite the disease burden, Latinx individuals remain underrepresented in cancer clinical trials, accounting for only 2.3 to 3.9 percent of participants in therapeutic studies. This disparity limits the applicability of research findings and contributes to inequities in outcomes. Barriers such as limited awareness, language discordance, mistrust in the medical system, and structural inequities impact participation. Culturally tailored educational interventions may help address these gaps. This investigator-initiated trial aims to investigate whether a brief, bilingual educational video can improve willingness to participate in clinical trials among Latinx adults diagnosed with genitourinary (GU) malignancies.

Methods

This is investigator-initiated, randomized, controlled, multi-center trial conducted. Eligible participants are adults aged 18 or older with a histologically confirmed diagnosis of a GU malignancy, including prostate, bladder, kidney, testicular, or penile cancer, or with tumor markers consistent with metastatic germ cell neoplasia. All participants must speak either English or Spanish and be attending their first consultation in Medical Oncology, Radiation Oncology, or Urology. Patients are randomized in a 1 to 1 ratio to either the experimental or control arm (Figure 1). Randomization is stratified by cancer type (prostate versus non-prostate) and language preference (English versus Spanish) to ensure balance across key variables. In the experimental arm, participants watch a 10-minute culturally adapted video in their preferred language. The video was developed in collaboration with clinicians, patient advocates, and community partners. It explains the purpose, risks, and benefits of clinical trials, emphasizes ethical protections, and highlights the importance of Latinx representation in research. Immediately afterward, participants complete the 31-item Attitudes and Intention to Enroll in Therapeutic Clinical Trials (AIET) questionnaire. This validated tool assesses willingness to participate in trials and explores attitudes across six domains, including fear, mistrust, privacy concerns, and knowledge gaps. In the control arm, participants complete the AIET questionnaire without viewing the video. After the survey, they are offered the opportunity to watch the video to ensure equitable access to educational content. The primary endpoint is the proportion of Latinx participants who express willingness to participate in a clinical trial, based

Trial Schema



on responses to item 31 of the AIET questionnaire. Based on prior data, a baseline willingness of 15 percent is assumed. The study is powered to detect an increase to 35 percent with a sample size of 110 participants (55 per arm), using a one-sided alpha of 0.1 and 80 percent power. Secondary endpoints include the proportion of Latinx participants who enroll in a clinical trial within six months of the intervention and changes in AIET subscale scores that reflect trust, perceived fairness, and understanding of clinical research. Additional questions assess general clinical trial literacy. Exploratory analyses will examine the same outcomes in non-Latinx participants. Statistical comparisons will be made using Fisher's exact test and Wilcoxon rank-sum tests. Proportions will be reported with exact 95 percent confidence intervals.

Significance & Vision

The study is currently open to enrollment and is designed to inform scalable, culturally responsive strategies to improve equity in clinical trial participation for Latinx patients with cancer.

Keywords

Clinical trial, Latino, inclusion, education